LAKE FOREST COLLEGE

Senior Thesis

# Characterization of Familial Mutants and Splice Variants of Parkinson's Disease Protein α- Synuclein in Yeast Models

by

Natalie Ann Kukulka

April 19, 2013

The report of the investigation undertaken as a

Senior Thesis, to carry two courses of credit in

the Department of Biology and the Program of Neuroscience.

| | |
|---|---|
| Michael T. Orr<br>Chairperson<br><br>Krebs Provost and Dean of the Faculty | Shubhik K. DebBurman, |
| | Douglas B. Light |
| | Matthew R. Kelley |

**Abstract**

The misfolding of the protein α-synuclein is a major contributor to Parkinson's disease (PD). Three mutations (A53T, A30P and E46K) cause familial PD, and three newly discovered spliced variant forms of the protein (syn-126, syn-112, and syn-98) are also found in many PD patients. Little is known about whether these familial mutants can influence each other's contributing properties and whether the spliced variants are protective or harmful. Each familial mutant distinctively affects α-synuclein's cellular localization, aggregation, and toxicity. For my thesis, I first tested the hypothesis that all three familial mutants equally influence a-synuclein's pathological contributions in yeast models and found unexpected support for the dominance of the A30P mutant over E46K and A53T, shedding new light on A30P's influence of a-synuclein's conformation. Using polymerase chain reaction-based strategies, I have also made significant progress in creating the three spliced-variants for future evaluation in yeasts to assess their contributions to PD.

**Dedication**

To my family, for their unconditional love and support

To God, for the gift of wisdom

**Acknowledgments**

First and foremost, I would like to thank Dr. Shubhik DebBurman for accepting me in his laboratory as a Richter Scholar and inspiring me to begin my own research project. Without his support I would have been able to develop that work through the years into this final senior thesis. I am forever grateful to have been given the opportunity to conduct undergraduate research in Dr. DebBurman's lab, and to have developed my skill set under his constant guidance.

Furthermore, I am eternally grateful to my mentors: Mike Fiske '10 and Keith Solvang '11, who have taught me basic skills in the lab that blossomed into this work. I would like to thank all of the past and current lab mates without who none of the years would have been as exciting as they were: Jaime Perez Pineda'10, Alina Konnikova'11, Madhavi Senagolege'12, Galina Lipkin'15, and Wase Tembo'15. Each one of you deepened my passion for science and research. Galina—thank you for commencing the future tradition of dancing Gangnam Style Dance with me during any and every lab outing; we shall pass this tradition to future Richters. Wase—thank you for always being there for me and bringing humor into my life. Aside from my lab mates, I would like to thank one of the most important and essential people in Johnson, Mrs. Elizabeth Herbert. Beth—thank you for keeping me sane through these four years!

I would like to thank my family for always supporting me every step of the way—from a clueless and hyper freshman, to a mature,but a bit stressed senior. Thank you to: my grandmother for her amazing cooking, which got me through numerous long nights in the lab, my sister for her never-ending humor, and my parents for their unconditional love and always needed words of wisdom and support. I would like to

thank Kevin Youkhana for his encouragement, Sylwia Dakowicz ’13 for her caffeinated motivation, and Pete Jansen ’13 for sharing a nocturnal lifestyle with me.

Lastly, I would like to thank my thesis committee members, Dr. Douglas Light, Dr. Matthew Kelley, and Dr. Shubhik DebBurman for not only taking part in reviewing my senior thesis but constantly supporting me for the past four years.

Dr. Light, thank you for always filling my thesis days with humor and music critiques; I promise *never* to pay back the toll fees I have accumulated.

Dr. Kelley, thank you for implanting statistical skills in me through Research and Statistics; unfortunately I still think you need to ‘step-up’ your game with Cognitive Psychology so that people do not take it abroad.

Dr. DebBurman, thank you for all of your patience and faith in me and for leading me through the unforgettable four-year-long voyage. You have told me that I take on too much, but it is because I strive to show my passion and involvement in things I care about as successfully as you do! ...still much practice needed.

**Table of Contents**

## List of Figures

## List of Tables

## Appendix List

**List of Abbreviations**

**PD:** Parkinson's disease

**LB:** Lewy Body

**BY 4741:** Parent yeast strain in Budding Yeast

**TCP1:** Parent yeast strain in Fission Yeast

**Sph+:** Parent yeast strain in Fission Yeast

**WT:** Wild-type α-synuclein

**GFP:** Green fluorescent protein

**eGFP:** Enhanced green fluorescent protein

**A30P:** Familial PD point mutation, Alanine → Proline at the $30^{th}$ amino acid

**E46K:** Familial PD point mutation, Glutamic acid → Lysine at the $46^{th}$ amino acid

**A53T:** Familial PD point mutation, Alanine → Threonine at the $53^{rd}$ amino acid

**A30P-A53T:** Combinatory double point mutation in α-synuclein where Alanine → Proline at the $30^{th}$ amino acid and Alanine → Threonine at the $53^{rd}$ amino acid

**A30P-E46K:** Combinatory double point mutation in α-synuclein where Alanine → Proline at the $30^{th}$ amino acid and Glutamic acid → Lysine at the $46^{th}$ amino acid

**E46K-A53T:** Combinatory double point mutation in α-synuclein where Glutamic acid → Lysine at the $46^{th}$ amino acid and Alanine → Threonine at the $53^{rd}$ amino acid

**A30O-E46K-A53T:** Combinatory triple point mutation in α-synuclein where Alanine → Proline at the $30^{th}$ amino acid, Glutamic acid → Lysine at the $46^{th}$ amino acid, and Alanine → Threonine at the $53^{rd}$ amino acid

# INTRODUCTION

## Nerve-Racking Protein Responsibilities

Understanding of the complexity of the human body is one of the most sought after abilities that doubtfully will ever be acquired. Take into consideration the human brain; it is a mass of about three pounds composed of one hundred billion nerve cells and trillions of supporting cells (Purves et al., 2012). This fundamental processing unit is responsible for everything one does, sees, smells, interacts with, has an emotional responses to or ignores altogether. Anatomically speaking, the brain is a part of the central nervous system, and along with the spine, both are responsible for integrating information and coordinating activity (Purves et al., 2012). In addition to this command system, the peripheral nervous system helps communicate with the rest of the body, thereby establishing a circuit of sensing, integrating, and acting.

As a newborn develops from an inexperienced 'creature' to a skilled adult, the range of processed information increases exponentially. Such overload of information is sequentially synchronized by the establishment of neuronal connections, which can either be retained with repetition or lost due to their irrelevance (Purves et al., 2012). On the molecular level, each neuron operates by an array of proteins whose functions are determined through their specific shapes. Although proteins are made up of as few as twenty amino acids, the sequence of the amino acid assortment is what leads to the diversity in protein shapes and consequent varied functions. While the protein folding machinery is quite robust, it operates best at an equilibrium state between

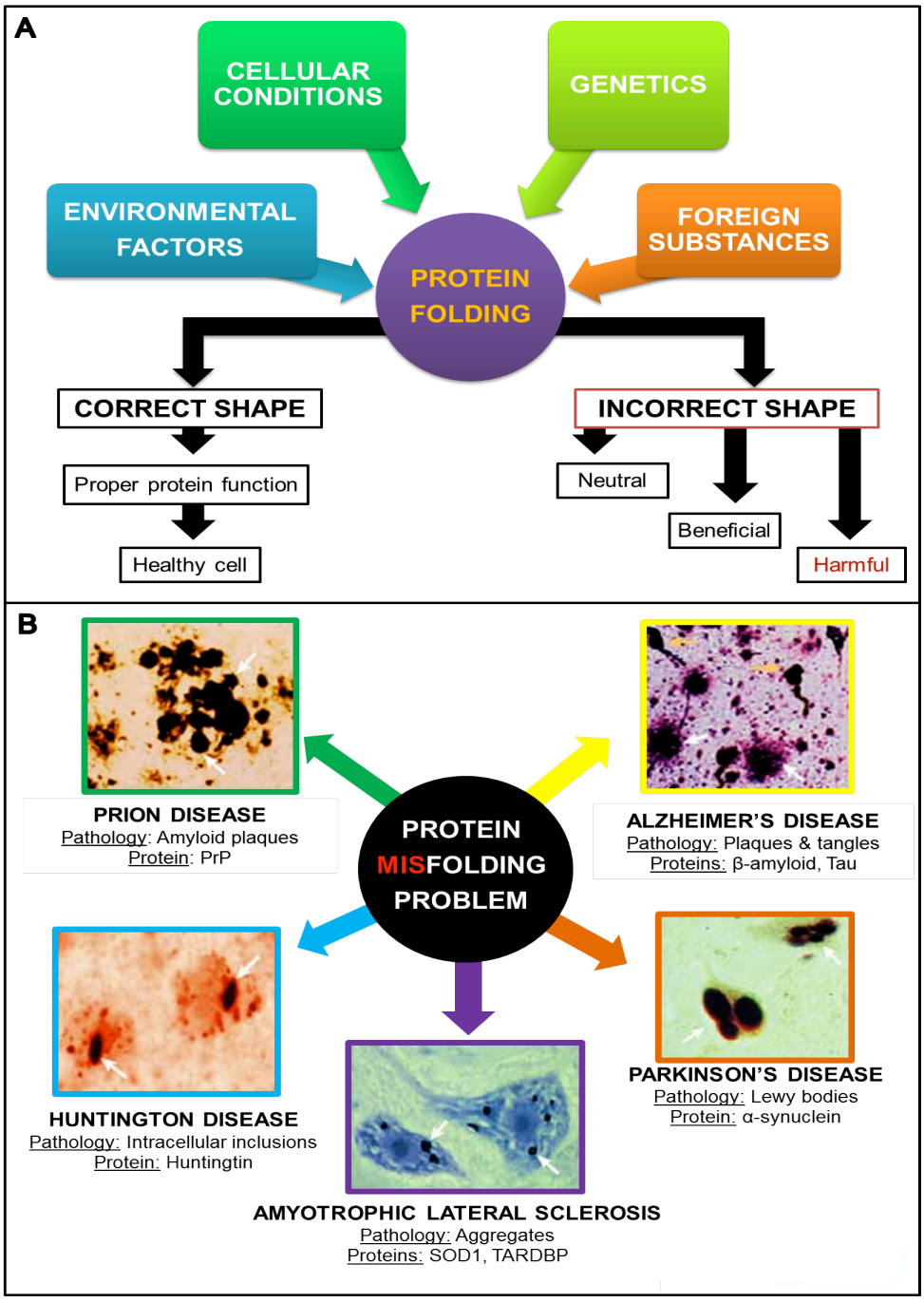
A
CELLULAR CONDITIONS
GENETICS
ENVIRONMENTAL FACTORS
FOREIGN SUBSTANCES
PROTEIN FOLDING
CORRECT SHAPE
Proper protein function
Healthy cell
INCORRECT SHAPE
Neutral
Beneficial
Harmful
B
PRION DISEASE
Pathology: Amyloid plaques
Protein: PrP
ALZHEIMER'S DISEASE
Pathology: Plaques & tangles
Proteins: β-amyloid, Tau
PROTEIN MISFOLDING PROBLEM
HUNTINGTON DISEASE
Pathology: Intracellular inclusions
Protein: Huntingtin
PARKINSON'S DISEASE
Pathology: Lewy bodies
Protein: α-synuclein
AMYOTROPHIC LATERAL SCLEROSIS
Pathology: Aggregates
Proteins: SOD1, TARDBP

*Figure 1*. *Protein folding.* A) There are many factors that affect the folding process of the protein. Exhibited are just some of the factors that will influence protein conformation: environmental factors, cellular conditions, genetics, and exposure to foreign substances. If the environmental factors do not provide any harm to the organism, cellular conditions are appropriate, genetic information is not impaired, and exposure to foreign substances is minimal, then the protein will fold correctly. The proper conformation will then lead to a well-functioning protein and a healthy cell. However, if the balance between these factors is disrupted or they individually become unfavorable for the organism, then the protein may misfold. The altered shape will lead to neutral, beneficial, or harmful consequences. B) Neurodegenerative diseases are one branch of harmful consequences due to protein misfolding. Exemplified are five common neurodegenerative diseases along with a list of their pathological characteristics and the misfolded protein(s). The images for various neurodegenerative diseases were acquired from http://www.nature.com/nrn/journal/v4/n1/fig_tab/nrn1007_F1.html.

environmental factors, cellular conditions, genetic influences, and foreign substances (Shin et al., 2009; Figure 1A). Increased exposure to negative environmental factors such as pollution or UV radiation or prolonged exposure to metals or toxins (such as pesticides) could contribute to the misfolding of the protein (Alberts et al., 2011). The molecular factors negatively influencing protein conformation could arise from incorrect encoding/ transcription of the DNA via various pathways or the failure of one of the intermolecular organelles like the mitochondria that serves as the power house for the cell (Shin et al., 2009). Still, more often than not, the brain withstands the negative factor of various sources and allows us to function flawlessly on a daily basis.

**Neurodegeneration Initiated by Protein Misfolding**

One of the negative consequences of improper protein folding can lead to selective death of neurons consequently leading to a neurodegenerative disorder (Figure 1B). Neurodegenerative diseases are disorders that are derived from the progressive deterioration of a specific portion of the nervous system, or in other words, a specific part of the brain that specializes in a particular ability (Ross & Poirier, 2004). Some of the leading neurodegenerative diseases are: Alzheimer's disease (AD), Parkinson's disease (PD), Huntington disease (HD), Multiple sclerosis (MS), amyotrophic lateral sclerosis or Lou Gehrig's disease (ALS), and Prion diseases (Figure 1B). While each of these diseases differs in the progressive death of highly specialized neurons, the common feature among the pathology of neurodegenerative disease is the formation of protein aggregates from the misfolded protein in the affected neurons (Taylor et al., 2002; Figure 1B). The vast spectrum of neurodegenerative disease can be further narrowed down by focusing on the

exact protein that misfolds. Synucleinopathies are thus neurodegenerative diseases in which the α-synuclein protein misfolds. They include dementia with Lewy bodies (DLB), multiple system atrophy (MSA), Lewy body dysphagia (LBD) and Parkinson's disease (Galvin & Trokanowscki, 2001). Despite years of extensive research, cures for any of these neurodegenerative diseases remain elusive, afflicting several regions of the brain. Due to the shared pathology**,** understanding the mechanisms of α-synuclein protein misfolding in one disease may unlock mysteries for the other synucleinopathies and neurodegenerative diseases. *My thesis focuses on gaining insight into the molecular basis of α-synuclein that contributes to familial and sporadic PD. Nevertheless, my findings have the potential to help understand the basis of protein misfolding-linked problems in all synucleinopathies.*

**Understanding Parkinson's Disease**

PD is the second most common neurodegenerative disease and the first most common bradykinesia disorder, known as the slowness of movement disorder (National Institute of Neurological Disorders and Stroke, 2004). While its occurrence was first noted by James Parkinson and documented in 1817 as a short article called "An Essay on Shaking Palsy", it continues to persist in even higher frequency two centuries later (Parkinson, 1817). PD afflicts close to ten million people worldwide and approximately 60,000 Americans annually (Parkinson's Disease Foundation, 2012). While the search for a cure for PD has broadened worldwide, so did the cost of possible treatments. With no possible cure on the horizon, patients try their luck with administering L-Dopa or using much more invasive treatment options, such as surgical implantation of metal electrodes

for deep brain stimulation (Parkinson's Disease Foundation, 2012). While some of the symptoms may be initially suppressed, such as rigidity, resting tremors, masked facial expressions, patients ultimately die of organ failure (Olanow & Tatton, 1999; Galvin & Trokanowscki, 2001; Figure 2A).

*PD Causes*

PD can be classified as sporadic, which accounts for 90% of all diagnoses, or familial, which accounts for the remaining 10%. The sporadic form of PD can be initiated by various factors similar to those influencing protein misfolding (Figure 1A). For a long time, environmental factors were neglected in relation to the onset of PD, and it was not until a famous incident with the use of MPTP (1-Methyl-4-phenyl-1,2,5,6-tetrahydropyridine), a by-product of synthetic heroin, that people began pay closer attention (Sian et al., 1999). For example, exposure to chemicals like rotenone (an organic farming pesticide), (Betarbet et al*.,* 2000), heavy metals (Calne et al., 1994), and free radicals (Maguire-Zeiss *et al.*, 2005) have been linked with sporadic PD (Figure 2B).

Another factor, classified as a long-term environmental influence, was linked with traumatic brain injury, such as a traumatic blow to the head or a severe concussion. In terms of cellular dysfunction, oxidative stress (Jenner & Olanow, 1996; Maguire-Zeiss et al., 2005) and mitochondrial incapability (Langston et al., 1983; Langston et al., 1984) have been tied into PD (Figure 2B). Nevertheless, the precise mechanisms behind these factors are not well known, hence researchers tend to focus on the genetic factors within the familial branch of PD. The most common gene mutations that lead to PD occur in *SNCA* (Polymeropoulos et al., 1997; Kruger et al., 1998; Zarranz et al., 2004), *Parkin*

A

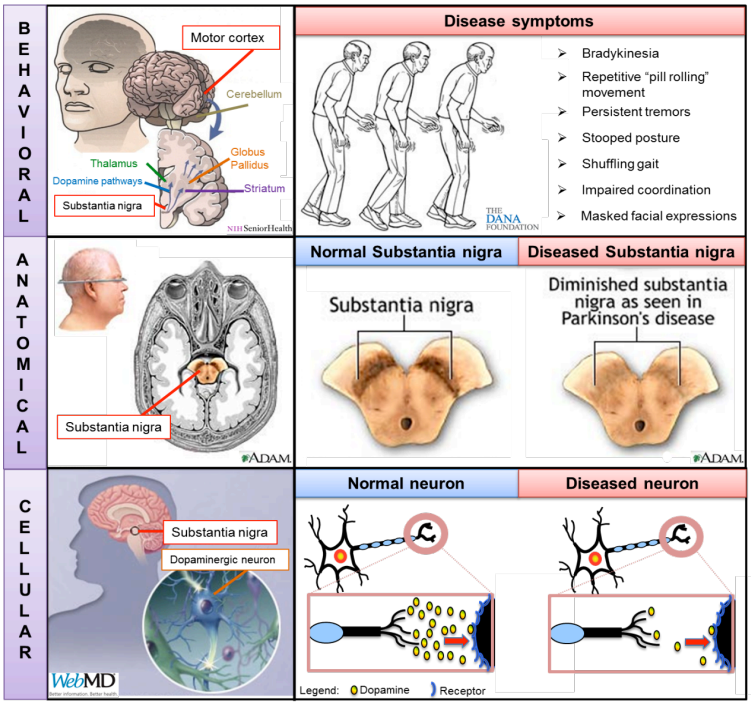
BEHAVIORAL
Motor cortex
Cerebellum
Thalamus
Globus Pallidus
Dopamine pathways
Striatum
Substantia nigra
NIH SeniorHealth
Disease symptoms
Bradykinesia
Repetitive "pill rolling" movement
Persistent tremors
Stooped posture
Shuffling gait
Impaired coordination
Masked facial expressions
THE DANA FOUNDATION
ANATOMICAL
Substantia nigra
ADAM.
Normal Substantia nigra
Diseased Substantia nigra
Substantia nigra
Diminished substantia nigra as seen in Parkinson's disease
ADAM.
CELLULAR
Substantia nigra
Dopaminergic neuron
WebMD
Normal neuron
Diseased neuron
Legend: Dopamine Receptor

B

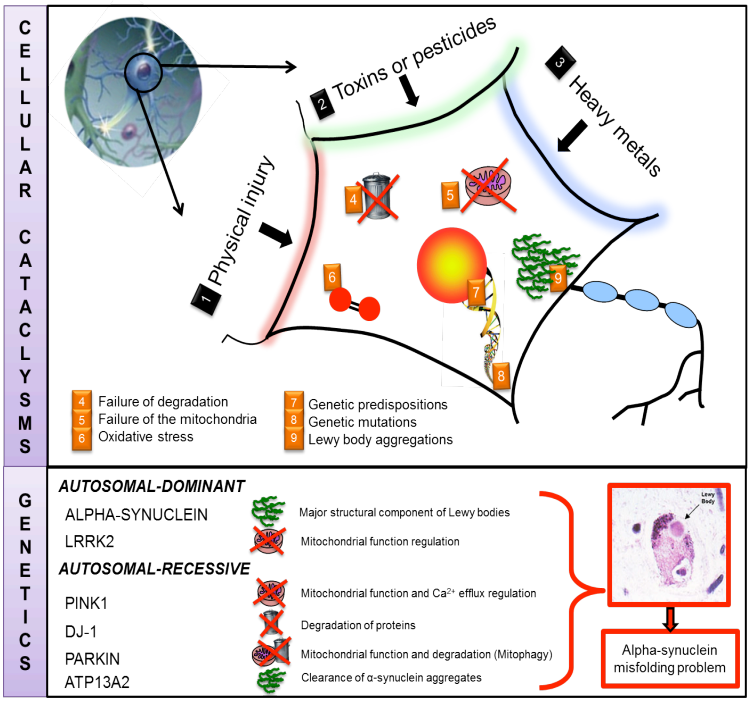
CELLULAR CATACLYSMS
1 Physical injury
2 Toxins or pesticides
3 Heavy metals
4 Failure of degradation
5 Failure of the mitochondria
6 Oxidative stress
7 Genetic predispositions
8 Genetic mutations
9 Lewy body aggregations
GENETICS
AUTOSOMAL-DOMINANT
ALPHA-SYNUCLEIN
Major structural component of Lewy bodies
LRRK2
Mitochondrial function regulation
AUTOSOMAL-RECESSIVE
PINK1
Mitochondrial function and Ca2+ efflux regulation
DJ-1
Degradation of proteins
PARKIN
Mitochondrial function and degradation (Mitophagy)
ATP13A2
Clearance of α-synuclein aggregates
Lewy Body
Alpha-synuclein misfolding problem

*Figure 2. The basis of PD.* A) Showcased are behavioral, anatomical, and cellular consequences of PD pathology demonstrated by restricted range of movement, neuronal death and reduced neurotransmitter signaling, respectively. The behavioral panel showcases the affected brain circuitry leading to the symptoms of the disease (image borrowed from https://www.dana.org/news/brainhealth/detail.aspx?id=9860). The anatomical panel shows the midbrain region of the substantia nigra, where at the onset of the disease, 90% of dopaminergic neurons die; this demise of neural cells can be clearly identified during patient autopsy through the lack of dark pigmentation (melanin) as exemplified on the right-side panel (image borrowed from http://www.umm.edu/patiented/articles/what_parkinsons_disease_what_causes_it_000051_1.htm). The cellular panel shows the release of the neurotransmitter, dopamine, from the specific dopaminergic neurons and how it diminishes during PD (image borrowed from http://www.webmd.com/parkinsons-disease/guide/parkinsons-causes). B) Showcased are molecular causes leading to the onset of the disease. The cellular cataclysms panel shows both the external influences on the neuron, as well as the molecular dysfunctions that lead to neurodegenration, especially in regard to PD. The genetics panel shows different genes that result in specific molecular consequences leading to the formation of Lewy bodies.

Kidata et al., 1998), *UCH-L1* (Liu et al., 2002), *DJ-1* (Bonifati et al., 2003), *PINK1* (Valente et al., 2004) and *LRRK2/PARK8* (Funayama et al., 2002; Paisan-Ruiz et al., 2004, Liu et al., 2012), *PARK2, PARK7 (*Neuytemans et al., 2010) autosomal-dominant PD mutations in (*UCHL-1, SNCA, LRRK2*), and autosomal-recessive PD (*parkin*, *PINK1* and *DJ-1*; Figure 2B).

*Parkinson's Disease Pathology*

PD is characterized by the death of dopaminergic neurons predominately concentrated within the midbrain structure known as the substantia nigra, which is Latin for "black substance" (Figure 2A). The substantia nigra is critical in the circuitry known to govern reward, addiction, and movement, which is further consistent with the exhibited symptomatic death of these neurons (Figure 2A). PD pathology reveals protein aggregates within degenerating neurons, which Frederick Lewy first named Lewy bodies in 1912. It was not until 1997 that Polymeropoulos and colleagues found a mutation in the α-synuclein gene, SNCA, on the fourth human chromosome, that caused autosomal-dominant PD through the A53T mutation in the α-synuclein protein (Polymeropoulos, 1997). The identified misfolded and aggregated α-synuclein protein was thus recognized as the major component that makes up Lewy bodies (Spillantini et al., 1998). Recently, it has been shown that Lewy bodies are formed from both full length and truncated versions of α-synuclein, indicating that the balance between these isomers plays an important role in the onset and progression of the disease (McLean et al., 2102).

**Insight into α-Synuclein**

The synuclein protein was first isolated from *Torpedo californica,* or Pacific electric ray,

but now its complete sequence has been analyzed in more than 20 species with its respective mutations, posttranscriptional modifiers, polymorphisms and truncations (Xiong et al., 2010). While much about the α-synuclein protein is still unknown, it appears to play a role in regulation of cell differentiation, synaptic plasticity, size of presynaptic vesicular pools, and dopaminergic neurotransmission (Luckin et al., 2000, Beyer et al., 2004). This is further supported by its history of binding to the phospholipid membranes *in vitro* and co-localization with synaptic vesicles *in vivo* (Luckin et al., 2000). While α-synuclein is predominantly expressed in the central nervous system, it is not a brain-specific protein because its presence is recognized in other tissues, such as the heart, muscles and pancreas (Beyer et al., 2004, Beyer et al., 2006). Further research has specified and confirmed its high expression in skin, lungs, kidney, spleen, heart, liver and muscle samples (Beyer et al., 2008). Still, its highest expression is found in the brain (Beyer et al., 2008).

Structurally speaking, α-synuclein is a small, 140-amino-acid-long acidic protein, which is encoded by the SNCA gene on chromosome 4q21 (Beyer et al., 2006). Its native unfolded form increases its predisposition to self-aggregate based on varying environmental conditions, making it a very dynamic molecule (Lucking & Brice, 2000, Beyer et al., 2006, Bisaglia et al., 2009). More specifically, in an aqueous solution, it conserves its unfolded and randomly coiled structure. However, when it comes in contact with acidic phospholipid vesicles, it folds into an α-helical structure or forms insoluble fibrils with a high beta-sheet structure leading to formation of Lewy bodies (Beyer et al., 2006, Beyer et al., 2008).

Aside from environmental conditions, there are genetic factors that may alter the characteristics of a protein. Three distinct α-synuclein single amino acid point mutations lead to

the development of familial PD. The data in my thesis depends heavily upon the understanding of each individual mutant's characteristics. Therefore, I will elaborate on them in the overview for study one. In additional genetic mutations, there are more than three hundred different posttranslational protein modifications which lead to changes in protein size, charge, structure, and conformation, affecting key protein characteristics. As part of background information for study two, I will provide insight into understanding one of these posttranslational protein modifications: the formation of splice variants.

***STUDY 1***

***Understanding Familial PD Point Mutations***

*A53T:*

This missense mutation, where alanine charges to threonine on the 53$^{rd}$ amino acid of the α-synuclein protein, was the first familial PD point mutation identified in the Contursi family and three additional unrelated Greek families (Polymeropoukous et al., 1997; Figure 3). In *in vitro* studies, the A53T mutant showed that in the absence of other Lewy body-associated molecules, it was disordered in dilute solution just as WT, but at high concentrations it formed discrete spherical assemblies at the fastest rate (Conway et al., 1998; Figure 3). Further *in vitro* experimentation supported A53T's ability to aggregate best at lower concentrations and showed that A53T had greater propensity to polymerize than A30P, one of the other familial mutants (Giasson et al., 1998). In 2000, Conway et al.'s research findings added that the fibrillation of A53T was relative to that of WT, and faster than that of A30P, while the consumption of the A53T monomer was the most rapid.

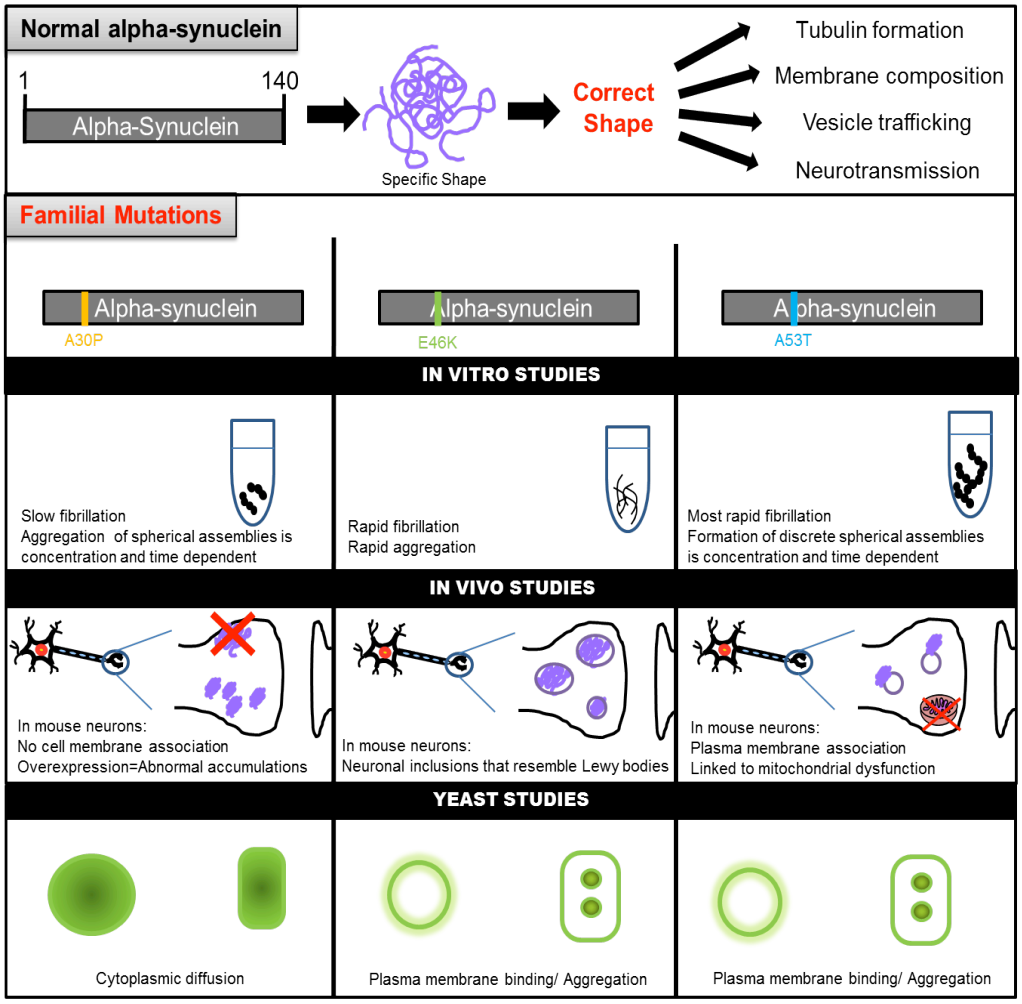


*Figure 3. Familial mutations of* α*-synuclein.* The top panel demonstrates the roles of the properly folded and corrently functioning α-synuclein prtein. This description is then contrasted by the portrayal of consequences from each of the familal mutations: A30P, E46K, and *A53T in vitro, in vivo,* and in yeast studies.

In 2001, the study conducted by Sharon et al. not only shed more light into the properties of the A53T α-synuclein mutation, but also into the function of the α-synuclein protein itself. In their transgenic mouse model, they found an enhanced association of the A53T mutation with microsomal membranes consequently leading to the conclusion that α-synuclein is a novel member of the lipid-binding protein family (Sharon et al., 2003; Figure 3). Further spectroscopy analysis showed no significant difference from WT in the second structure upon membrane binding of α-synuclein (Jo et al., 2002). Studies in living organisms, more precisely in yeast models, revealed that in budding yeast the A53T mutation showed plasma membrane binding, just like WT, and in fission yeast it was exhibited as accumulation of small vesicles or the presence of aggregates (Sharma et al., 2006, Brandis et al., 2006; Figure 3). Depending on the strain that was being used as the model, A53T did not show any toxicity in budding yeast, yet in fission yeast it was always toxic in either the TCP1 or Sph+ strains. (Sharma et al., 2006, Brandis et al., 2006; Figure 3).

In respect to human dopamine transporter (hDAT) the mutation did not form strong protein-to-protein bonds, and unlike A30P, it did not modulate dopamine uptake from hDAT in any way (Wersinger et al., 2003). Nevertheless, the hDAT-dependent toxicity was higher than with either WT or A30P (Wersinger et al., 2003). In transgenic mice models, the A53T mutant of α-synuclein led to development of severe and complex motor impairment, leading to paralysis and death (Giasson et al., 2002). Further immunoelectron microscopies supported the argument that the extensively formed filaments were toxic and lead to neurodegeneration (Giasson et al., 2002). The latest research further elaborates upon A53T's effects and shows that the overexpression of the mutant leads to massive mitochondrial destruction and loss, which is a

bioenergetics deficit characteristic of neural degeneration (Choubey et al., 2011).

*A30P:*

This missense mutation was the second point mutation identified in the involvement of the onset of familial PD after A53T. In 1998, members of a British family lacking the A53T mutation revealed a hereditary progression of the development of PD. After further investigation, Kruger at al. identified the A30P missense mutation (a switch of Alanine to Proline on the 30$^{th}$ amino acid in the α-synuclein) as a familial PD point mutation in accordance with the UK Parkinson's Disease Society Brain Bank's criteria (Figure 3).

When tested in a vesicle binding assay, the A30P mutation lacked significant plasma membrane binding, which was initially proposed to lead to the assembly of Lewy body filaments in the rat optic system (Jensen et al., 1998; Figure 3). Subsequent *in vitro* studies showed that in the absence of other Lewy body-associated molecules, the A30P α-synuclein mutant was disordered in dilute solution, just as WT, whereas at high concentrations it only formed small spherical species (Conway et al. 1998). Further *in vitro* experimentations showed that A30P demonstrated an ability to aggregate, which depended on both concentration and time (Giasson et al., 1998). In 2000, Conway et al.'s research findings explained that although the fibrillation of A30P was slower than that of WT and A53T, the consumption of the A30P monomer was comparable to or slightly faster than WT, but slower than the rate of A53T. Such findings could be attributed to the fact that unlike other Parkinson's disease mutations, A30P has been shown to substantially alter the three-dimensional conformation of the α-synuclein protein, which may be due to the failure to undergo a typical structural transition from random coil to α-helix (McLean

et al., 2000, Jo et al., 2002).

Later studies in living organisms, for instance in yeast models, revealed that in both budding and fission yeast the A30P mutant exhibited cytoplasmic diffusion throughout the cell and was not toxic in either of the models (Sharma et al., 2006, Brandis et al., 2006; Figure 3). In 2000, Kahle et al. demonstrated that the A30P human α-synuclein mutant in a transgenic mouse's brain did not fail to be transported to the synapse, despite its inhibited ability to bind plasma membranes. In fact, A30P's transgenic overexpression lead to abnormal cellular accumulations (Kahle et al., 2000). In relation to human dopamine transporter (hDAT), the mutation did form strong protein-to-protein complexes, and unlike A53T, it negatively modulated hDAT function, leading to reduced uptake of the extracellular dopamine and dopamine-mediated hDAT-dependent toxicity (Wersinger et al., 2003).

*E46K:*

In 2004, E46K was identified as the third familial PD point mutation in α-synuclein leading to familial PD (Zarranz et al., 2004). In E46K, the dicarboxylic amino acid—the glutamic acid—changes to lysine on the 46$^{th}$ position (Figure 3). Published by Zarranz et al. in 2004 as the first instance of its identification in a Spanish family, the mutation pathologically contributed to the death of dopaminergic neurons within the substantia nigra and presence of numerous Lewy bodies, which are key trademarks of PD. Additionally, the aggregations of the protein proved to be unresponsive to ubiquitin in cortical and subcortical areas, further supporting its role in the onset of PD (Zarranz et al., 2004). That same year, this missense mutation was characterized in terms of its phospholipid properties and ability to assemble filaments in comparison to the WT α-synuclein and the other two familial mutations, A30P and

A53T. It turns out that E46K caused two fold higher proportion of liposomal binding and resulted in the same or slightly less high rate of formation of fibrils as A53T(Choi et al. 2004, Greenbaum et al., 2004; Figure 3).

Shortly after its identification, E46K was biochemically and biophysically characterized, revealing that it resulted from rather subtle changes to the conformation of the α-synuclein protein (Fredenburg et al., 2007). When tested *in vitro,* E46K formed insoluble fibrils more rapidly than WT but the total amount of protofibrils was reduced (Fredenburg et al., 2007). Using high-resolution atomic force microscopy, researchers established that structurally, E46K formed fibrillar aggregates of a smaller diameter and periodicity than WT (Raaij et al., 2006). At the same time, E46K yielded a larger amount (4.4-fold) of total accumulation and assembly of amyloid fibrils than WT at 25°C (Kamiyoshihara et al., 2007).

In culture systems, such as human neuroblastoma cells, E46K exhibited highest percentage of aggregation (in comparison to WT, A30P, and A53T), as well as phenotypic characteristics reminiscent of the formation of Lewy bodies (Pandey et al., 2005). At the same time, when E46K was tested in a live organism, budding yeast, it revealed a major lag in cell growth in the optical density assay, but those findings were contradicted by the toxicity results of the spotting assay that did not reveal any noticeable change in the rate of growth with the E46K mutation (Herrera & Shrestha, 2005; Figure 3). In transgenic mice, E46K human α-synuclein mutation expressed in SNpc resulted in neuronal inclusions that reiterated the biochemical, histological and morphological characteristics of Lewy bodies (Emmer et al., 2011).

*Combinatory Mutations until Now*

Although the knowledge on the individual familial PD mutations (A30P, E46K, and A53T) is vast and specific in areas such as *in vitro,* cell cultures, model organisms and human populations, there is little to no information in the literature about any combinatory mutations. Certainly none of the human patients has been found to exemplify more than one familial mutation at the time, but due to the varied properties exemplified by each mutant, combining them would provide a novel insight into the structural dynamics of the α-synuclein protein. The earliest recognition of the significance of studying combinatory missense mutations appears in the literature in 2002 when Jo et al., characterize the A30P-A53T mutant in an *in vitro* study. Their results showed a defective membrane binding which mimicked that of A30P, therefore suggesting dominance of the proline mutation in regard to lipid membrane binding behavior (Jo et al., 2002, Fuller et al., 2002). Furthermore, these results were supported and further elaborated upon in experiments in budding and fission yeast. In both budding and fission yeast, the A30P-A53T α-synuclein mutation showed cytoplasmic diffusion throughout the cell (Sharma et al., 2006, Brandis et al., 2006). In budding yeast, the combinatory mutant appeared not be toxic, and in fission yeast, the A30P-A53T mutant was less toxic than either one of the individual mutations (Sharma et al., 2006, Brandis et al., 2006).

The earliest animal (rodent) model bearing any one of the combinatorial mutations was described by Ikeda et al., in 2008 where the researchers created TgαSYN transgenic mice to study the A30P-A53T mutation. Overall, within the striatum they found significantly decreased levels of dopamine and the rotarod test revealed motor impairment making their model useful for analyzing the pathological cascade (Ikeda et al., 2008). Later on in 2011, Lelan et al. used a transgenic Sprague Dawley rat to gather a better insight of the properties of the A30P-A53T

α-synuclein mutation. The researchers hoped to gather further insight into neuropathological intricacies of PD. They found that the rat solely displayed olfactory deficits without any motor impairment which would be characteristic of an early onset PD, making it a good model to test olfactory deficits. While there was no α-synuclein aggregation localized in the subventricular zone, there was cell proliferation in the glomerular layers of the olfactory bulb and the subventricular zone (Lelan et al., 2011).

***Gap in Knowledge***

Despite minimal research available for A30P-A53T combinatory mutant, there is no literature on the other combinatory mutations, such as A30P-E46K, E46K-A53T or A30P-E46K-A53T. This lack of any sign of experimental analysis needs to be fulfilled, allowing for better understanding of the significance of these specific amino acids within α-synuclein.

***STUDY TWO:***

Molecular research focused on uncovering a specific set of protein properties can be initiated in two ways. The first option is to create synthetic variants that mimic one or more of the post-transitional modifications that the protein could be exposed to. The second technique is to recreate natural protein variants in a laboratory setting, which would allow for better control over protein expression leading to more specific insight.

*Synthetic Variants*

Three examples of post-transitional modification of α-synuclein that can be studied

through designer mutants are phosphorylation, nitrosylation and sumoylation. LBs are known to be composed of highly phosphorylated α-synuclein, particularly at two serine locations: amino acid 87 and 129 (Fujiwara et al., 2002, Paleolegou et al., 2010). The kinase involved in the α-synuclein phosphorylation is yet to be identified; nevertheless, simulating this condition can bring further insight into PD pathology and possible kinases identification.

In regard to nitrosylation, there are four sites that have been linked to PD, which can be studied through four mutation mimics: T39K, T125K, T133K, T136K (Clayton & George, 1998). One of the more interesting findings from 2004, done by Hodara et al., showed that a nitration of Tyrosine 39 hindered the protein's ability to bind lipids and caused it to behave like the familial A30P mutation.

The process of sumoylation was recently linked to a novel family of proteins called SUMO that is believed to have the capacity to influence inter- and molecular interactions of α-synuclein. This modification could potentially prevent the protein from binding to itself, consequently reducing aggregation (Geiss-Friedlaner & Melchoir, 2007). Specifically, SUMO has been shown to modify lysine residues on proteins through establishing covalent bonds of which the most prominent two are K96 and K102 (Wilkinson et al., 2010, Bossis & Melchoir, 2006). Designer mutants such as K96R and K102R could therefore bring valuable insight into the role of this protein family.

*Natural Variants*

Aside from post-translational modifications, there are other changes that may lead to formation of new protein variants such as polymorphisms and truncations of the protein. Protein

polymorphisms occur when different genetic variants (alleles) become expressed. In one of the initial studies from 2003, conducted by Holzmann and his colleagues, two polymorphisms (-116C>G and -668T>C) of the α-synuclein promoter defining four haplotypes have been characterized in 315 German PD patients. In a later study from 2004, which focused on the Norwegian population, Myhre et al. identified several markers associated with PD such as Rep1 263 base pare allele, rs356165 and rs356219. In the Korean population the *MAPT* H1 haplotype and *SNCA* single nucleotide polymorphism (SNP) rs356219 have been reported to have a synergistic effect on the risk of PD (Kim et al., 2010). In regard to protein truncations, it has been established that about 15% of α-synuclein structures are truncated forms, which *in vitro* show high tendency for aggregation (Liu et al., 2005, Beyer & Ariza, 2012). Most specifically, the known forms of truncations are due to 20 S proteasome-mediated cleavage (Li et al., 2005), calpain-I-mediated cleavage (Dufty et al., 2007) and matrix metalloproteinase 3 mediated cleavage (Beyer & Ariza, 2012). Additionally, recently three naturally occurring splice variants have been identified resulting in the formation of α-synuclein-112, -126 and -98 (McLean et al., 2012).

*Introduction to α-synuclein splice variants*

The initial notion of the presence of splice variants of the α-synuclein protein was documented in 2004 in the study conducted by Beyer et al. The researchers identified an α-synuclein splice variant that was 112 amino acids long and was missing the region that accounted for the fifth exon (that was eliminated during alternative splicing), consequently deleting the amino acids from position 103 to 130 (Beyer et al., 2004; Figure 4). This alteration

deletes the possible phosphorylation site at position 129, which plays an important role in accumulation (Xiong et al., 2010).

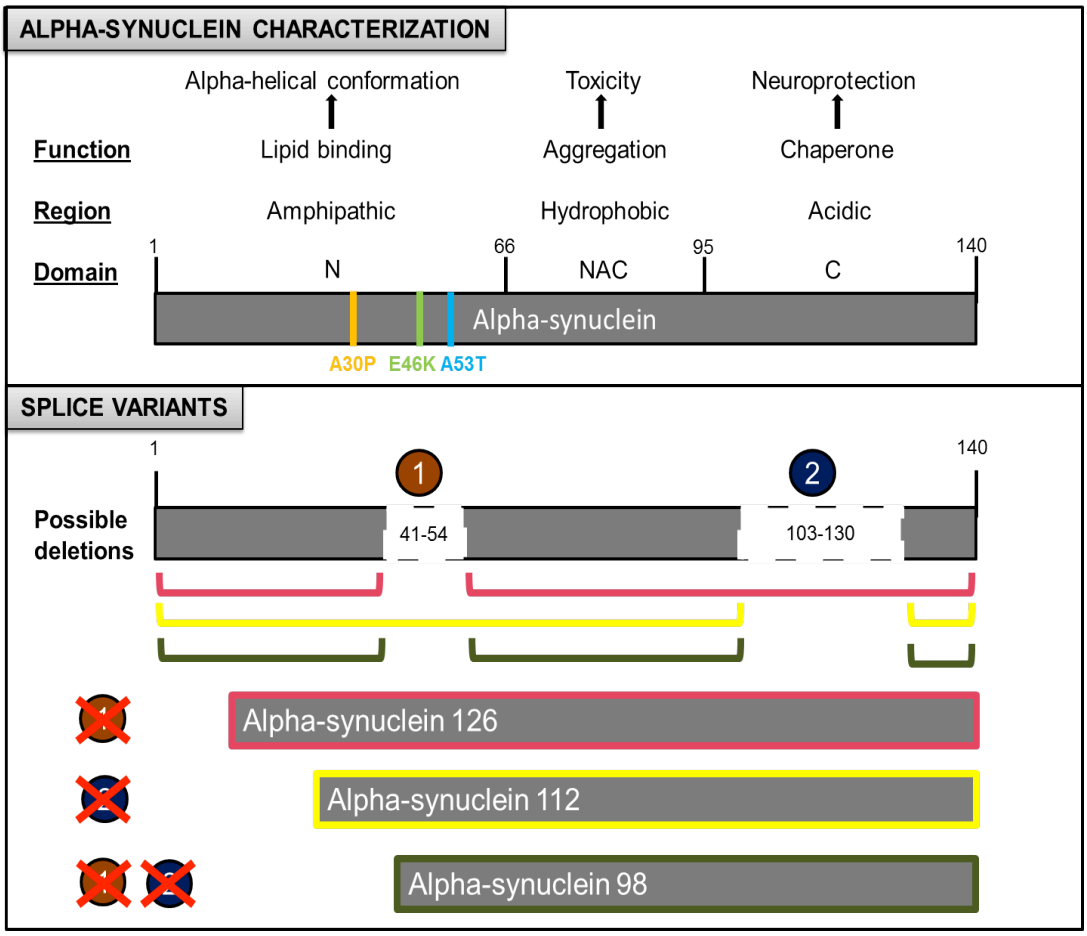


*Figure 4. Natural variants of alpha-synuclein protein*. The top panel (Alpha-Synuclein Characterization) breaks down the structural topography of the α-synuclein protein and provides the functions that each region is believed to be responsible for. The second panel (Splice Variants) shows the formation of natural splice variants through alternative splicing of α-synuclein gene, SNCA.

Furthermore, this truncation is highly hydrophobic because it is missing the majority of its hydrophilic amino acids located in exon five in this acidic C domain (Xiong et al., 2010).

In 2004, Beyer and his collogues compared the α-synuclein protein abundance levels of the full length version (140 amino acids long) and the spliced variant (α-synuclein-112) in human patients. They chose to analysis the prefrontal cortices of six patients with dementia with Lewy bodies (DLB), eight patients with Alzheimer's disease (AD) and six control subjects. They found that the level of α-synuclein-112 was greatly elevated in patients with DLB as opposed to AD, while the levels of alpha-synuclein 140 were diminished in both cases (Beyer et al. 2004).

Later on, another splice variant was identified, α-synuclein126, which is caused by the absence of the 3$^{rd}$ exon (amino acids: 41-53) due to alternative splicing (Figure 4). These splice variant results in the deletion of two familial PD mutations, E46K and A53T, and based on the location of the deletion, it affects the α-helix structures at the N-terminus (Xiong et al., 2010). In 2006, Beyer et al. characterized α-synuclein-126 based on similar brain analysis conducted with brain tissues from patient deceased from DLB, AD, and controls. They found that in all cases, α-synuclein-126 levels were markedly diminished in comparison to that of α-synuclein-140 (Beyer et al., 2006).

Finally, in 2007, Beyer at al. identified the third splice variant called α-synuclein-98 (Figure 4). Due to alternative splicing, this protein lacks both exons 3 and 5, resulting in missing amino acids in the region from 41-53 and 103-130. Aside from the fact that this truncation is missing familial point mutations E46K and A53T, as well as the phosphorylation site at S129, its function is not yet fully understood (Xiong et al., 2010). Nevertheless, mRNA expression

analyses revealed that α-synuclein-98 is a brain-specific splice variant and its expression varies based on location in fetal and adult brains (Beyer et al., 2008).

In the most recent study on α-synuclein splice variants published in 2012, McLean et al. analyzed both human brain regions and conducted studies on transgenic mice. In PD patients, they found that the truncations were expressed specifically in the cortex, substantia nigra, and cerebellum (McLean et al., 2012). The results in human α-synuclein expressing mice (ASO) revealed that while most transcript levels were elevated in comparison to WT mice, the highest levels were in the midbrain in 15-month old ASO mice (McLean et al., 2012).

***Gap in Knowledge***

Due to the recent identification of three α-synuclein splice variants, there is an absence of studies where each of the spliced variants would be individually expressed in any research model. Thus far, α-synuclein-126, -112, and -98 have only been examined during simultaneous expression in a model organism. Therefore, the gap in knowledge comes in understanding the function of each splice variant and later on the dynamics of their interactions.

**MY EFFORTS**

Earlier, I identified two gaps of knowledge that currently exist in understanding the PD protein α-synuclein. In order to narrow down the first presented gap of knowledge, I decided to create and assess α-synuclein combinatory mutants in several yeast models. In order to bridge the second gap, I set out to create at least two of the three splice variants, α-synuclein-126 and -112. The evidence mounted for this first study is compiled into the first chapter of my thesis, while the data gathered for the second study is compiled into the second chapter of my thesis.

The overall goal of my thesis was to gather further insight into the properties of α-synuclein and its relation to PD pathology. I attained that goal through: 1) assessing combinatory mutants in yeast models that allowed for the analysis of the α-synuclein's two hallmark PD related pathology characteristics, 2) creating tools for future assessment of the roles of each splice variant and their individual contribution to LB formation.

***STUDY ONE:***

*Hypothesis and Aims*

I hypothesized that combinatory mutants would exhibit: a blend of phenotypic features, high toxicity, and high protein accumulation (Figure 5). To test this hypothesis, I first created α-synuclein combinatory mutants: A30P-A53T, A30P-E46K, E46K-A53T, and A30P-E46K-A53T. Then, I assessed their properties in regard to α-synuclein localization, toxicity, and expression in several yeast models (Table 1).

*Main Findings*

Combinatory mutants were successfully created and expressed in low and high level protein expression yeast models. In terms of protein localization, A30P dominated the phenotype in combinatory variants. Furthermore, combinatory mutants did not enhance toxicity or protein expression.

***STUDY TWO:***

*Hypothesis and Aims*

I hypothesize that alpha-synuclein-98 and -126 will show diffusion throughout the cell, due to the impairment of regions responsible for plasma membrane binding; while α-synuclein-112 will show the formation of aggregates. Furthermore, I hypothesize that α-synuclein-112 and -98 will be more toxic than α-synuclein-126. Based on results from patients' data, I hypothesize that in yeast the protein expression will be the highest for α-synuclein-126, followed by -98, and finally -112. In order to test my hypothesis, I aimed to create tools for future assessment of each splice variant's role and contribution to PD pathology. My first goal was to create α-synuclein-126 and -112.

Main Findings

α-synuclein-126 and -112 were created through PCR splicing and α-synuclein-126 was successfully TOPO cloned.. Although none of the created α-synuclein splice variants have been sequenced, the α-synuclein-126 and -112 both seem to be of the appropriate sizes.

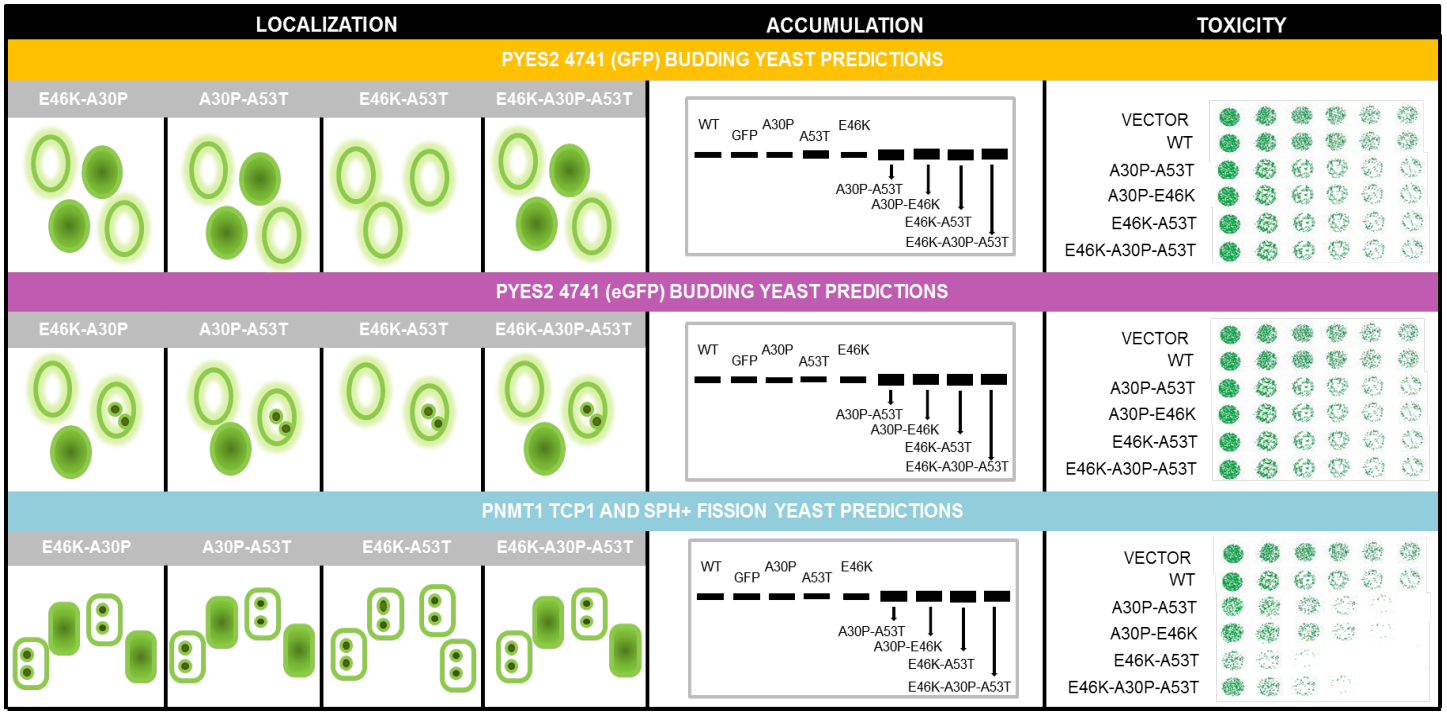


*Figure 5. Hypothesis for α-synuclein familial combinatory mutant properties.* A) This is a visual representation of the hypothesis for the behavior of combinatory mutants in two budding yeast models: BY 4741 with GFP, BY4141 with eGFP and the two fission yeast models: TCP1 and Sph+. The following assays were of interest: localization, accumulation and toxicity.

## METHODS AND MATERIALS

The methods utilized in the laboratory were adapted from Sharma et al. (2006), Brandis et al. (2006), and Fiske et al. (2011). Below is a succinct overview of the techniques utilized to acquire all data showcased in this thesis.

### *STUDY ONE:*

*Yeast Mutagenesis*

The combinatory mutants, A30P-A53T, A30P-E46K, E46K-A53T, and A30P-E46K-A53T, tagged with either green fluorescent protein (GFP) or enhancing green fluorescent protein (eGFP), were mutagenized according to the GENEART Site-Directed Mutagenesis System Protocol provided by Invitrogen Life Technologies. The mutagenized products were then transformed into One Shot Max Efficiency Dh5α-T1 component cells according to the TOPO TA Expression Kit from Invitrogen. Each vector was then purified using the mini-prep technique from the Qiagen Mini-prep Kit and sent out for sequencing at the University of Chicago DNA Sequencing Facility.

*Yeast Transformation*

The correctly sequenced α-synuclein expression plasmid vectors for each combinatory mutation were then transformed into selected yeast strains for budding and fission yeast models as described in Burke et al., 2000. Yeast cells were selected for by growing them on synthetic-complete media that for budding yeast strains lacked uracil (SC-Ura) and for fission yeast strains lacked thymine. A polymerase chain reaction

(PCR) was performed to confirm the presence of α-synuclein vector by identifying the appropriate band on a 1% agarose gel.

*Yeast Strains*

The two main species utilized were budding and fission yeast. In experiments involving budding yeast, the vector was pYES2.1 and was expressed in BY4741. The individual as well as combinatory mutants were tagged with either GFP or eGFP. In experiments concentrated on fission yeast, the vector was pNMT1 and the two strains were TCP1 and Sph+. In fission yeast models, all mutations were tagged with GFP.

*Yeast Expression*

The repression or expression of the α-synuclein protein in buddying yeast was controlled by the repression or induction of the GAL promoter that was incorporated in the yeast vector. Furthermore, the media lacked the uracil nucleotide indicated by the SC-Ura abbreviation. Thus, SC-Ura Glucose, which serves as the GAL repressor, repressed the production of the mutagenized α-synuclein protein, whereas the SC-Ura Galactose media, which induced the GAL promoter, expressed the protein. Fission yeast cells were grown in Edinburg Minimal Media, and could be repressed or expressed through the addition or lack of thiamine. Therefore, EMM+T media repressed the expression of the protein, and EMM-T expressed the protein.

*GFP Fluorescent Microscopy*

Yeast cells were grown overnight in either 5mL of SC-URA Glucose media for buddying yeast, or EMM+T media for fission yeast. After pelleting the cells at 1500 x g for 5 minutes at 4˚C and two water washes, a density of $2.0x10^7$ cells/mL was transferred from the initially non-expressive media to an expressive media for either organism: SC-Ura Galactose for budding yeast, or EMM-T for fission yeast. At both 24 and 48 hours, 1 mL of cell culture was removed and pelleted at 5000 rpm for one minute for further analysis. 900 µl of supernatant was removed and a sample of 4 µL was taken from the remaining 100 µL. The cells were observed under the Nikon TE2000-U fluorescent microscope under 60X magnification facilitated by the use of oil drops. Metamorph 4.0 software was used to collect and quantify an appropriate amount of cells per trial. For fission yeast models ~750 cells were counted per sample per trial and for budding yeast models ~1000 cells were counted per sample per trial. Overall, five trials were conducted for each sample in every yeast model for both 24 and 48 hours.

*Statistics*

The GFP fluorescent microscopy data was represented as a graph of each sample per yeast strain per specific time period with standard deviation error bars. Chi-square analysis was performed for specific combination of mutants. The phenotype of each cell was classified in accordance to the appropriate criteria for each yeast model. No other statistical analysis was carried out for any other assay.

For budding yeast models each cell's phenotype was classified as one of the following:

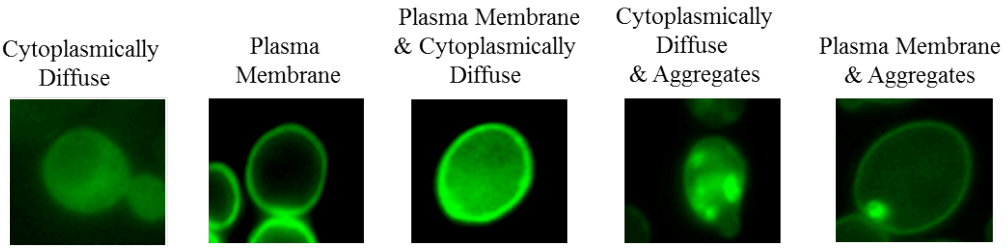


For fission yeast models each cell's phenotype was classified as one of the following:

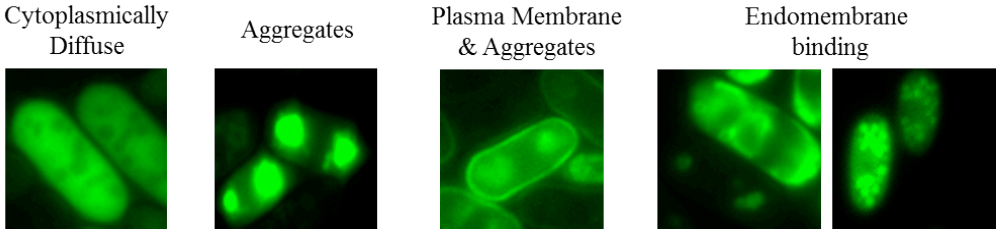


*Spotting Assay*

Yeast cells were cultured in 5 ml SC-Ura Glucose/EMM+T media overnight. To collect cells, yeast cells were pelleted at 1500 x g for 5 minutes at 4°C. Cells were then washed twice with 5 ml of $H_2O$, re-suspended in 10 ml $H_2O$, and counted using a hemocytometer to determine cell density. $2.0x10^6$ cells/ml were removed and pelleted. The supernatant was removed and cells were resuspended in 1 ml of $H_2O$. Cells were then diluted 10-fold (5X) in a 96 well microtitier plate and spotted onto repressing media, SC-Ura Glucose/ EMM+T, and inducing media growth plates, SC-Ura Galactose/ EMM-T. Pictures of the plates were taken at 24 and 48 hours through an HP Canoscan scanner using Adobe Photoshop CS3.

*Survival Assay*

Budding yeast cells (with a GFP tag) were grown in 5mL of SC-Ura Glucose overnight at 30°C at 200rpm. Cells were then washed twice with 5 mL of water using centrifugation at 1500 x g for 5 minutes at 4°C each time. Next, the cells were re-suspended in 10 mL of water and counted using a hemocytometer to determine equal cell densities between samples. The flasks containing SC-Ura Galactose were inoculated to a density of $2.0x10^6$ cells/mL. Between 15-18 hours, $1.8x10^6$ cells/mL were removed, washed once with 1 mL of water, then resuspended in 1 mL of water and diluted to 1:1000. 100µl of cells of each sample were spread on a pair of plates: SC-Ura Glucose and SC-Ura Galactose. Measurements were taken 3 days post-plating.

*Western Blot Assay*

Budding and fission yeast cells were first grown overnight in a repressive media, SC-Ura Glucose or EMM+T respectively. The next day, cells were pelleted at 1500 x g for 5 minutes at 4°C, washed twice with water and transferred into expressive media. 24 hours later, the cells indicative of a $2.5x10^7$ cells/mL concentration were washed with 100 mM $NaN_3$ and solubilized in electrophoresis sample buffer (ESB), as described in Burke et al., 2000. ESB consisted of 2% sodium dodecyl sulfate (SDS), 80 mM Tris (pH 6.8), 10% glycerol, 1.5% dithiothreitol, 1 mg/ml bromophenol blue, and a mixture of protease inhibitors and solubilizing agents: 1% Triton-X 100, 1 mM phenylmethylsulfonyl fluoride, 1 mM benzamidine, 1 mM sodium orthovanadate, 0.7 mg/mL pepstatin A, 0.5 mg/mL leupeptin, 10 mg/mL E64, 2mg/mL aprotinin, and 2

mg/mL chymostatin. The attained cell lysates were then electrophoresed at 130 volts on a 10-20% Tris-Glycine gel (acquired form Invitrogen) using 1 x SDS running buffer, and the SeeBlue ladder (acquired form Invitrogen) as the standard molecular ladder.

After running the SDS gels, they were equilibrated in 1x SDS transfer buffer and transferred to Polyvinylidene fluoride (PVDF) membranes using the semi-dry transfer method. α-Synuclein was detected using a mouse monoclonal anti-V5 (acquired form Invitrogen) followed by an anti-mouse secondary antibody. The anti-phosphoglycerokinase (PGK) antibody (acquired form Molecular probes) was used as a loading control for budding yeast, whereas anti-beta-actin (acquired from Abcam) was utilized for fission yeast. The last step, used to visualize the protein, was washing the membrane with a solution consisting of NBT (nitro-blue tetrazolium chloride), BCIP (5-bromo-4-chloro-3'-indolyphosphate p-toluidine salt), and alkaline phosphatase buffer. In order to ensure the interpretation of the proper protein, the SeeBlue® Plus2 Pre-Stained Standard was employed.

In the end, due to a series of unsuccessful Western blot developments, the WesternBreeze Chromogenic Kit-Anti-Mouse (from Invitrogen) was ordered and the membranes were developed according to the kit's protocol. The antibodies remained the same, but they were diluted with the kit's solutions and in accordance to the guidelines.

***STUDY TWO:***

*Primer Design*

In order to create α-synuclein-126, -112 and -98 splice variants flanking primers were designed. According to the protocol for PCR splicing devised by Dr. Alexei Gratchevs, the two flanking complimentary primers should comprise a region of -15 base pairs to +15 base pairs around the intended area of deletion. For α-synuclein-126 the area that needed deletion was from 41-54 amino acids, α-synuclein-112 needed a deletion in the range of 103-130 amino acids, and α-synuclein-98 needed a double deletion in both of these regions. Therefore, the following primers were designed:

To ensure the proper functionality of each primer I calculated the proper size for each segment necessary for the formation of α-synuclein-126 and -112 splice variants. Additionally, two controls would be utilized to test the primers necessary to read the full length of the protein. The following table represents the calculated segment sized according to the number of amino acids (aa) and base pairs (bp):

*PCR Design*

The following PCR program was devised in the DebBurman lab in order to optimize the quality of products obtained from PCR splicing:

Step 1-Heat up to 98 ˚C - 1 minute
Step2-Heat up to 72 ˚C - 1 minute
Step 3-Heat up to 54˚C - 2 minutes
Repeat the cycle 36 times
Step 4-Heat up to 72 ˚C - 10 minutes
Step 5-Hold at 4 ˚C - indefinitely

*Table 1. α-Synuclein splice variant primer design.* The following primers were designed in order to truncate the appropriate regions of the α-synuclein protein to create splice variants. Primers 3 and 4 were designed to delete the region for α-synuclein-126, while primer 5 and 6 were designed to delete the region for α-synuclein-112. FP stands for forward primer and RP stands for reverse primer.

| **DESIGNED PRIMER** | **SEQUENCE** |
|---|---|
| Primer 3 (α-syn-126 RP) | 5'-GGT CTT CTC AGC CAC TAC ATA GAG AAC ACC-3' |
| Primer 4 (α-syn-126 FP) | 5'-GGT GTT CTC TAT GTA GTG GCT GAG AAG ACC-3' |
| Primer 5 (α-syn-112 RP) | 5'-GTC TTG ATA CCC TTC CTT GCC CAA CTG GTC-3' |
| Primer 6 (α-syn-112 FP) | 5'-GAC CAG TTG GGC AAG GAA GGG TAT CAA GAC-3' |

*Table 2. Splice variant segment sizes.* Above are indicated sizes for each of the segments. A and B indicates the first and second segments that ought to be fused to attain α-synuclein-126, while segments C and D indicate the two parts that would be fused to create α-synuclein-112. For control 1 and 2, the full-length protein was amplified during PCR using primer 2 (starts at the beginning of α-synuclein and moves forward), primer 1 (reads the sequence starting from the promoted and moves forward) and primer 7 (reads the sequence starting from the eGFP tag and moves backward).

| Segment | Forward Primer | Reverse Primer | Size (aa) | Size (bp) |
|---|---|---|---|---|
| A (part of α-syn-126) | Primer 2 | Primer 3 | 40 | 120 |
| B (part of α-syn-126) | Primer 4 | Primer 7 | 324 | 972 |
| C (part of α-syn-112) | Primer 2 | Primer 5 | 102 | 306 |
| D (part of α-syn-112) | Primer 6 | Primer 7 | 249 | 747 |
| Control 1 | Primer 2 | Primer 7 | 379 | 1137 |
| Control 2 | Primer 1 | Primer 7 | 450 | 1349 |

*DNA Band Purification*

The Geneclean Turbo Kit was utilized (from MP Bio) to purify the DNA product acquired from the PCR product for splice variants that was ran in the form of a band on an ethidium bromide 1 % agarose gel. All steps were followed in accordance with the provided manual.

*TOPO Cloning*

In order to input the truncated isoform into the pYES2.1 vector, the TOPO TA Expression Kit from Invitrogen was used. All steps were followed from the provided manual.

*Table 3. List of α-synuclein constructs.*

| α-Synuclein Construct | Vector | Yeast Strain | Chapter |
|---|---|---|---|
| LOW EXPRESSION BUDDING YEAST MODEL | | | |
| No cDNA (Parent Plasmid) | pYES2.1 | BY4741 | 1 |
| GFP | pYES2.1 | BY4741 | 1 |
| WT-GFP | pYES2.1 | BY4741 | 1 |
| A30P-GFP | pYES2.1 | BY4741 | 1 |
| E46K-GFP | pYES2.1 | BY4741 | 1 |
| A53T-GFP | pYES2.1 | BY4741 | 1 |
| A30P-A53T-GFP | pYES2.1 | BY4741 | 1 |
| A30P-E46K-GFP | pYES2.1 | BY4741 | 1 |
| E46K-A53T-GFP | pYES2.1 | BY4741 | 1 |
| A30P-E46K-A53T-GFP | pYES2.1 | BY4741 | 1 |
| HIGH EXPRESSION FISSION YEAST MODELS | | | |
| No cDNA (Parent Plasmid) | pNMT1 | TCP1, Sph+ | 1 |
| GFP | pNMT1 | TCP1, Sph+ | 1 |
| WT-GFP | pNMT1 | TCP1, Sph+ | 1 |
| A30P-GFP | pNMT1 | TCP1, Sph+ | 1 |
| E46K-GFP | pNMT1 | TCP1, Sph+ | 1 |
| A53T-GFP | pNMT1 | TCP1, Sph+ | 1 |
| A30P-A53T-GFP | pNMT1 | TCP1, Sph+ | 1 |
| A30P-E46K-GFP | pNMT1 | TCP1, Sph+ | 1 |
| E46K-A53T-GFP | pNMT1 | TCP1, Sph+ | 1 |
| A30P-E46K-A53T-GFP | pNMT1 | TCP1, Sph+ | 1 |
| HIGH EXPRESSION BUDDING YEAST MODEL | | | |
| WT-eGFP | pYES2.1 | BY4741 | 1 |
| A30P-eGFP | pYES2.1 | BY4741 | 1 |
| E46K-eGFP | pYES2.1 | BY4741 | 1 |
| A53T-eGFP | pYES2.1 | BY4741 | 1 |
| A30P-A53T-eGFP | pYES2.1 | BY4741 | 1 |
| A30P-E46K-eGFP | pYES2.1 | BY4741 | 1 |
| E46K-A53T-eGFP | pYES2.1 | BY4741 | 1 |
| A30P-E46K-A53T-eGFP | pYES2.1 | BY4741 | 1 |
| SPLICE VARIANTS | | | |
| 112-eGFP | pYES2.1 | in progress | 2 |
| 126-eGFP | pYES2.1 | in progress | 2 |

# CHAPTER 1

*CHARACTERIZATION*

OF COMBINATORY α-*SYNUCLEIN FAMILIAL MUTANTS IN YEAST*

## RESULTS

### Experimental Design

*Analysis Overview*

To fully acquire an understanding of the properties of the α-synuclein combinatory mutants, I decided to characterize them in several models. First in a budding yeast model using the GFP tag, then in two fission yeast models: TCP1 and Sph+ (data for Sph+ fission yeast model is available in the appendix), and lastly again in the budding yeast model but using the eGFP tag. The reason I chose to employ these models in such a sequence is due to differences in the level of expression and exhibited properties by α-synuclein, which link back to PD pathology. The budding yeast model with GFP tag is a low protein expression model that shows α-synuclein's ability to bind to plasma lipid membranes. The two fission yeast models are high protein expression models that show α-synuclein's ability to form aggregates. The last assessed model, budding yeast with the eGFP tag, serves as a bridge between the two previously stated models because at 24 hours α-synuclein showcases aggregation, but by 48 hours, the protein exhibits lipid plasma membrane localization.

In order to replicate the findings on the characteristics of individual mutants and assess the yet unknown properties of combinatory mutants, I asked three questions: 1) Where does α-synuclein localize within the cell? 2) Is α-synuclein toxic to the cells? 3) Does α-synuclein accumulate? In order to gather answer for these questions, I evaluated protein localization, toxicity, and accumulation.

*Assay Overview*

In order to acquire all of the data suitable to address the aspects of protein localization, toxicity, and accumulation within the cell, I focused on three assays: green fluorescent protein (GFP) live cell microscopy, serial dilution spotting, and Western analysis. The green fluorescent protein (GFP) live cell microscopy allowed for the visualization of the α-synuclein protein within yeast cells. The spotting assay indicated the toxicity of the cells based on the comparison of the rate of cell growth between the control and tested mutations. In the absence of any levels of toxicity in individual mutants (in budding yeast GFP), I reassessed toxicity with a survival assay, which served preliminarily as another toxicity assay that focused on colonies' growth process and size. The Western analysis indicated the protein expression through accumulation levels within the cells.

**Low Expressing Budding Yeast Model (GFP)**

*A30P Phenotypic Dominance*

In this low-level protein expressing model, WT α-synuclein shows membrane lipid localization (Figure 6A, column 1), which is mimicked by two individual familial mutants: A53T and E46K ($\chi^2(2)=1.655$; $p=0.44$) (Figure 6A, columns 2 and 4). The third point mutation, A30P (Figure 6A, column 3), exemplifies cytoplasmic diffusion that is a distinctively different phenotype. Out of the analyzed combinatory mutants, every variant that included A30P (A30P-E46K, A30P-A53T, A30P-E46K-A53T; Figure 6A, columns 5, 7, 8) exhibited a characteristic cytoplasmically diffused protein localization

within cells ($\chi^2(2)=3.698$; $p=0.30$). The only combinatory mutant that showed plasma membrane localization consistent with E46K and A53T was E46K-A53T (Figure 6A, column 6; $\chi^2(2)=0.978$; $p=0.61$). These phenotypes were conserved throughout time course microscopy from 24 to 48 hours in the five conducted trials. Additionally, the frequency of the exhibited characteristic localization was quantified (Figure 6B).

*No Toxicity Due to Combinatory Mutants*

In comparison to three different controls, BY4741 (cells lacking the α-synuclein vector), GFP, and WT, none of the individual mutants (A30P, E46K, and A53T) showed any signs of toxicity (Figure 7A – upper panel). Upon further analysis, combinatory mutants also seemed not to be toxic (Figure 7A – lower panel). The uniform growth on the repressive medium serves as a control that eliminates any factors other than the protein that would affect cell growth on the inductive medium.

*A30P Expression Dominance*

Based on the acquired Western blot, visible in Figure 7B, the levels of protein accumulation were relatively uniform between WT, A30P, and E46K. Out of the three individual mutants, only A53T showed higher α-synuclein protein levels. In combinatory mutant, every variant that included A30P (A30P-E46K, A30P-A53T, A30P-E46K-A53T) showed comparably low protein levels as those in A30P. Only one combinatory mutant, E46K-A53T, showed high protein accumulation, which could be attributed to the observed high protein levels in A53T. Nevertheless, in the presence of A30P, as in the

A30P-E46K-A53T mutant, the A53T's higher protein accumulation levels were no longer exhibited. All of these observations were made possible due to a loading control that showed consistent protein amount for each sample (Figure 7B – lower panel).

*Preliminary Toxicity Reassessment*

Although I did not find any toxicity in the GFP budding yeast model for either the individual or combinatory mutants, I decided to reassess the possible toxicity levels through the survival assay. As showcased in Figure 8A, the production of the α-synuclein protein is induced for a specific amount of time after which the cells are plated on the repressive and inductive media (Figure 8B). Based on this early, yet interesting data, there seems to be a trend with a higher colony count on the repressive media for E46K, A30P-E46K, E46K-A53T, and A30P-E46K-A53T (Figure 8C). Thus, it would appear that, in this case, the presence of E46K dominated the survival rates. Based on colony size comparison, the inductive media led to smaller colonies for all individual and combinatory mutants. As mentioned above, due to the lack of replication of these findings, no conclusions can be made at this point, thus further trials are necessary.

**High Expressing Fission Yeast Models**

The characterization of combinatory mutants were assessed in two fission yeast models: TCP1 and Sph+. Due to similar findings between the two models, I will discuss the data acquired for TCP1 and exemplify representative figures below. The data from Sph+ assays are attached in the appendix (Figures 21-22) and only differences will be

emphasized in the analyses below.

*A30P Phenotypic Dominance*

In the TCP1 strain both A53T and E46K mimic the WT phenotype by showing aggregation within the cells ($\chi^2(2)=1.995$; $p=0.37$; Figure 9A, columns 1, 2 and 4). Similarly to the low expressing yeast model, A30P's phenotype is cytoplasmically diffused protein localization (Figure 9A, column 2). In Sph+, predominately at 24 hours, WT and E46K show a serpentine-like pattern of endomembrane binding in addition to the formation of aggregates (Appendix: Figure 21A, columns 1 and 4). By 48 hours, however, that dynamic seems to change and more aggregates are visualized in the cells (Appendix: Figure 21B). During the examination of combinatory mutants, A30P again dominated the phenotype, resulting in cytoplasmic diffusion exhibited by A30P-E46K, A30P-A53T, and A30P-E46K-A53T in both models (Figure 9A, Appendix: Figure 21A; columns 5, 7 and 8). E46K-A53T exhibited the phenotype of A53T and/or E46K at both 24 and 48 hours (Figure 9A, Appendix: Figure 21A; column 6). Thus, just as in the low expression model, A30P dominated the phenotype for combinatory mutants.

*No Toxicity Enhancement Caused by Combinatory Mutants*

Unlike the budding yeast model, both fission yeast models reveal individual α-synuclein familial mutant toxicity patterns. In TCP1, A53T is the most toxic followed by slightly toxic E46K and nearly non-toxic A30P, all in comparison to the PNMT1 strain control (Figure 10A). That pattern was maintained in Sph+, although the severity

of the toxicity of A53T and E46K was smaller compared to the control (Appendix: Figure 22A). In terms of toxicity patterns for combinatory mutants, only E46K-A53T showed to be slightly toxic, but less toxic that the individual mutants themselves. In fact, once again, any combination variant including A30P exhibited no toxicity levels (Figure 10A, Appendix: Figure 22A). The analysis was based on 5 trials per each strain in terms of phenotypic determination and its quantification.

*Expression Assay Inconclusive*

The Western blot interpretation for both fission yeast models was unsuccessful due to varied protein loading levels and membrane development issues. The tested sample included WT, individual mutants, and combinatory mutants. Included in Figures 10B and in 22B (available in the appendix) are representative blots indicative of my attempts at testing protein accumulation levels in this model.

**High Expressing Budding Yeast Model (eGFP)**

*A30P Phenotypic Dominance*

The high and low level protein expressing budding yeast models vary solely in the type of tag attached to the α-synuclein protein that helps in its visualization. In this model the eGFP tag enhances the expression of α-synuclein, allowing for the exemplification of the protein's characteristics in a time-dependent manner. At 24 hours, WT α-synuclein shows its ability to form aggregates, while at 48 hours the only visible phenotype is plasma membrane localization (Figure 11A, column 1). A30P shows strong

diffusion throughout the cell at both examination periods (Figure 11A, column 3), while A53T and E46K show similar pattern to WT ($\chi^2(4)=4.566$; p=.33) (Figure 11A, columns 2 and 4). Upon examination of the combinatory mutants, A30P dominated the phenotype at 24 and 48 hours within A30P-E46K, A30P-E46K, and A30P-E46K-A53T (Figure 11A, columns 5, 7 and 8). The only combinatory mutant that mimicked the phenotype of A53T and/or E46K was E46K-A53T ($\chi^2(4)=5.746$; p=0.22) (Figure 11A, column 6). These phenotypes were observed in five separate trials and quantified (Figure 11B).

*No Toxicity Enhancement Caused by Combinatory Mutants*

In comparison to the other high protein level expressing models, in this model there were no signs of strong toxicity patterns. Individually, A53T appears to be slightly toxic in relation to all of the controls, yet never as toxic as in fission yeast. Furthermore, the combinatory mutants did not enhance the individual mutants' toxicity. It fact, they appeared not be toxic at all, which was more consistent with the GFP budding yeast finding.

*Expression Assay Inconclusive*

To determine α-synuclein expression, I performed a Western blot analysis of WT alongside the individual and combinatory mutants. Unfortunately, as in fission yeast, the protein expression cannot be interpreted due to the unequal protein loading levels and poor development of the membrane. Included in Figure 12B is a representative blot of my attempts at testing protein expression levels in this model.

**A. LOCALIZATION**

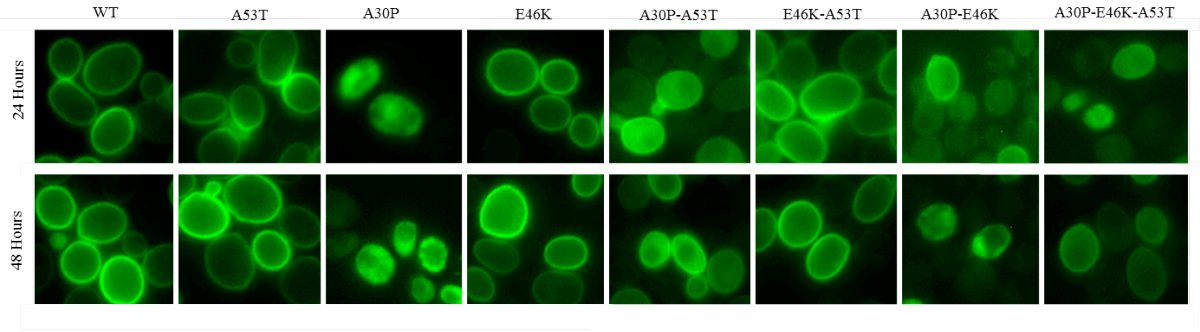


**B. QUANTIFICATION**

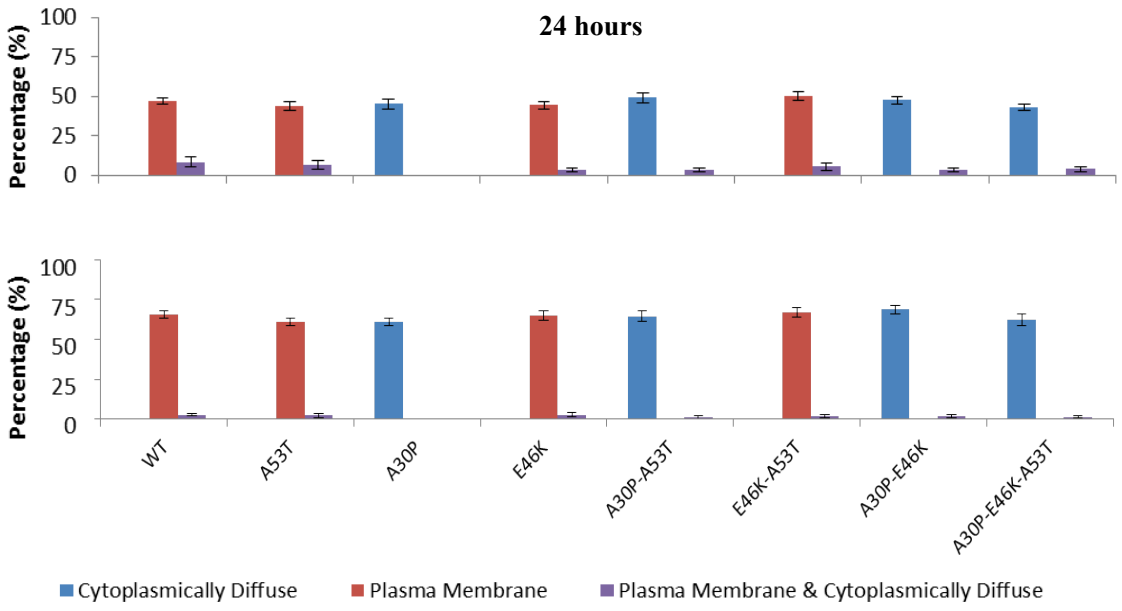


*Figure 6. Protein localization in a low expressing yeast model.*

A. Time course fluorescent microscopy. The following mutations of α-synuclein were evaluated in comparison to its WT localization: A53T, A30P, E46K, A30P-A53T, E46K-A53T, E46K-A30P, and E46K-A30P-A53T. Microscopy photographs were captured at 24 and 48 hours post induction with SC-Ura Galactose (n=5).

B. Time course quantification. WT, A53T, A30P, E46K, A30P-A53T, A53T-E46K, E46K-A30P, and E46K-A30P-A53T were quantified for photographs captured at 24 and 48 hours post induction with SC-Ura Galactose (n=5). The error bars represent standard deviation based on the averaged results.

**A. TOXICITY**

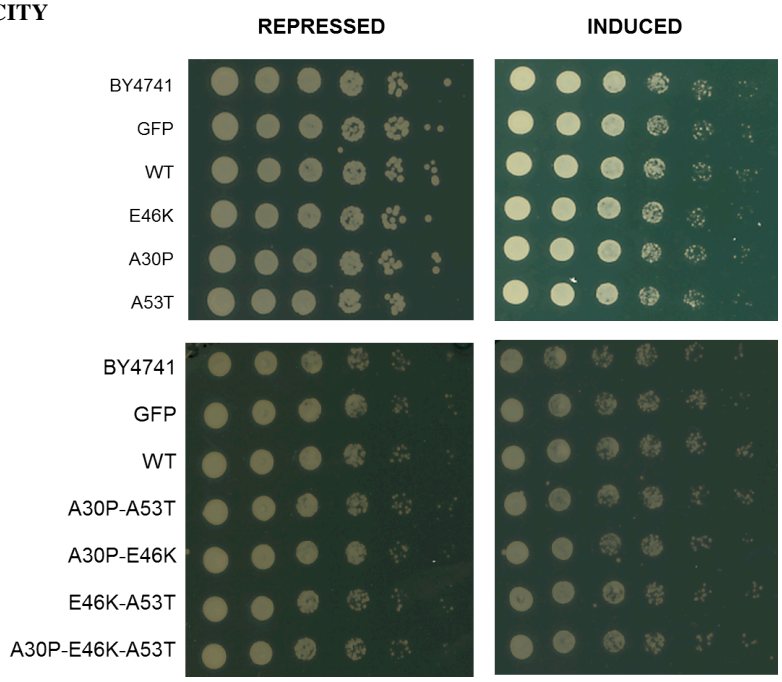


**B. EXPRESSION**

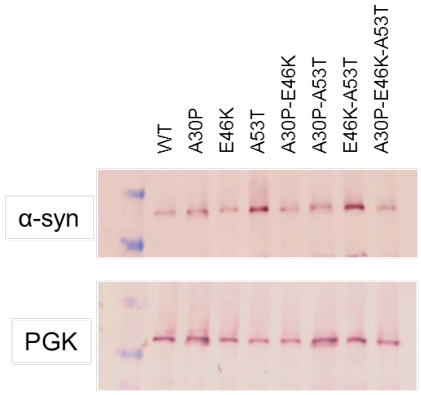


*Figure 7.Toxicity and protein expression in a low expressing yeast model.*

A. Spotting. Yeast expressing BY4741, GFP, WT, A30P, A53T, E46K, A30P-A53T, E46K-A30P, E46K-A53T and E46K-A30P-A53T α-synuclein spotted onto repressive media (SC-Ura Glucose) and inductive media (SC-Ura Galactose) after five-fold serial dilutions (n=5).

B. Expression. Western Blot at 48 hours of WT, A30P, E46K, A53T, A30P-E46K, A30P-A53T, E46K-A53T, and E46K-A30P-A53T expression (anti-V5) with the loading control below (PGK) (n=3).

**A. EXPERIMENTAL DESIGN**

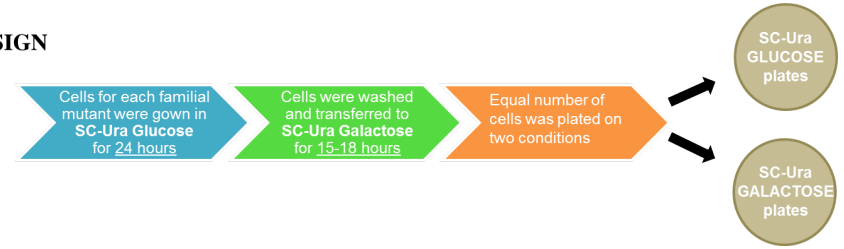


**B. SURVIVAL ASSAY**

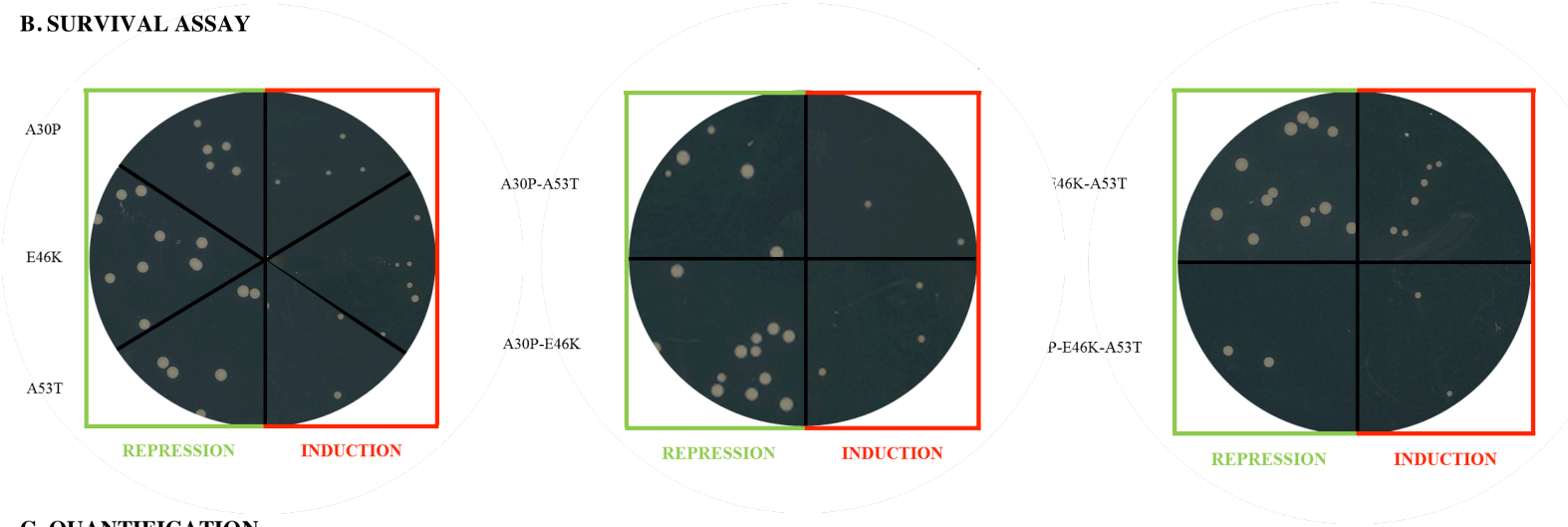


**C. QUANTIFICATION**

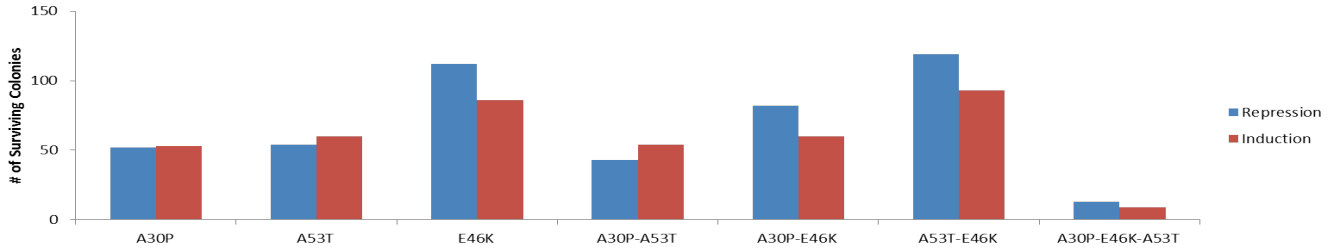

*Figure 8.Survival assessment in a low expressing yeast model.*

A. Experimental design. The cells were grown in SC-Ura Glucose for 24 hours. Next the cells were washed and transferred to SC-Ura Galactose. After 15-18 hours, an equal number of cells was counted and plated on SC-Ura Glucose and SC-Ura Galactose plated. The colonies were allowed to grow for 3 days.

B. Survival assay. Representative images of grown and quantified colonies were taken 3 days post experiment. The left circle represents the survival of individual mutants (controls), A30P, E46K, and A53T. The middle and right circles represent the survival of colonies in combinatory mutants: A30P-A53T, A30P-E46K and A53T-E46K, E46K-A30P-A53T, respectively. In each circle the left panel represents repression (SC-Ura Glucose), marked in green, and the right panel represents induction (SC-Ura Galactose), marked in red (n=1).

C. Time course quantification. The number of colonies grown for A30P, A53T, E46K, A30P-A53T, A30P-E46K, A53T-E46K, and E46K-A30P-A53T were counted at 3 days post experiment (n=1).

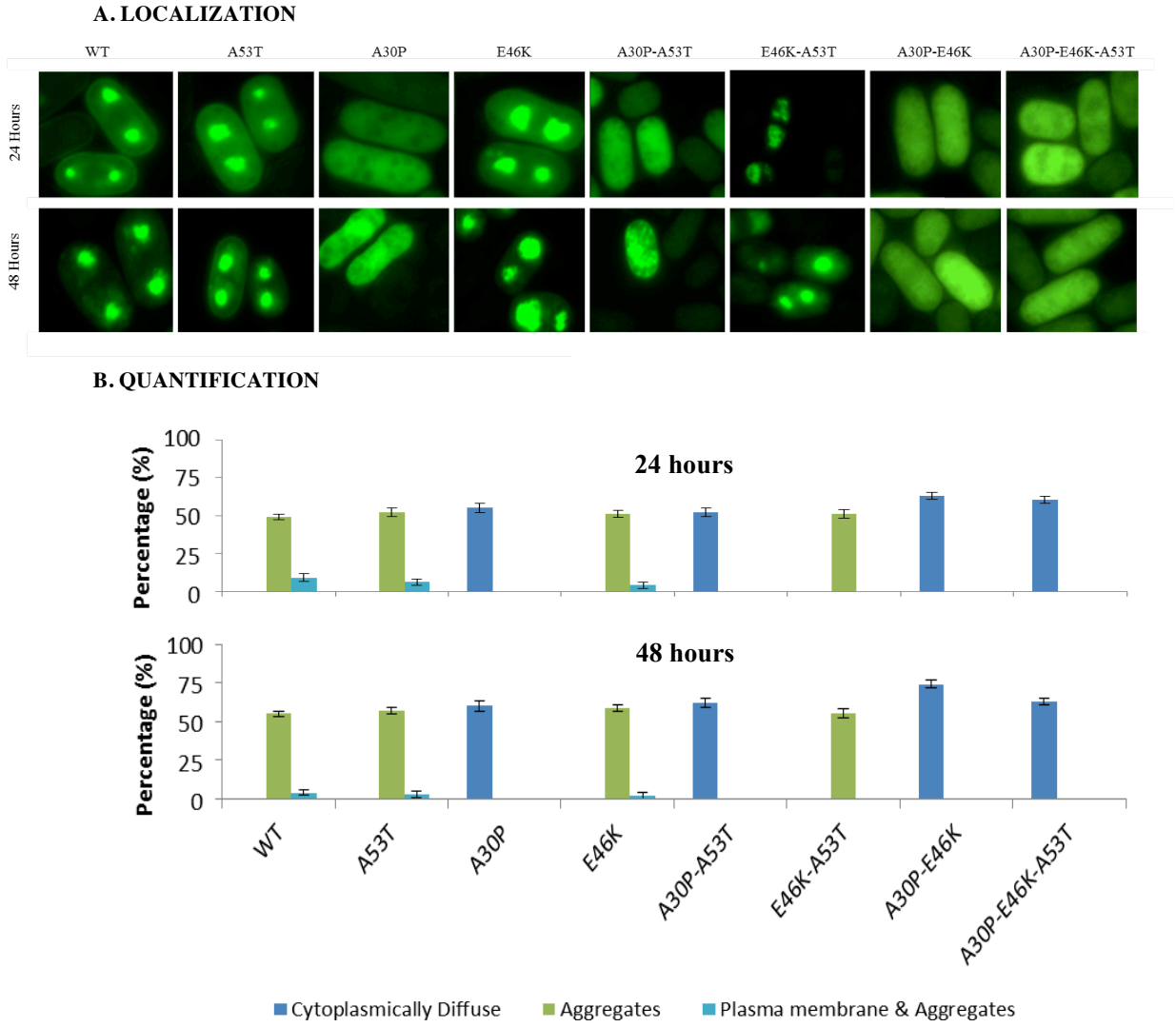


*Figure 9. Protein localization in a high expressing fission yeast model.*

A. Time course fluorescent microscopy. The following mutations of α-synuclein were evaluated in comparison to its WT localization: A53T, A30P, E46K, A30P-A53T, E46K-A53T, A30P-E46K, and A30P-E46K-A53T. The mutants were expressed in the TCP1 strain of fission yeast. Microscopy photographs were captured at 24 and 48 hours post induction with EMM-T (n=5).

B. Time course quantification. WT, A53T, A30P, E46K, A30P-A53T, E46K-A53T, A30P-E46K, and A30P-E46K-A53T were quantified for photographs captured at 24 and 48 hours post induction with EMM-T (n=5). The error bars represent standard deviation based on the averaged results.

**A. TOXICITY**

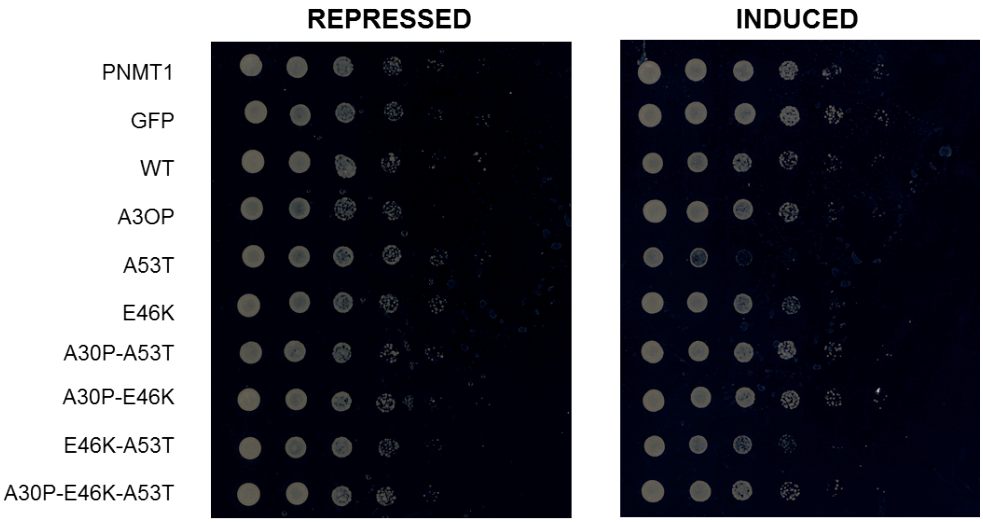


**B. EXPRESSION**

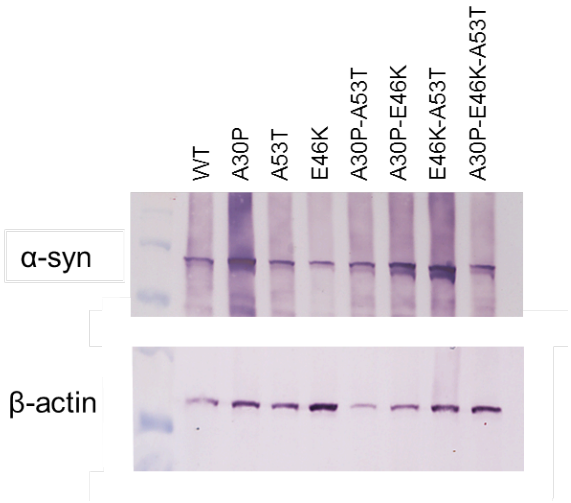


*Figure 10. Toxicity and protein accumulation in a high expressing fission yeast model.*

A. Spotting. Yeast expressing PNMT1, GFP, WT, A30P, A53T, E46K, A30P-A53T, E46K-A30P, E46K-A53T and E46K-A30P-A53T α-synuclein spotted onto repressive media (EMM+T) and inductive media (EMM-T) after five-fold serial dilutions (n=5).

B. Expression. Western Blot at 48 hours of WT, A30P, E46K, A53T, A30P-E46K, A30P-A53T, E46K-A53T, and E46K-A30P-A53T expression (anti-V5) with the loading control below (β-actin) (n=4).

**A. LOCALIZATION**

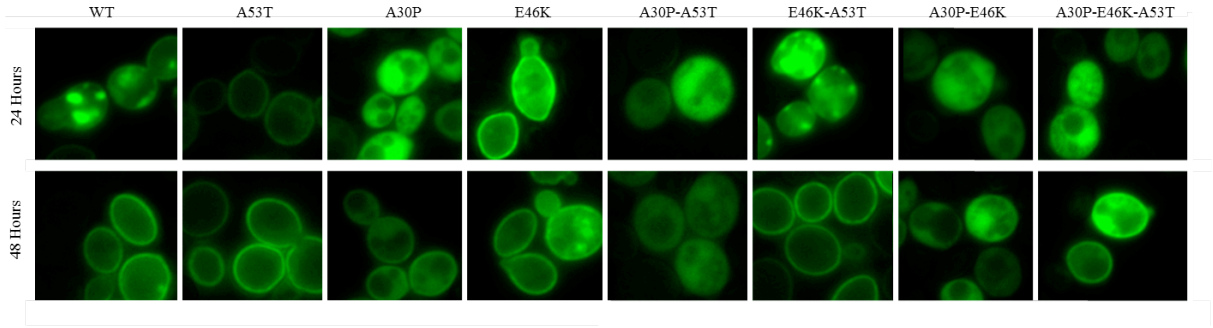


**B. QUANTIFICATION**

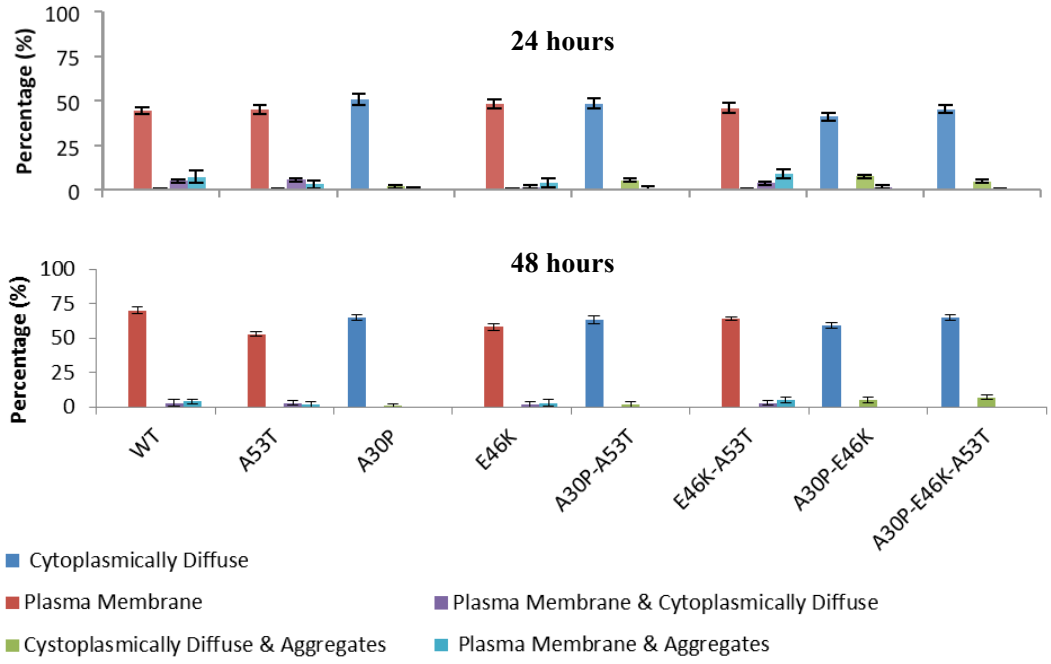


*Figure 11. Protein localization in a high expressing budding yeast model.*

A. Time course fluorescent microscopy. The following mutations of α-synuclein were evaluated in comparison to its WT localization: A53T, A30P, E46K, A30P-A53T, E46K-A53T, A30P-E46K, and A30P-E46K-A53T. Microscopy photographs were captured at 24 and 48 hours post induction with SC-Ura Galactose (n=5).

B. Time course quantification. WT, A53T, A30P, E46K, A30P-A53T, E46K-A53T, A30P-E46K, and A30P-E46K-A53T were quantified for photographs captured at 24 and 48 hours post induction with SC-Ura Galactose (n=5). The error bars represent standard deviation based on the averaged results.

**A. TOXICITY**

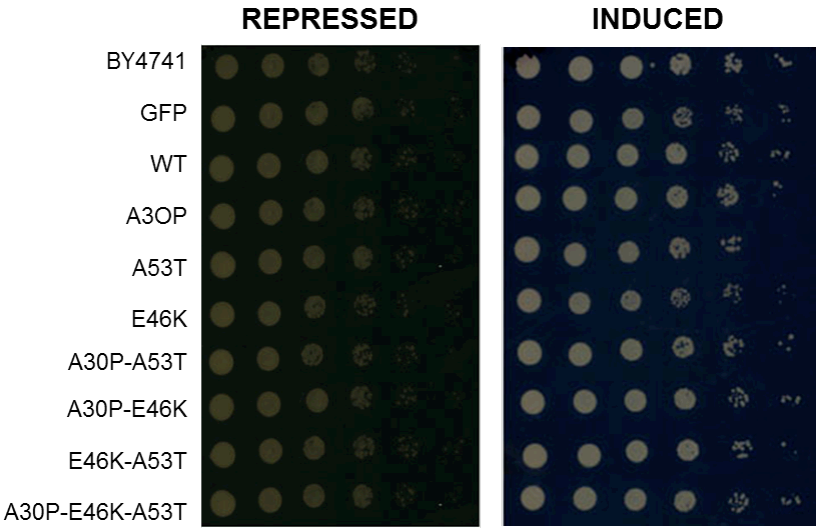


**B. EXPRESSION**

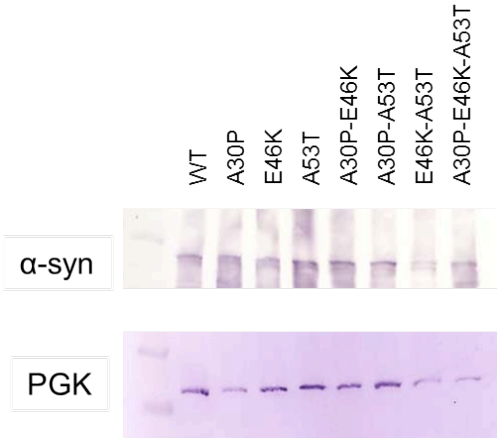


*Figure 12. Toxicity and protein accumulation in a high expressing budding yeast model.*

A. Spotting. Yeast expressing BY4741, GFP, WT, A30P, A53T, E46K, A30P-A53T, E46K-A30P, E46K-A53T and E46K-A30P-A53T α-synuclein spotted onto repressive media (SC-Ura Glucose) and inductive media (SC-Ura Galactose) after five-fold serial dilutions (n=5).

B. Expression. Western Blot at 48 hours of WT, A30P, E46K, A53T, A30P-E46K, A30P-A53T, E46K-A53T, and E46K-A30P-A53T expression (anti-GFP) with the loading control below (PGK) (n=1).

**DISCUSSION:**

The onset of any neurodegenerative disease can be attributed to sporadic factors, familial factors, or a combination of both. In Parkinson's disease, 10% of all cases can be solely linked to an inheritance of a genetic mutation in one of several PD associated genes. In the α-synuclein protein, coded by the SNCA gene, three single-point mutations account for a portion of familial PD cases and are identified as: A53T, A30P, and E46K (Polymeropoulos et al., 1998; Kruger et al., 1998; Zarrans et al., 2004). While each of these mutations have been individually characterized and studied in various model organisms, only a small amount of research has been conducted on any combinatorial mutations within the α-synuclein protein. Aside from the characterization of the A30P-A53T mutation in *in vitro* (Jo et al., 2002), budding yeast (Sharma et al., 2006), fission yeast (Brandis et al., 2006), transgenic mice (Ikeda et al., 2008), mouse lines (Prasad et al., 2011) or rats (Lelan et al., 2011), no other combinatory mutant has been assessed. Insight into the dynamics of interactions between α-synuclein's familial mutants in combinatory variants could provide important clues about the significance of each amino acid's location, switch, and impact on final protein conformation. Furthermore, combinatory variants would further characterize the properties of α-synuclein protein.

Thus, the first goal of my thesis was to create α-synuclein familial combinatory mutations and characterize them in terms of protein localization, toxicity and expression. To complete my analysis I utilized four models: 1) a low-expression yeast model that exemplified α-synuclein's ability for plasma lipid membrane binding; 2) two high-expression yeast models that exemplified α-synuclein's aggregation; 3) a high expression

model where both characteristics were exhibited in a time-dependent manner. My three findings were: 1) A30P dominated the phenotype, 2) Combinatory mutants did not enhance toxicity, and 3) A30P suppressed protein expression.

**Cumulative Data Reveal Unexpected A30P dominance**

In my thesis, the four created combinatory mutants, A30P-A53T, A30P-E46K, E46K-A53T, A30P-E46K-A53T, were assessed on protein localization (through fluorescent microscopy), toxicity (through the spotting assay), and expression (through Western blot analysis). Based on the data derived from assays completed in the four models, the characteristics of A30P mutation dominated within the combinatory variants in terms of exhibited phenotype, suppressed toxicity, and lower protein accumulation, (indicative of lower protein expression).

*A30P Phenotypic Dominance*

My hypothesis of phenotypic expression based on a combination of individual mutant localization patterns was not fully supported due to A30P phenotypic dominance in combinatory variants. A30P dominance can be concluded because of mimicked exhibition of its individual characteristics in combination variants. Based on *in vitro* studies of independent A30P expression, the mutant shows disorder in dilute solutions and the formation of small spherical species (Conway et al., 1998), which may lead to further aggregation in a concentration and time-dependent manner (Giasson et al., 1998). In both budding and fission yeast models, the A30P phenotype is characterized as cytoplasmic diffusion of the protein throughout the cell (Sharma et al., 2006; Brandis et

al., 2006). The hindered ability of A30P to bind to plasma membranes is also exhibited in transgenic models. However, its overexpression can lead to abnormal cellular accumulation (Kahale et al., 2000).

Based on first analysis of A30P-A53T *in vivo*, Jo et al. (2002) noted that, compared to WT, the double mutant showed an almost identical inability to bind lipids and a decreased α-helicity just like that of A30P. In previous fission and budding yeast studies, A30P-A53T showed predominately cytoplasmic diffusion throughout the cell that was conserved across time (Sharma et al., 2006; Brandis et al., 2006).

In my thesis, I was able to replicate such findings and exemplify the A30P-A53T phenotype of cytoplasmic protein diffusion in all four models. Additionally, one of my high-expression yeast models (budding yeast with eGFP) showed a small amount of visible aggregation of the protein at 24 hours, which could be representative of previous *in vitro* and mouse studies of abnormal cellular accumulation in regard to A30P overexpression (Giasson et al., 1998; Kahale et al., 2000). The appearance of these foci was also noted in the low expression model at 24 hours as a minor phenotype in Sharma et al. (2006), but was not replicated in my low expression model. The feature of protein aggregation due to A30P-A53T was also noted in transgenic mice (Lelan et al., 2011).

The A30P dominance noted in my thesis research was further exemplified in the phenotypes of two other combinatory mutants, A30P-E46K and A30P-E46K-A53T. Due to the lack of any previous characterization of these mutations (A30P-E46K and A30P-E46K-A53T), my findings offer neither a replication nor an opposition. However, they can serve as further support for the dominance of A30P. Furthermore, by utilizing both

budding and fission models, my findings further strengthen the A30P dominance in its inability to bind plasma membrane and form aggregates (Jo et al., 2002; Brandis et al., 2006). While E46K and A53T have been vastly characterized in different models, the E46K-A53T mutant was never previously assessed. Both E46K and A53T show plasma membrane association *in vivo* (Fredenburg et al. 2007; Conoway et al., 1998; Giasson et al., 1998) and in the budding yeast model (Sharma et al., 2006), but they show aggregation in the fission yeast model (Brandis et al., 2006). In my low-expression model, the E46K-A53T shows plasma membrane localization, whereas in both of my fission yeast models, the double mutant shows formation of aggregates. In my high-expression budding yeast model, the double mutant exhibits some signs of aggregation at 24 hours in addition to predominant plasma membrane localization at both 24 and 48 hours. Such a phenotype could be interpreted as a blend of individual mutant phenotypes and thus serves as the only support for my hypothesis. Nevertheless, it should be noted that there is a possibility that either A53T or E46K could be dominating the observed phenotype. While that distinction was not possible to assess by observational means, further quantification using statistical analysis and the chi-square value revealed no difference between the phenotypic patterns of A53T, E46K, and A53T-E46K.

*A30P Toxicity Suppression*

With regard to toxicity patterns, I hypothesized that the combinatory mutants would enhance the individual mutant's toxicity in all of my studied models. In the end, my hypothesis was refuted in each model because none of the combinatory mutants

enhanced individual mutant toxicity. This lack of enhanced toxicity can be supported by previous toxicity assessment of A30P-A53T in fission yeast (Brandis et al., 2006), but it is novel for all other combinatory mutants. Furthermore, my data further strengthens the dominance of A30P because in both fission yeast models utilized, the presence of A30P in combination mutants suppressed the toxicity exhibited by A53T and E46K independently (clearly evident in the triple mutant). The lack of toxicity due to the A30P-A53T mutant can be further supported by transgenic mouse model studies, in which the double mutant showed an inducement of formation of new dopaminergic neurons as opposed to killing them (Lelan et al., 2011).

*A30P Expression Suppression*

My assessment of protein expression was hindered by complications with Western blot development in three of the four utilized models. Nevertheless, the data acquired from the low expression model refuted my hypothesis and did not support the notion of higher protein expression in all combinatory mutations. In fact, only E46K-A53T showed high protein accumulation, however A53T independently showed heightened levels of protein expression, which were comparable to those of combinatory mutant. Therefore, the double mutant did not enhance the individually noted expression patterns. On the other hand, what can be concluded is that A30P suppressed protein expression because the A30P-A53T mutant showed much lower protein expression than A53T. This finding is supported by previous Western analysis of A30P-A53T in budding and fission yeast (Sharma et al., 2006; Brandis et al., 2006).

**Structural Insight into A30P Dominance**

The significance of protein conformation lies within the notion that structure determines function. Therefore, due to a previously established A30P dominance within the combinatory mutants based on exhibited characteristic in protein localization, toxicity, and expression, one should take into consideration structural influences induced by A30P. Three of the combinatory mutants I created have never been analyzed before, thus I cannot provide any support for the broad A30P dominance in structural composition from the literature, but I will provide simulated data from computer generated programs. In addition, I will also discuss the significance of the amino acid switch.

*Structural Simulation Analysis*

One of the structural characteristics of a protein that influences its function is the rate at which a protein folds, because that, in turn, will indicate its susceptibility to form fibers or aggregates. By definition, the protein folding rate indicates how fast or slow the folding, from an unfolded state to a 3-D structure, will occur. The data for this assessment are visible in the first row in Table 4 (Gromiha, 2003, courtesy of http://psfs.cbrc.jp/fold-rate). Note that the three combinatory mutants that include A30P showcase the slowest folding rate (Table 4). In *in vitro* studies, A30P showed the slowest rate of fibrillation, thus the association between slow protein folding and further low fibrillation for such combinatory mutants can be assumed.

Another measurement that can be utilized is center of mass (COM), which is an

*Table 4. Simulated structural characteristics of α-synuclein's mutants.*

| **Property** | **WT** | **A30P** | **E46K** | **A53T** | **E46K-A53T** | **A30P-E46K** | **A30P-A53T** | **A30P-E46K-A53T** |
|---|---|---|---|---|---|---|---|---|
| Foling rate (folds/second) | 10.6/sec | 9.55/sec | 9.27/sec | 11.5/sec | 10.1/sec | 9.04/sec | 9.53/sec | 7.49/sec |
| X-coordinate of COM | 233.208 | 233.220 | 233.208 | 233.216 | 233.208 | 233.213 | 233.229 | 233.221 |
| Y-coordinate of COM | 29.798 | 29.880 | 29.772 | 29.902 | 29.757 | 29.735 | 29.983 | 29.839 |
| Z-coordinate of COM | -15.252 | -15.226 | -15.250 | -15.278 | -15.247 | -15.195 | -15.251 | -15.221 |
| **Z-score** | | | | | | | | |
| Cβ interaction energy | -2.06 | -1.88 | -2.12 | -2.03 | -2.03 | -1.88 | -1.84 | -1.85 |
| All-atom pairwise energy | 0.84 | 0.88 | 0.58 | 0.84 | 0.83 | 0.87 | 0.88 | 0.87 |
| Solvation energy | -3.26 | -3.22 | -3.27 | -3.23 | -3.26 | -3.25 | -3.17 | -3.2 |
| Torsion energy | -3.44 | -3.54 | -3.46 | -3.51 | -3.54 | -3.57 | -3.62 | -3.64 |
| QMEAN4 score | -3.77 | -3.84 | -3.89 | -3.83 | -3.86 | -3.88 | -3.90 | -3.93 |
| **Raw score** | | | | | | | | |
| Cβ interaction energy | -5.04 | -5.90 | -4.78 | -5.20 | -5.18 | -5.88 | -6.07 | -6.05 |
| All-atom pairwise energy | -687.80 | -697.68 | -648.93 | -690.94 | -689.15 | -695.66 | -700.47 | -698.71 |
| Solvation energy | 7.38 | 7.09 | 7.45 | 7.19 | 7.37 | 7.28 | 6.80 | 6.98 |
| Torsion energy | 2.83 | 4.11 | 3.11 | 3.76 | 4.04 | 4.40 | 5.05 | 5.33 |
| QMEAN4 score | 0.452 | 0.445 | 0.440 | 0.446 | 0.443 | 0.441 | 0.440 | 0.437 |

*Table 4. Simulated structural characteristics of α-synuclein's mutants.* The first property is the folding rate of the protein (Gromiha, 2003, courtesy of http://psfs.cbrc.jp/fold-rate) followed by three coordinates specifying the protein's center of mass (COM) (courtesy of Gert Vriend and http://swift.cmbi.ru.nl/servers/html/index.html). The second part of the table provides the Z-scores for five other properties: Cβ interaction energy, All-atom pairwise energy, Solvation energy, Torsion energy and the QMEAN4 score, while the last part of the table provides the raw scores for the same properties (courtesy of the SWISS-MODEL, swissmodel.expasy.org, (Schwede et al., 2011) and QMEAN (Benkert et al., 2011)). C-beta atoms and all-atom potentials are two measures of distance-dependent interaction potentials that assess long-range interaction. The residue-level implementation is indicated by Cβ interaction energy measure, while the all-atom potential indicates secondary structure specific interaction potential. The solvation energy indicates the burial status of the residues. The torsion energy measure analyzes the local geometry over three consecutive amino acids. The QMEAN4 is a reliability score of the whole model. Z-scores relay the quality estimates to scores obtained from high-resolution reference structures solved experimentally by X-ray crystallography, in this case the native α-synuclein.

artificial point used for detecting important and simple features of proteins structure, shape, and association (Namdeo et al., 2011). COM thus reflects the behavior of the whole system and can be used to predict protein tertiary models or assess the global shape of protein in protein-protein complexes (Namdeo et al., 2011). The COM measure comprises of the assessment of three axes X, Y, and Z, which were calculated for each mutant and are visible in Table 4. Note that in combinatory mutants whose characteristics were dominated by A30P, the COM coordinates are most closely related to that of A30P. Potentially, three out of the four combinatory mutants resembled A30P properties because they adapted a slow folding rate and closely related COM coordinates (Table 4).

While the problem of protein conformation simulation is still pertinent in biology, a computer generated model available online provides a way to predict possible protein structures based on certain measurements. The Swiss-Model simulates Cβ interaction energies, all-atom pairwise energies, solvation energies, torsion energies and QMEAN4 score based on the provided amino acid sequence (Schwede et al., 2011; Benkert et al., 2011). The acquired data for each of these measurements are shown in Table 4, and it should be noted that the values for A30P-E46K, A30P-A53T, and A30P-E46K-A53T reflect the values of A30P. To make interpretation easier, each measurement was defined in the legend (Table 4).

*Amino Acid Characterization*

Twenty amino acids have been identified that give rise to all of the different proteins utilized by all organisms. To promote diversity, amino acids differ in charge, hydrophobicity, and polarity. The amino acids involved in creation of A30P, A53T, and

E46K have been represented in Table 5. Due to the dominance of A30P on E46K and A53T, I will limit the discussion to A30P. As previously established, the A30P mutant is made by a switch of Alanine to Proline on the 30$^{th}$ amino acid location. Alanine is an L-isomer with the alpha carbon atom bound to a methyl group, thus classifying the amino acid aliphatic (Alberts et al., 2010). Proline, formally not an amino acid, but an animino acid, is a secondary amine because of its connection to two bulky alkyl groups, and it is known to loosen the stability of the protein to bind lipids (Alberts et al., 2010). Neither of the amino acids are charged, and whereas alanine is aliphatic, proline likes to promote turns, which would result in the breaking of α-synuclein's α-helix (Alberts et al., 2010). The result of a switch from an alanine to a proline is ultimately showcased in *in vivo* comparison of A30P to WT, which supports A30P's inability to bind lipid membranes (Conway et al., 1998). This alternation thus results in a characteristic A30P phenotype of diffusion of the protein throughout the cell. This feature is contrary to the natural form of the α-synuclein protein, which is known to present itself in an aggregated form (Spilantini et al., 1998) and in association to phospholipid membranes (Clayton & George, 1998).

**Importance of Designer Mutants**

In reality, the onset of familial PD in human patients due to one of the combinatory mutations is very minimal. However, due to their characterization, a lot of new insight about the α-synuclein protein may be gained, as well as the significance of its amino acid locations and properties in regard to final protein conformation. Progress is not only attained through studying naturally occurring mutations, but, in PD

*Table 5. Amino acid characterization*. This table represents each of the amino acids involved in the familial mutations and their properties in regard to charge, hydrophobicity, polarity and other properties important for protein conformation changes (Alberts et al., 2010).

| **Amino Acid:** | **Charge:** | **Hydrophobicity:** | **Polarity:** | **Other properties:** |
|---|---|---|---|---|
| Alanine (A) | None | Hydrophobic | None | Aliphatic |
| Lysine (K) | Positive | Hydrophilic | Polar | Basic |
| Proline (P) | None | Not hydrophobic | None | Promotes turns |
| Glutamate (E) | Negative | Hydrophilic | Polar | Acidic |
| Threonine (T) | None | Hydrophilic | Polar | |

Especially, knowledge has been gained through various designer mutants. Individual point mutations have been used in order to gather a better understanding of the protein's properties in relation to specific regions. For example, Fiske et al., (2011) assessed contributions of alanine-76 and serine phosphorylation, which gave insight on membrane association and aggregation. Other posttranslational modification mutants for phosphorylation (Fujiwara et al., 2002; Paleologou et al., 2010), nitrosylation (Clayton & George, 1998) or sumoylation (Wilkinson et al., 2003) have contributed to better understanding of PD pathology. Therefore, the majority of research focus should not be on the type of mutation, but rather on the level of insight that it provides.

**The Future of Studying Combinatory Mutants**

To strengthen the characterization of combinatory mutants I could conduct other tests such as loss of induction and optical density curve assessment, and I could replicate the survival assay. The analysis of combinatory mutants has an enormous range of application because their characteristics could be assessed within different pathways implicated in PD onset such as endocytosis or autophagy. Furthermore, the properties of combinatory mutants should be assessed with regard to additional PD associated phosphorylation, nitrosylation, or sumoylation of the α-synuclein protein.

Unexpectedly, in February of 2013, a fourth PD familial mutation was identified as G51D (Kiely et al., 2013). Upon initial analysis, is has shown to exhibit clinical and neuropathological properties resembling those of A53T, such as presence of neuronal grains and threads and severe neuronal loss (Kiely et al., 2013). However, G51D also shows features including dense accumulation of a-synuclein-positive inclusions in the

striatum, and very severe pathology that affects both superficial and deep cortical laminae that ultimately distinguishes G51D from other SNCA mutations (Kiely et al., 2013). Thus, it would be appropriate to create combinatory variants with G51D and determine whether A30P dominance would still be conserved, especially in the quadruple mutant. From a biochemical perspective, the combinatory mutations ought to be crystalized, or at least 3D structures should be constructed in the most representative fashion. These techniques would provide more insight into α-synuclein protein's conformation that would be beneficial to understanding the mechanism behind this protein's shape acquisition.

**Protein Expression Improvement Strategy**

As exhibited in my data set, the Western blot development and analysis was one of the biggest struggles of my thesis. The problem seemed to evolve across many areas from initial lack of visualization of any bands to the ineffectiveness of secondary antibody and unequal loading. After re-making all of the solutions I was still not able to visualize the bands, which is when WesternBreeze was ordered. As a new strategy, I would count the samples three times instead of two to establish uniform cell density and perhaps even confirm it using the machine responsible for determination of optical density of solutions. Additionally, if within the lab's budget, I will develop my Westerns using the WesternBreeze kit in order to perfect my loading skills. Once representative results are acquired, I will go back to self-making lab solutions for Western blot analysis. In the future, if Western development is not problematic, I intend on conducting a loss of induction assay in a time-dependent manner to determine whether the acquired α-synuclein concentration was due to less degradation.

# CHAPTER 2

*CREATION OF α-SYNUCLEIN SPLICE VARIANTS*

## RESULTS

### Experimental Design

In order to understand the properties of the three, newly-discovered α-synuclein natural splice variants (α-synuclein-126, -112, -98), the initial step was to strategize an appropriate series of techniques for protein truncation. Through the literature, I identified the two regions of α-synuclein that needed elimination. For α-synuclein-112 it was the amino acid range of 41-54, and for α-synuclein-126 it was the amino acid range of 103-130 (McLean et al., 2012; Figure 14A). Then I designed appropriate primers for the formation of these splice variants (for primer design details please refer to p.34, for a schematic refer to Figure 14B). I also chose to wait for the correct sequencing of either α-synuclein-112 or -126 in order to use either one as a template for the last splice variant, α-synuclein-98.

The next step was to design a suitable sequence of PCR reactions. As a model method, I adopted Dr. Alexei Gratchev's general protocol for creating a deletion in a protein by PCR splicing (Figure 15). According to his strategy, the pair of designed primers should flank the region intended for the deletion. During the first round of PCR, the outer most primers along with the designer primers would form and help amplify the desired segments. Then, during the second round of PCR, only the outer most primers would then be utilized to fuse the segments and contribute to product amplification. In alignment to Gratchev's design, I predicted that using the first round of PCR my designed primers would yield four segments called A, B, C, and D (Figure 14B).

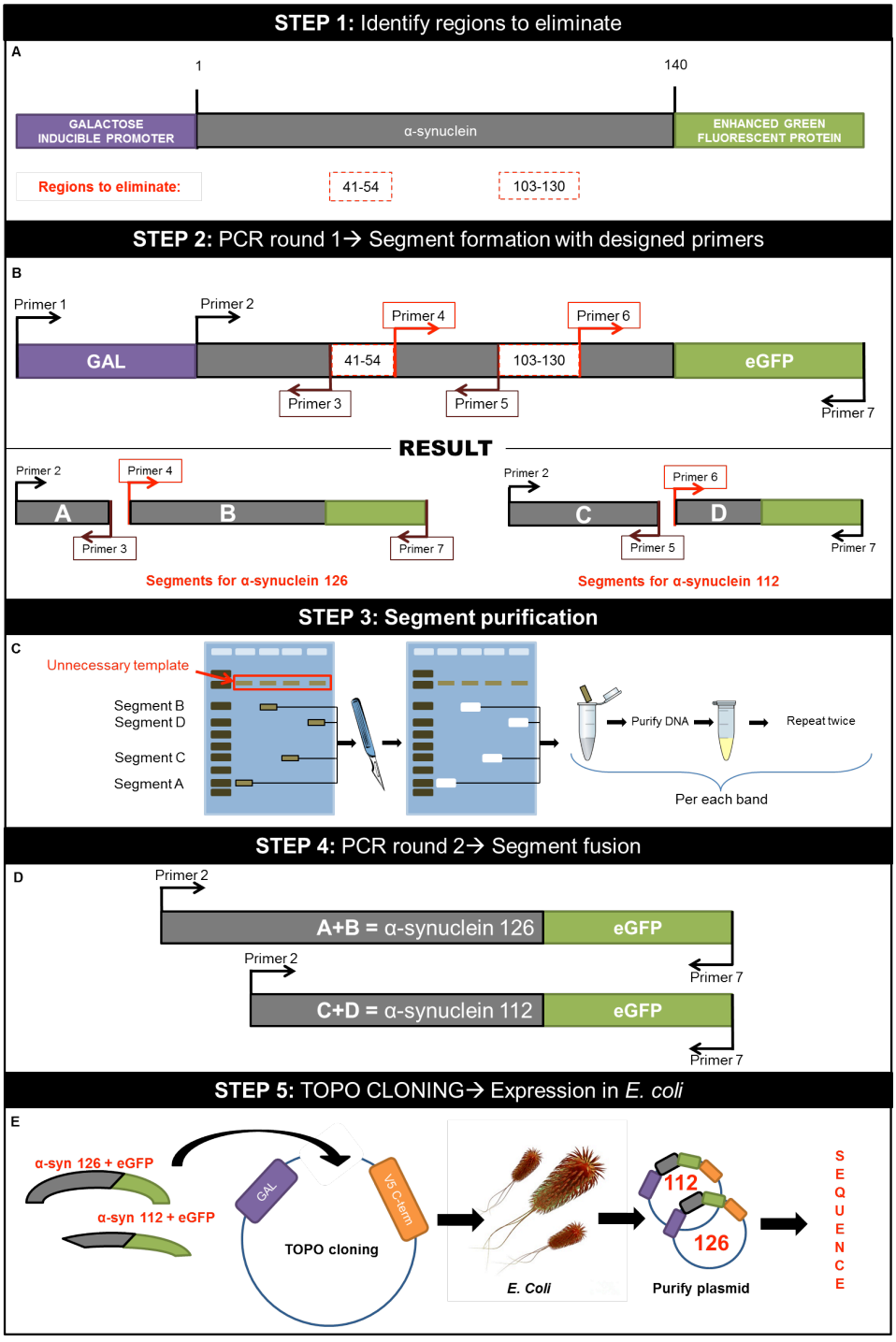
STEP 1: Identify regions to eliminate
A
1
140
GALACTOSE INDUCIBLE PROMOTER
α-synuclein
ENHANCED GREEN FLUORESCENT PROTEIN
Regions to eliminate:
41-54
103-130
STEP 2: PCR round 1→ Segment formation with designed primers
B
Primer 1
Primer 2
Primer 4
Primer 6
GAL
41-54
103-130
eGFP
Primer 3
Primer 5
Primer 7
RESULT
Primer 2
Primer 4
A
B
Primer 3
Primer 7
Segments for α-synuclein 126
Primer 2
Primer 6
C
D
Primer 5
Primer 7
Segments for α-synuclein 112
STEP 3: Segment purification
C
Unnecessary template
Segment B
Segment D
Segment C
Segment A
Purify DNA
Repeat twice
Per each band
STEP 4: PCR round 2→ Segment fusion
D
Primer 2
A+B = α-synuclein 126
eGFP
Primer 7
Primer 2
C+D = α-synuclein 112
eGFP
Primer 7
STEP 5: TOPO CLONING→ Expression in E. coli
E
α-syn 126 + eGFP
α-syn 112 + eGFP
GAL
V5 C-term
TOPO cloning
E. Coli
112
126
Purify plasmid
SEQUENCE

*Figure 13. Experimental design for the formation of splice variants.*

A. Step 1: Identification of regions for elimination within the α-synuclein protein to create proper segments.
B. Step 2: Understanding of the use of correct primers for intended segment acquisition in the first round of PCR. The specifically designed flanking primers (3,4,5, and 6) are indicated by a box and their directionality is showcased by the direction of an arrow. Additionally, the color indicates the type of the designed primer: red for forward and brown for reverse. The first round of PCR will thus result in four segments: A and B as parts of α-synuclein-126 and B and C as parts of α-synuclein-112.
C. Step 3: Segment purification to increase the quality of the final product. Each PCR product was run independently on the gel. The band was then cut out on a UV table and purified. In order to purify the entire PCR product, the process was repeated twice for each PCR product per each segment.
D. Step 4: Segment fusion through the second round of PCR. In order to create the splice variants, Primers 2 and 7 were utilized to fuse segments A and B for α-synuclein-126 and segments C and D for α-synuclein 112.
E. Step 5: TOPO cloning of the spliced α-synuclein-126 and -112 variants in *E. coli* and plasmid purification followed by sequencing.

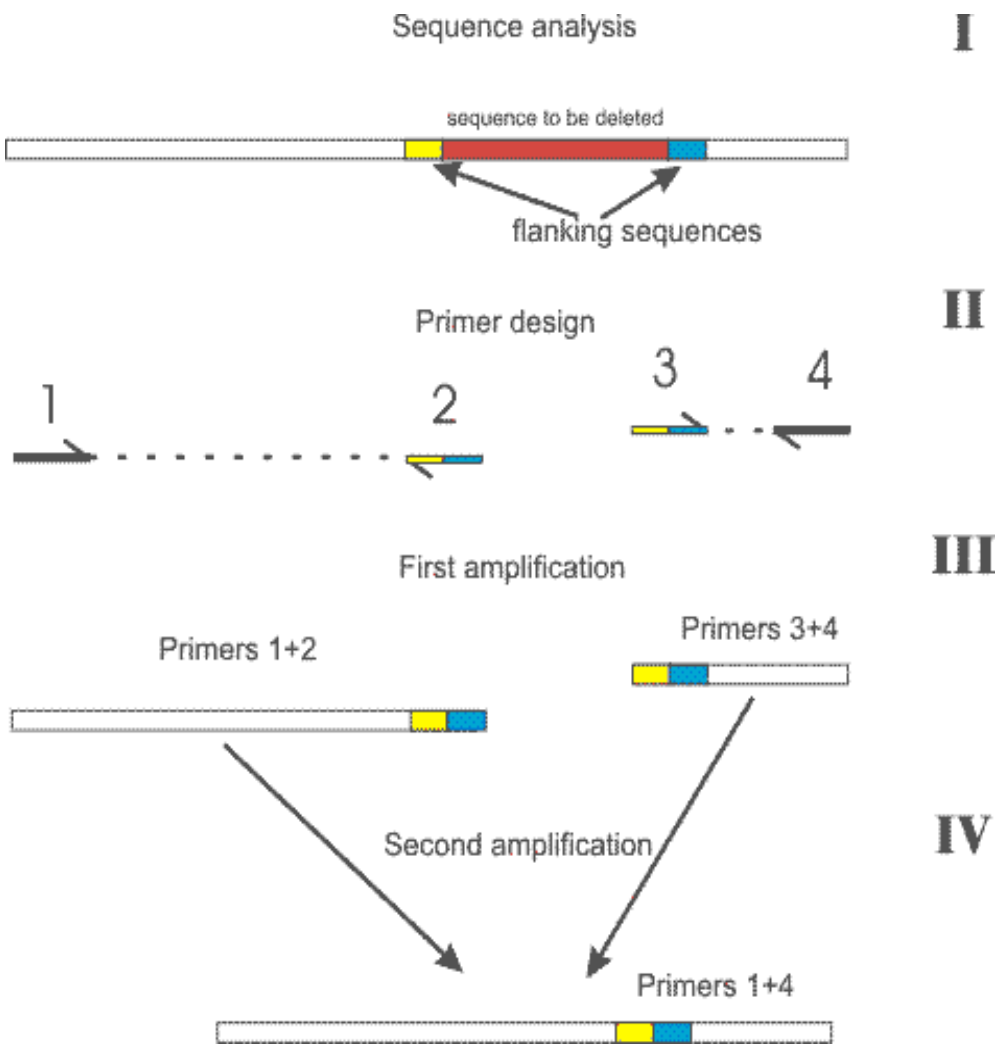


*Figure 14. PCR splicing.* This is an illustration of Dr. Alexei Gratchev's general protocol for a segment deletion within any protein through PCR splicing. It is available on his website (http://www.methods.info/Methods/Mutagenesis/PCR_splicing.html) and serves as a simplistic representation of his model. The four steps in his schematic are: I) Identify the desired region of deletion; II) Design primers (2 and 3); III) Carry out the first PCR with the designed primers (2 and 4) and the primers that will read the front of the protein (1) and the back (4); IV) Carry out the second round of PCR with the primers that will fuse the two segments together (1 and 4).

Since each PCR product would contain more than just the intended segment, for example the original template or unused primers, I decided to individually purify the entire PCR product for each segment (Figure 14C). Only then did I continue with the second round of PCR that was intended to yield the fused α-synuclein-126 and -112 spliced variants (Figure 14D).

**Formation of Spliced Variants' Segments**

The entire process of forming α-synuclein's splice variants has been attempted three times. The first effort occurred during the summer of 2012, however, the acquired final sequences were incorrect. The second try took place during the fall of 2012, but the acquired splice variants were never TOPO cloned due to the poor quality of the end product. Nevertheless, the data for that trial is available in the appendix. The third attempt happened during the spring semester of 2013, and this is the set of data I will present and analyze.

After the sequences of the designed primers were to be correct, I carried out the first round of PCR to create individual segments for α-synuclein-126 and -112 (Figure 16A). Based on the anticipated sizes of the individual segments (Table 2), the acquired PCR products appeared to be the correct sizes. Segment A, visible in lane 2, seemed to be 120 base pairs in size, while segment B, visible in lane3, represented the anticipated size of 972 base pairs (Figure 16B). Segment C, visible in lane 4, appeared to be 306 base pairs in size, while segment D, visible in lane 5, was indicative of 747 base pairs in size (Figure 16B). The reason why no controls were run in this gel is because the primers were already confirmed to work correctly by generating two correct products for two

controls (Appendix: Figure 23, lanes 6 and 7). Based on the acquired PCR results in Figure 16B, the bands for the front segments of each splice variant were weaker (segments: A and C, lanes 2 and 4) than the back segments (segments: B and D, lanes 3 and 5). Due to the impurity of the PCR products for each segment, the next step would be DNA purification.

**Purification of Spliced Variants' Segments**

To assess any loss of the product during the purification process, the purified product was compared to the original PCR product (Figure 17 B). Since only half of the PCR product could be loaded into a gel well at once, each PCR product yielded two purified products (Figure 17A). Both AmpliSize ladders in the resulting gel picture are visible in Figure 17 B lanes 1 and 11. Lane 2 is the PCR product for segment A, followed by the purified products in lanes 3 and 4 (Figure 17 B). Lane 6 is the PCR product for segment C, followed by the purified products in lanes 7 and 8 (Figure 17 B). Lane 5 is the PCR product for segment B followed by the purified products in lanes 9 and 10 (Figure 17 B). Lane 12 is the PCR product for segment D followed by the purified products in lanes 13 and 14 (Figure 17 B). Based on the visible band intensities, overall the product was conserved during the purification process, although some was lost in the second purification of the first segment of 126, segment A. The success of the purification technique was also supported by the fall results (Appendix: Figure 24).

**Segment Fusion**

After the products indicative of each segment were purified, they were used in the

second round of PCR. In order to fuse the protein, primers 2 and 7 were employed (Figure 18A). Furthermore, to optimize the quality of the final product, this was the step where I could alter the amounts of front and back segments used for each splice variant because, as discussed earlier, they varied in band intensity qualities. During the fall semester of 2012 I created multiple conditions, such as three variants for equal and varying template ratios, to help me acquire the best product (Appendix: Figure 25). Thus, this time I only tested two conditions: first—both segments are utilized at equal ratio; second—2.5 times as much of the weaker product (Figure 18B). The only condition that yielded a product was where both segments were used at an equal ratio (Figure 18B, lanes 2 and 3). In Figure 18B, lane 1 is the AmpliSize ladder, lanes 2 and 4 represent α-synuclein-112 splice variant, and lanes 3 and 5 show α-synuclein 126 splice variant.

**Expression of Splice Variants**

Based on the second round of PCR, a strong product for each splice variant was generated, thus the next step was to insert the acquired α-synuclein-126 and -112 into a pYES2.1 vector through TOPO cloning (Figure 19A). In the end, only α-synuclein-126 was successfully TOPO cloned and nine randomly picked colonies were screened for the presence of the α-synuclein-126 product (Figure 19B). Lane 1 is the AmpliSize ladder followed by confirmation PCR products using colonies 1-9 respectively, placed in lanes 2-10 (Figure 19B). The final sequences will be confirmed once α-synuclein-112 is also successfully TOPO cloned.

**B. EXPERIMENTAL DESIGN**

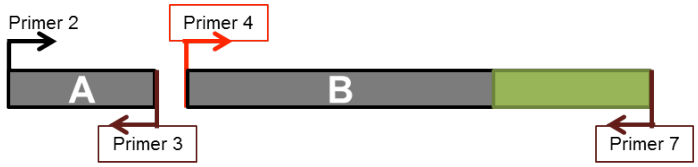


Segments for α-synuclein 126

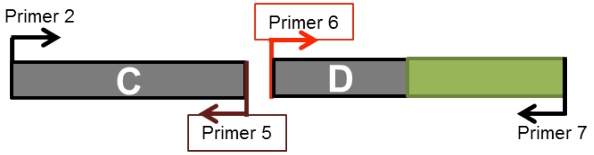


Segments for α-synuclein 112

**A. EXPERIMENTAL OUTCOME**

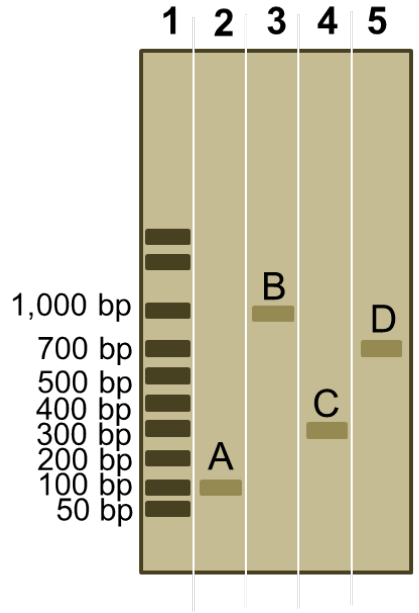


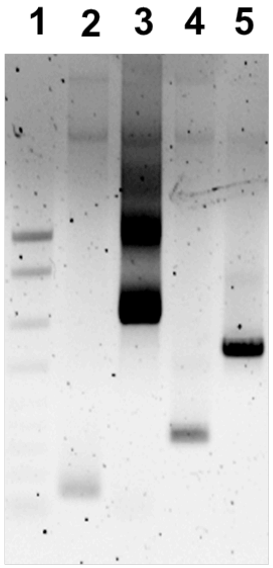


**Legend:**
1. AmpliSize Ladder
2. Segment A
3. Segment B
4. Segment C
5. Segment D

*Figure 15. Formation of splice variants' segments.*

A. Experimental design. Desired segments for each splice variant created through the first round of PCR with the appropriate primers.
B. Experimental outcome. First round PCR results. Lane 1 is the ApliSize ladder, lane 2 is segment A, lane 3 is segment B, lane 4 is segment C, and lane 5 is segments D. Segments A and B will be used to create α-synuclein-126, and segments C and D will give rise to α-synuclein-112.

**B. EXPERIMENTAL DESIGN**

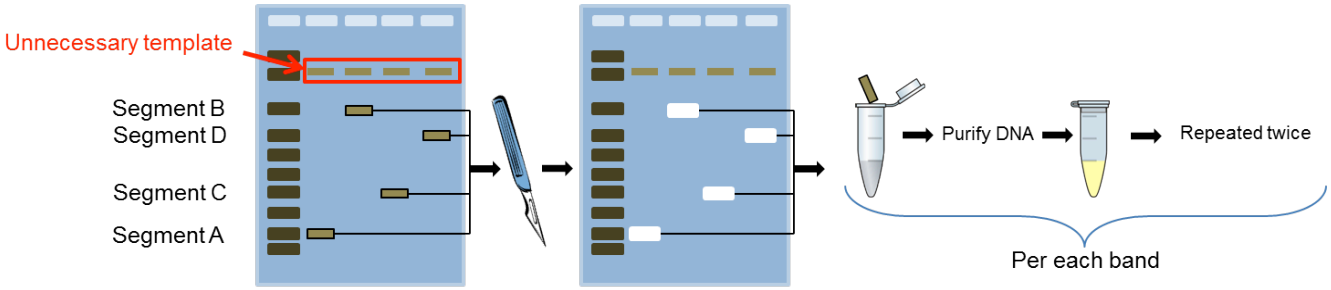


**A. EXPERIMENTAL OUTCOME**

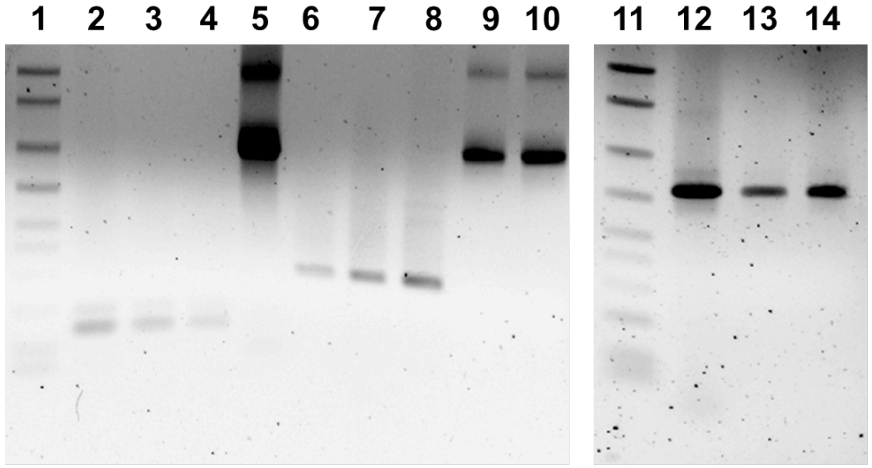


**Legend:**

1. AmpliSize Ladder
2. Segment A original PCR
3. Segment A purified PCR
4. Segment A purified PCR
5. Segment B original PCR
6. Segment C original PCR
7. Segment C purified PCR
8. Segment C purified PCR
9. Segment B purified PCR
10. Segment B purified PCR
11. AmpliSize Ladder
12. Segment D original PCR
13. Segment D purified PCR
14. Segment D purified PCR

*Table 4. Simulated structural characteristics of α-synuclein's mutants.*

| **Property** | **WT** | **A30P** | **E46K** | **A53T** | **E46K-A53T** | **A30P-E46K** | **A30P-A53T** | **A30P-E46K-A53T** |
|---|---|---|---|---|---|---|---|---|
| Foling rate (folds/second) | 10.6/sec | 9.55/sec | 9.27/sec | 11.5/sec | 10.1/sec | 9.04/sec | 9.53/sec | 7.49/sec |
| X-coordinate of COM | 233.208 | 233.220 | 233.208 | 233.216 | 233.208 | 233.213 | 233.229 | 233.221 |
| Y-coordinate of COM | 29.798 | 29.880 | 29.772 | 29.902 | 29.757 | 29.735 | 29.983 | 29.839 |
| Z-coordinate of COM | -15.252 | -15.226 | -15.250 | -15.278 | -15.247 | -15.195 | -15.251 | -15.221 |
| **Z-score** | | | | | | | | |
| Cβ interaction energy | -2.06 | -1.88 | -2.12 | -2.03 | -2.03 | -1.88 | -1.84 | -1.85 |
| All-atom pairwise energy | 0.84 | 0.88 | 0.58 | 0.84 | 0.83 | 0.87 | 0.88 | 0.87 |
| Solvation energy | -3.26 | -3.22 | -3.27 | -3.23 | -3.26 | -3.25 | -3.17 | -3.2 |
| Torsion energy | -3.44 | -3.54 | -3.46 | -3.51 | -3.54 | -3.57 | -3.62 | -3.64 |
| QMEAN4 score | -3.77 | -3.84 | -3.89 | -3.83 | -3.86 | -3.88 | -3.90 | -3.93 |
| **Raw score** | | | | | | | | |
| Cβ interaction energy | -5.04 | -5.90 | -4.78 | -5.20 | -5.18 | -5.88 | -6.07 | -6.05 |
| All-atom pairwise energy | -687.80 | -697.68 | -648.93 | -690.94 | -689.15 | -695.66 | -700.47 | -698.71 |
| Solvation energy | 7.38 | 7.09 | 7.45 | 7.19 | 7.37 | 7.28 | 6.80 | 6.98 |
| Torsion energy | 2.83 | 4.11 | 3.11 | 3.76 | 4.04 | 4.40 | 5.05 | 5.33 |
| QMEAN4 score | 0.452 | 0.445 | 0.440 | 0.446 | 0.443 | 0.441 | 0.440 | 0.437 |

*Table 4. Simulated structural characteristics of α-synuclein's mutants.* The first property is the folding rate of the protein (Gromiha, 2003, courtesy of http://psfs.cbrc.jp/fold-rate) followed by three coordinates specifying the protein's center of mass (COM) (courtesy of Gert Vriend and http://swift.cmbi.ru.nl/servers/html/index.html). The second part of the table provides the Z-scores for five other properties: Cβ interaction energy, All-atom pairwise energy, Solvation energy, Torsion energy and the QMEAN4 score, while the last part of the table provides the raw scores for the same properties (courtesy of the SWISS-MODEL, swissmodel.expasy.org, (Schwede et al., 2011) and QMEAN (Benkert et al., 2011)). C-beta atoms and all-atom potentials are two measures of distance-dependent interaction potentials that assess long-range interaction. The residue-level implementation is indicated by Cβ interaction energy measure, while the all-atom potential indicates secondary structure specific interaction potential. The solvation energy indicates the burial status of the residues. The torsion energy measure analyzes the local geometry over three consecutive amino acids. The QMEAN4 is a reliability score of the whole model. Z-scores relay the quality estimates to scores obtained from high-resolution reference structures solved experimentally by X-ray crystallography, in this case the native α-synuclein.

artificial point used for detecting important and simple features of proteins structure, shape, and association (Namdeo et al., 2011). COM thus reflects the behavior of the whole system and can be used to predict protein tertiary models or assess the global shape of protein in protein-protein complexes (Namdeo et al., 2011). The COM measure comprises of the assessment of three axes X, Y, and Z, which were calculated for each mutant and are visible in Table 4. Note that in combinatory mutants whose characteristics were dominated by A30P, the COM coordinates are most closely related to that of A30P. Potentially, three out of the four combinatory mutants resembled A30P properties because they adapted a slow folding rate and closely related COM coordinates (Table 4).

While the problem of protein conformation simulation is still pertinent in biology, a computer generated model available online provides a way to predict possible protein structures based on certain measurements. The Swiss-Model simulates Cβ interaction energies, all-atom pairwise energies, solvation energies, torsion energies and QMEAN4 score based on the provided amino acid sequence (Schwede et al., 2011; Benkert et al., 2011). The acquired data for each of these measurements are shown in Table 4, and it should be noted that the values for A30P-E46K, A30P-A53T, and A30P-E46K-A53T reflect the values of A30P. To make interpretation easier, each measurement was defined in the legend (Table 4).

*Amino Acid Characterization*

Twenty amino acids have been identified that give rise to all of the different proteins utilized by all organisms. To promote diversity, amino acids differ in charge, hydrophobicity, and polarity. The amino acids involved in creation of A30P, A53T, and

E46K have been represented in Table 5. Due to the dominance of A30P on E46K and A53T, I will limit the discussion to A30P. As previously established, the A30P mutant is made by a switch of Alanine to Proline on the 30$^{th}$ amino acid location. Alanine is an L-isomer with the alpha carbon atom bound to a methyl group, thus classifying the amino acid aliphatic (Alberts et al., 2010). Proline, formally not an amino acid, but an animino acid, is a secondary amine because of its connection to two bulky alkyl groups, and it is known to loosen the stability of the protein to bind lipids (Alberts et al., 2010). Neither of the amino acids are charged, and whereas alanine is aliphatic, proline likes to promote turns, which would result in the breaking of α-synuclein's α-helix (Alberts et al., 2010). The result of a switch from an alanine to a proline is ultimately showcased in *in vivo* comparison of A30P to WT, which supports A30P's inability to bind lipid membranes (Conway et al., 1998). This alternation thus results in a characteristic A30P phenotype of diffusion of the protein throughout the cell. This feature is contrary to the natural form of the α-synuclein protein, which is known to present itself in an aggregated form (Spilantini et al., 1998) and in association to phospholipid membranes (Clayton & George, 1998).

**Importance of Designer Mutants**

In reality, the onset of familial PD in human patients due to one of the combinatory mutations is very minimal. However, due to their characterization, a lot of new insight about the α-synuclein protein may be gained, as well as the significance of its amino acid locations and properties in regard to final protein conformation. Progress is not only attained through studying naturally occurring mutations, but, in PD

*Table 5. Amino acid characterization*. This table represents each of the amino acids involved in the familial mutations and their properties in regard to charge, hydrophobicity, polarity and other properties important for protein conformation changes (Alberts et al., 2010).

| **Amino Acid:** | **Charge:** | **Hydrophobicity:** | **Polarity:** | **Other properties:** |
|---|---|---|---|---|
| Alanine (A) | None | Hydrophobic | None | Aliphatic |
| Lysine (K) | Positive | Hydrophilic | Polar | Basic |
| Proline (P) | None | Not hydrophobic | None | Promotes turns |
| Glutamate (E) | Negative | Hydrophilic | Polar | Acidic |
| Threonine (T) | None | Hydrophilic | Polar | |

Especially, knowledge has been gained through various designer mutants. Individual point mutations have been used in order to gather a better understanding of the protein's properties in relation to specific regions. For example, Fiske et al., (2011) assessed contributions of alanine-76 and serine phosphorylation, which gave insight on membrane association and aggregation. Other posttranslational modification mutants for phosphorylation (Fujiwara et al., 2002; Paleologou et al., 2010), nitrosylation (Clayton & George, 1998) or sumoylation (Wilkinson et al., 2003) have contributed to better understanding of PD pathology. Therefore, the majority of research focus should not be on the type of mutation, but rather on the level of insight that it provides.

**The Future of Studying Combinatory Mutants**

To strengthen the characterization of combinatory mutants I could conduct other tests such as loss of induction and optical density curve assessment, and I could replicate the survival assay. The analysis of combinatory mutants has an enormous range of application because their characteristics could be assessed within different pathways implicated in PD onset such as endocytosis or autophagy. Furthermore, the properties of combinatory mutants should be assessed with regard to additional PD associated phosphorylation, nitrosylation, or sumoylation of the α-synuclein protein.

Unexpectedly, in February of 2013, a fourth PD familial mutation was identified as G51D (Kiely et al., 2013). Upon initial analysis, is has shown to exhibit clinical and neuropathological properties resembling those of A53T, such as presence of neuronal grains and threads and severe neuronal loss (Kiely et al., 2013). However, G51D also shows features including dense accumulation of a-synuclein-positive inclusions in the

striatum, and very severe pathology that affects both superficial and deep cortical laminae that ultimately distinguishes G51D from other SNCA mutations (Kiely et al., 2013). Thus, it would be appropriate to create combinatory variants with G51D and determine whether A30P dominance would still be conserved, especially in the quadruple mutant. From a biochemical perspective, the combinatory mutations ought to be crystalized, or at least 3D structures should be constructed in the most representative fashion. These techniques would provide more insight into α-synuclein protein's conformation that would be beneficial to understanding the mechanism behind this protein's shape acquisition.

**Protein Expression Improvement Strategy**

As exhibited in my data set, the Western blot development and analysis was one of the biggest struggles of my thesis. The problem seemed to evolve across many areas from initial lack of visualization of any bands to the ineffectiveness of secondary antibody and unequal loading. After re-making all of the solutions I was still not able to visualize the bands, which is when WesternBreeze was ordered. As a new strategy, I would count the samples three times instead of two to establish uniform cell density and perhaps even confirm it using the machine responsible for determination of optical density of solutions. Additionally, if within the lab's budget, I will develop my Westerns using the WesternBreeze kit in order to perfect my loading skills. Once representative results are acquired, I will go back to self-making lab solutions for Western blot analysis. In the future, if Western development is not problematic, I intend on conducting a loss of induction assay in a time-dependent manner to determine whether the acquired α-synuclein concentration was due to less degradation.

# CHAPTER 2

*CREATION OF α-SYNUCLEIN SPLICE VARIANTS*

## RESULTS

### Experimental Design

In order to understand the properties of the three, newly-discovered α-synuclein natural splice variants (α-synuclein-126, -112, -98), the initial step was to strategize an appropriate series of techniques for protein truncation. Through the literature, I identified the two regions of α-synuclein that needed elimination. For α-synuclein-112 it was the amino acid range of 41-54, and for α-synuclein-126 it was the amino acid range of 103-130 (McLean et al., 2012; Figure 14A). Then I designed appropriate primers for the formation of these splice variants (for primer design details please refer to p.34, for a schematic refer to Figure 14B). I also chose to wait for the correct sequencing of either α-synuclein-112 or -126 in order to use either one as a template for the last splice variant, α-synuclein-98.

The next step was to design a suitable sequence of PCR reactions. As a model method, I adopted Dr. Alexei Gratchev's general protocol for creating a deletion in a protein by PCR splicing (Figure 15). According to his strategy, the pair of designed primers should flank the region intended for the deletion. During the first round of PCR, the outer most primers along with the designer primers would form and help amplify the desired segments. Then, during the second round of PCR, only the outer most primers would then be utilized to fuse the segments and contribute to product amplification. In alignment to Gratchev's design, I predicted that using the first round of PCR my designed primers would yield four segments called A, B, C, and D (Figure 14B).

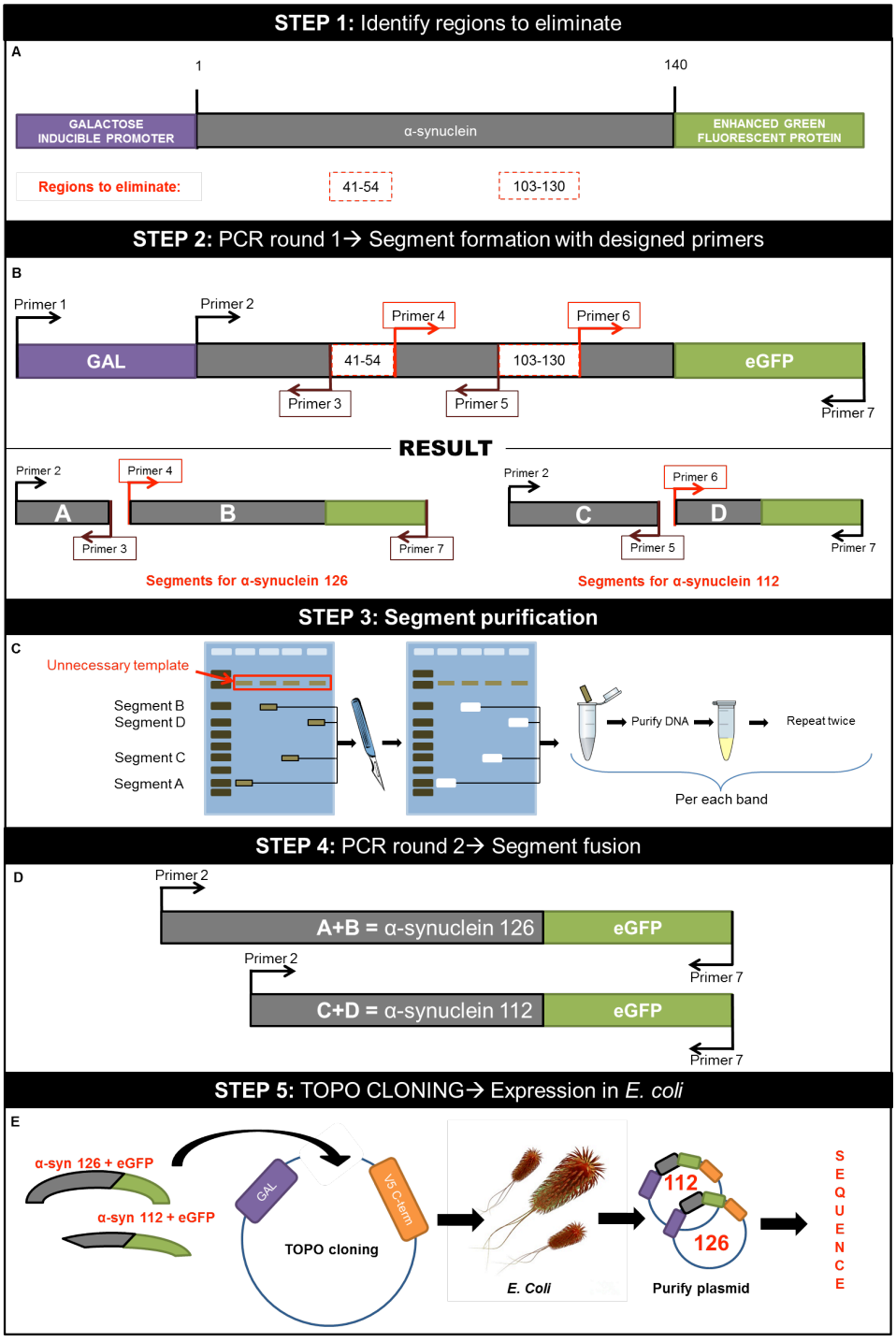
STEP 1: Identify regions to eliminate
A
1
140
GALACTOSE INDUCIBLE PROMOTER
α-synuclein
ENHANCED GREEN FLUORESCENT PROTEIN
Regions to eliminate:
41-54
103-130
STEP 2: PCR round 1→ Segment formation with designed primers
B
Primer 1
Primer 2
Primer 4
Primer 6
GAL
41-54
103-130
eGFP
Primer 3
Primer 5
Primer 7
RESULT
Primer 2
Primer 4
A
B
Primer 3
Primer 7
Segments for α-synuclein 126
Primer 2
Primer 6
C
D
Primer 5
Primer 7
Segments for α-synuclein 112
STEP 3: Segment purification
C
Unnecessary template
Segment B
Segment D
Segment C
Segment A
Purify DNA
Repeat twice
Per each band
STEP 4: PCR round 2→ Segment fusion
D
Primer 2
A+B = α-synuclein 126
eGFP
Primer 7
Primer 2
C+D = α-synuclein 112
eGFP
Primer 7
STEP 5: TOPO CLONING→ Expression in E. coli
E
α-syn 126 + eGFP
α-syn 112 + eGFP
GAL
V5 C-term
TOPO cloning
E. Coli
112
126
Purify plasmid
SEQUENCE

*Figure 13. Experimental design for the formation of splice variants.*

A. Step 1: Identification of regions for elimination within the α-synuclein protein to create proper segments.
B. Step 2: Understanding of the use of correct primers for intended segment acquisition in the first round of PCR. The specifically designed flanking primers (3,4,5, and 6) are indicated by a box and their directionality is showcased by the direction of an arrow. Additionally, the color indicates the type of the designed primer: red for forward and brown for reverse. The first round of PCR will thus result in four segments: A and B as parts of α-synuclein-126 and B and C as parts of α-synuclein-112.
C. Step 3: Segment purification to increase the quality of the final product. Each PCR product was run independently on the gel. The band was then cut out on a UV table and purified. In order to purify the entire PCR product, the process was repeated twice for each PCR product per each segment.
D. Step 4: Segment fusion through the second round of PCR. In order to create the splice variants, Primers 2 and 7 were utilized to fuse segments A and B for α-synuclein-126 and segments C and D for α-synuclein 112.
E. Step 5: TOPO cloning of the spliced α-synuclein-126 and -112 variants in *E. coli* and plasmid purification followed by sequencing.

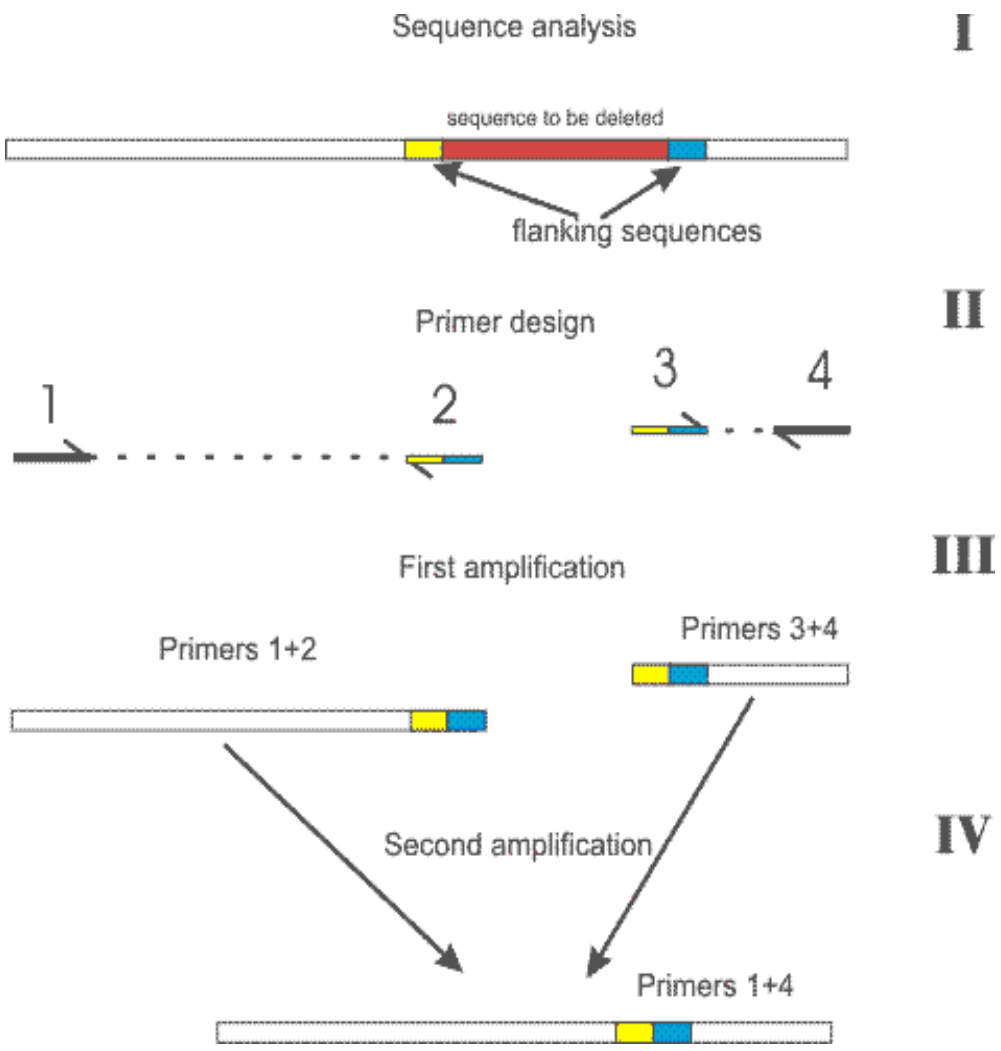


*Figure 14. PCR splicing.* This is an illustration of Dr. Alexei Gratchev's general protocol for a segment deletion within any protein through PCR splicing. It is available on his website (http://www.methods.info/Methods/Mutagenesis/PCR_splicing.html) and serves as a simplistic representation of his model. The four steps in his schematic are: I) Identify the desired region of deletion; II) Design primers (2 and 3); III) Carry out the first PCR with the designed primers (2 and 4) and the primers that will read the front of the protein (1) and the back (4); IV) Carry out the second round of PCR with the primers that will fuse the two segments together (1 and 4).

Since each PCR product would contain more than just the intended segment, for example the original template or unused primers, I decided to individually purify the entire PCR product for each segment (Figure 14C). Only then did I continue with the second round of PCR that was intended to yield the fused α-synuclein-126 and -112 spliced variants (Figure 14D).

**Formation of Spliced Variants' Segments**

The entire process of forming α-synuclein's splice variants has been attempted three times. The first effort occurred during the summer of 2012, however, the acquired final sequences were incorrect. The second try took place during the fall of 2012, but the acquired splice variants were never TOPO cloned due to the poor quality of the end product. Nevertheless, the data for that trial is available in the appendix. The third attempt happened during the spring semester of 2013, and this is the set of data I will present and analyze.

After the sequences of the designed primers were to be correct, I carried out the first round of PCR to create individual segments for α-synuclein-126 and -112 (Figure 16A). Based on the anticipated sizes of the individual segments (Table 2), the acquired PCR products appeared to be the correct sizes. Segment A, visible in lane 2, seemed to be 120 base pairs in size, while segment B, visible in lane3, represented the anticipated size of 972 base pairs (Figure 16B). Segment C, visible in lane 4, appeared to be 306 base pairs in size, while segment D, visible in lane 5, was indicative of 747 base pairs in size (Figure 16B). The reason why no controls were run in this gel is because the primers were already confirmed to work correctly by generating two correct products for two

controls (Appendix: Figure 23, lanes 6 and 7). Based on the acquired PCR results in Figure 16B, the bands for the front segments of each splice variant were weaker (segments: A and C, lanes 2 and 4) than the back segments (segments: B and D, lanes 3 and 5). Due to the impurity of the PCR products for each segment, the next step would be DNA purification.

**Purification of Spliced Variants' Segments**

To assess any loss of the product during the purification process, the purified product was compared to the original PCR product (Figure 17 B). Since only half of the PCR product could be loaded into a gel well at once, each PCR product yielded two purified products (Figure 17A). Both AmpliSize ladders in the resulting gel picture are visible in Figure 17 B lanes 1 and 11. Lane 2 is the PCR product for segment A, followed by the purified products in lanes 3 and 4 (Figure 17 B). Lane 6 is the PCR product for segment C, followed by the purified products in lanes 7 and 8 (Figure 17 B). Lane 5 is the PCR product for segment B followed by the purified products in lanes 9 and 10 (Figure 17 B). Lane 12 is the PCR product for segment D followed by the purified products in lanes 13 and 14 (Figure 17 B). Based on the visible band intensities, overall the product was conserved during the purification process, although some was lost in the second purification of the first segment of 126, segment A. The success of the purification technique was also supported by the fall results (Appendix: Figure 24).

**Segment Fusion**

After the products indicative of each segment were purified, they were used in the

second round of PCR. In order to fuse the protein, primers 2 and 7 were employed (Figure 18A). Furthermore, to optimize the quality of the final product, this was the step where I could alter the amounts of front and back segments used for each splice variant because, as discussed earlier, they varied in band intensity qualities. During the fall semester of 2012 I created multiple conditions, such as three variants for equal and varying template ratios, to help me acquire the best product (Appendix: Figure 25). Thus, this time I only tested two conditions: first—both segments are utilized at equal ratio; second—2.5 times as much of the weaker product (Figure 18B). The only condition that yielded a product was where both segments were used at an equal ratio (Figure 18B, lanes 2 and 3). In Figure 18B, lane 1 is the AmpliSize ladder, lanes 2 and 4 represent α-synuclein-112 splice variant, and lanes 3 and 5 show α-synuclein 126 splice variant.

**Expression of Splice Variants**

Based on the second round of PCR, a strong product for each splice variant was generated, thus the next step was to insert the acquired α-synuclein-126 and -112 into a pYES2.1 vector through TOPO cloning (Figure 19A). In the end, only α-synuclein-126 was successfully TOPO cloned and nine randomly picked colonies were screened for the presence of the α-synuclein-126 product (Figure 19B). Lane 1 is the AmpliSize ladder followed by confirmation PCR products using colonies 1-9 respectively, placed in lanes 2-10 (Figure 19B). The final sequences will be confirmed once α-synuclein-112 is also successfully TOPO cloned.

**B. EXPERIMENTAL DESIGN**

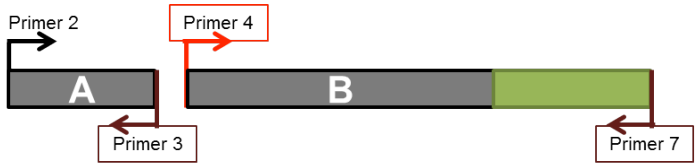


Segments for α-synuclein 126

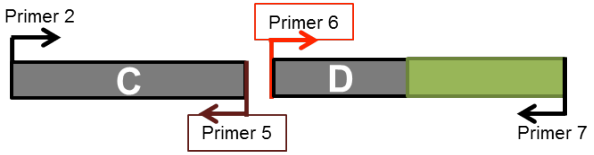


Segments for α-synuclein 112

**A. EXPERIMENTAL OUTCOME**

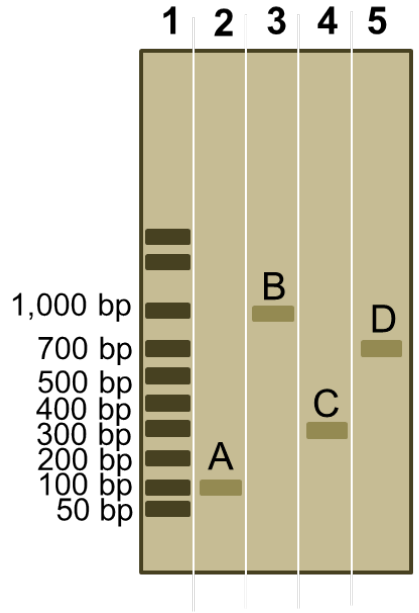


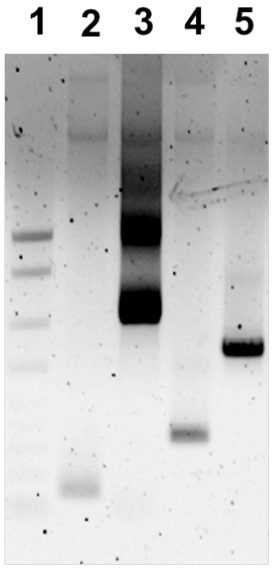


**Legend:**
1. AmpliSize Ladder
2. Segment A
3. Segment B
4. Segment C
5. Segment D

*Figure 15. Formation of splice variants' segments.*

A. Experimental design. Desired segments for each splice variant created through the first round of PCR with the appropriate primers.
B. Experimental outcome. First round PCR results. Lane 1 is the ApliSize ladder, lane 2 is segment A, lane 3 is segment B, lane 4 is segment C, and lane 5 is segments D. Segments A and B will be used to create α-synuclein-126, and segments C and D will give rise to α-synuclein-112.

**B. EXPERIMENTAL DESIGN**

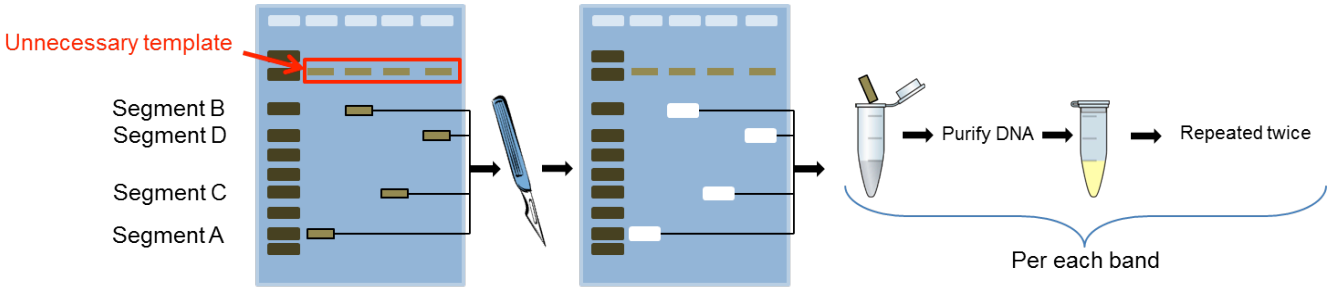


**A. EXPERIMENTAL OUTCOME**

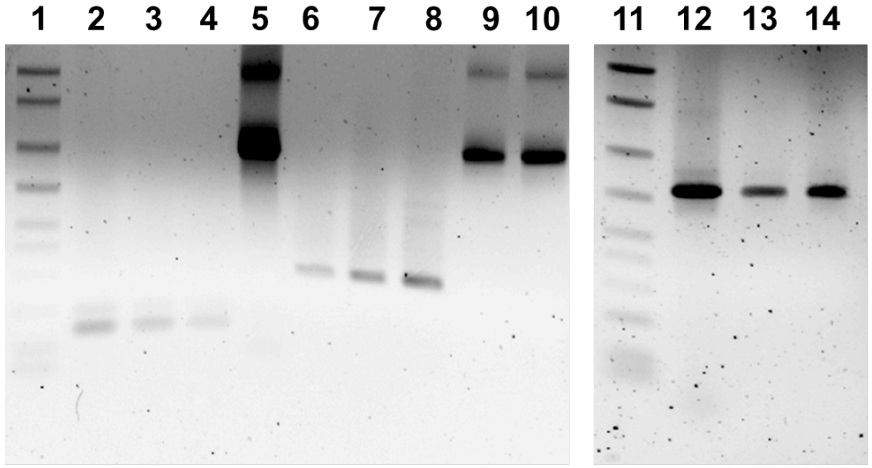


**Legend:**

1. AmpliSize Ladder
2. Segment A original PCR
3. Segment A purified PCR
4. Segment A purified PCR
5. Segment B original PCR
6. Segment C original PCR
7. Segment C purified PCR
8. Segment C purified PCR
9. Segment B purified PCR
10. Segment B purified PCR
11. AmpliSize Ladder
12. Segment D original PCR
13. Segment D purified PCR
14. Segment D purified PCR

*Figure 16. Purification of splice variants' segments.*

A. Experimental design. Exemplified is a cartoon of the purification process of the PCR product acquired for each segment. Each PCR product was run independently on the gel. The band was then cut out on a UV table and purified. In order to purify the entire PCR product the process was repeated twice for each PCR product per each segment.

B. Experimental outcome. To ensure minimal loss of product during the purification technique, the original PCR product was compared to the purified product for each segment. Lanes 1 and 11 are both AmpliSize ladders. Lane 2 is the PCR product for segment A followed by the purified products in lanes 3 and 4. Lane 6 is the PCR product for segment C followed by the purified products in lanes 7 and 8. Lane 5 is the PCR product for segment B followed by the purified products in lanes 9 and 10. Lane 12 is the PCR product for segment D followed by the purified products in lanes 13 and 14.

**A. EXPERIMENTAL DESIGN**

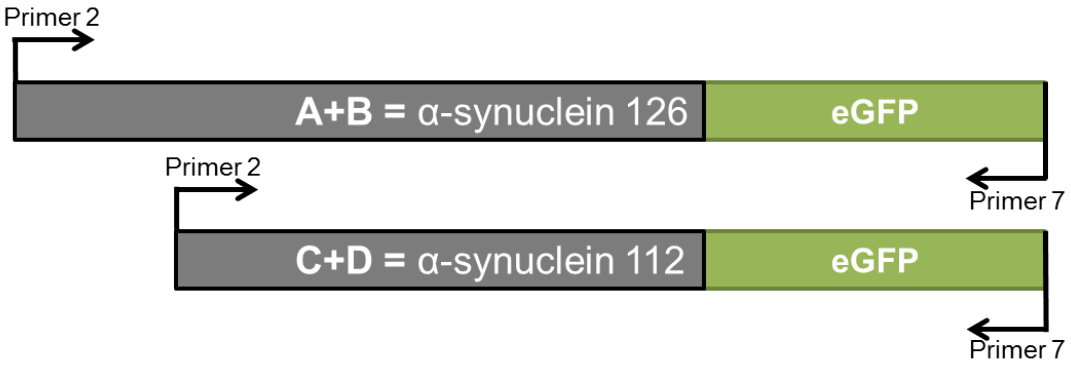


**B. EXPERIMENTAL OUTCOME**

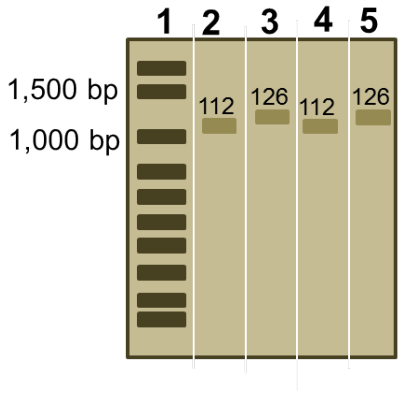


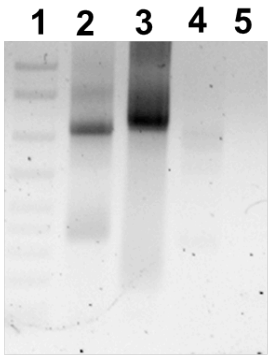


**Legend:**

1. AmpliSize Ladder
2. Segment 112 (1:1 template ratio)
3. Segment 126 (1:1 template ratio)
4. Segment 112 (1:2.5 template ratio)
5. Segment 126 (1:2.5 template ratio)

*Figure 17. Segment fusion.*

A. Experimental design. Desired splice variants for each α-synuclein isoform from fused segments acquired through the second round of PCR.
B. Experimental outcome. To acquire the best quality product two conditions were created. First: the same amount of the two segments for each splice variant was used; second: there was 2.5 times more of the weaker product (segment A and C) utilized when making each splice variant. Lane 1 is AmpliSize ladder, lanes 2 and 4 represent α-synuclein 112 splice variant, and lanes 3 and 5 show α-synuclein 126 splice variant.

A. EXPERIMENTAL DESIGN

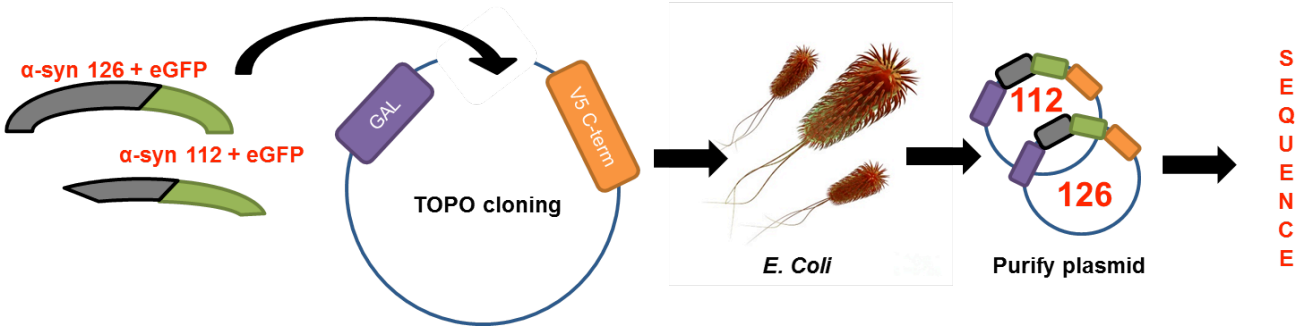


B. EXPERIMENTAL OUTCOME

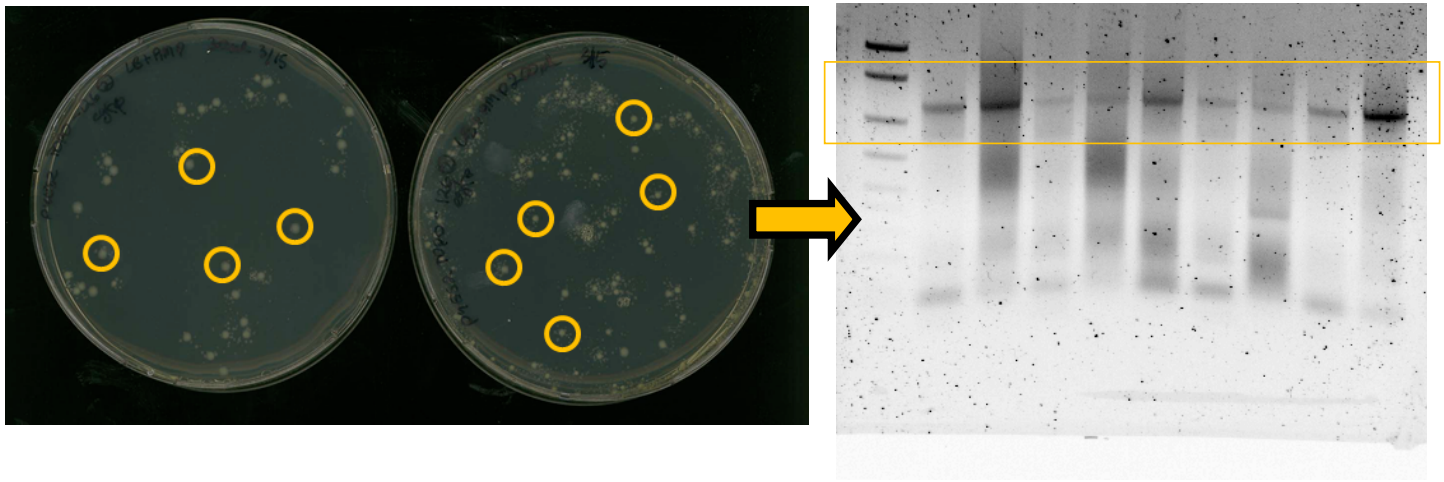

*Figure 18. Splice variant expression.*

A. Experimental design. Showcased is a cartoon representing the insertion of the splice variant into a vector then into *E. coli* using TOPO cloning technique and final variant formation confirmation though sequencing.

B. Experimental outcome. Showcased are photographs of plates representing the colonies of α-synuclein-126 splice variant, which indicate successful TOPO cloning. Circled are nine colonies that were selected for product confirmation. The gel represents the nine tested colonies and the acquired product confirmation. Lane 1 is the AmpliSize ladder followed by confirmation PCR products using colonies 1-9 respectively placed in lanes 2-10.

**DISCUSSION:**

Recently, three splice variants (α-synuclein-98, -112 and -126) were identified in various synucleinopathies (Beyer et al., 2006; Beyer et al., 2008; McLean et al., 2012) and in animal PD models (McLean et al., 2012). More specifically, these splice variants of the protein were identified as components of Lewy bodies which are a hallmark characteristic of PD pathology (McLean et al., 2012). In addition to PD, other diseases, such as: Dementia with Lewy bodies (DLB), Lewy body variant of Alzheimer disease (LBVAD), and multiple system atrophy (MSA) can be pathologically unified by the presence of Lewy bodies with α-synuclein as their main component (Beyer et al., 2004; Beyer, 2006; Dufty et al., 2007). Whether any of the α-synuclein splice variants can directly protect or harm cells is not known, thus there is a high need for their individual expression in model organisms to assess their functions. Thus, my goal was to construct at least two of the α-synuclein splice variants (α-synuclein-126 and -112) to create tools for future expression in various yeast models.

**Creation of α-Synuclein Splice Variants**

As part of the second goal of my thesis, I created two splice variants, α-synuclein-126 and α-synuclein-112, but I was only successful with the process of TOPO cloning in regard to α-synuclein-126. Although the generated splice variants for α-synuclein-126 and -112 have not yet been sequenced their base pair sizes seem appropriate for each one of the variants. The limitation of the process of splice-variant creation is that the indication of their correct splice variant acquisition is based on a the

ladder utilized in gel electrophoresis. With variants that are similar in size, such as α-synuclein-126 and α-synuclein-112, the differences between exemplified segments can be miniscule. Overall, the biggest drawback in the process of forming these isoforms is that one will not know if the progression was successful until the final sequencing.

**Uncovering the Roles of Splice Variants**

Based on the available literature about the three splice variants in neurodegenerative diseases, I developed a prediction for the roles of each α-synuclein isoform. If I was given the opportunity to express each one of them individually in a yeast model, I would expect specific features in regard to protein localization, toxicity and expression. According to my hypothesis, in budding and fission yeasts, α-synuclein-98 and -126 would show diffusion throughout the cell, due to the impairment of regions responsible for plasma membrane binding; while α-synuclein-112 would show the formation of aggregates (Figure 20). While the formation of such aggregates would not be visible in the low expression model with the regular green fluorescent tag (GFP), we could use the higher expression budding yeast model with the enhanced green fluorescent tag (eGFP) to note possibly different results.

The reason why I believe that α-synuclein-112 would form aggregates is because the deletion of amino acids 103-130 results in a characteristic shortening of the C-terminal, which makes the protein highly hydrophobic and prone for aggregation (Xiong et al., 2010). Studies have shown that C-terminally truncated α-synuclein demonstrates

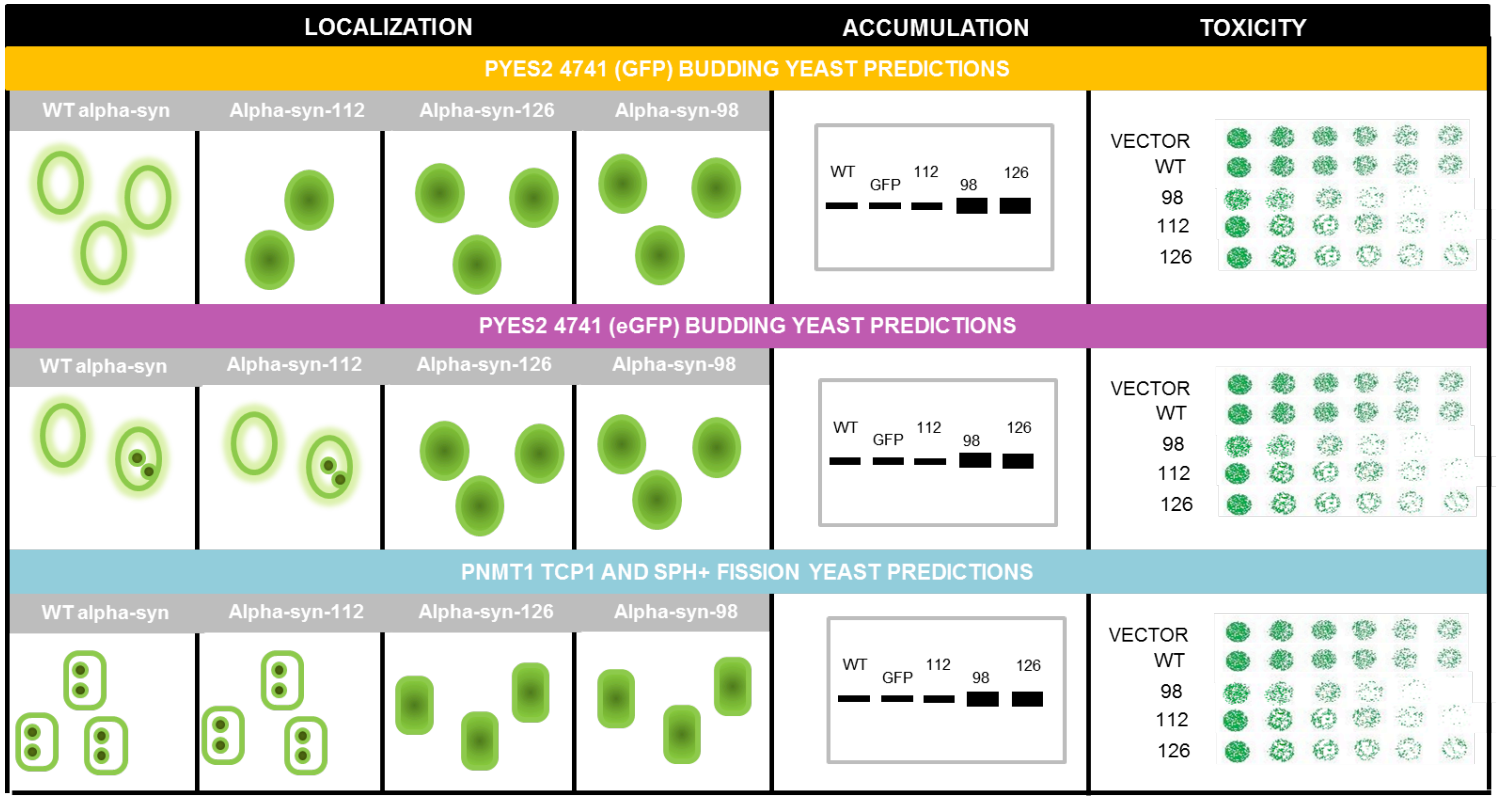


*Figure 20. Prediction for α-synuclein splice variants' properties.*

*Figure 20. Prediction for α-synuclein splice variants' properties.* This is a visual representation of the hypothesis for the behavior of splice variants in yeast models of low and high expression. The low expression model is budding yeast with GFP tag, while the high expression models are two fission yeast strains and budding yeast with eGFP tag. The following assays were of interest: localization, accumulation and toxicity. According to my predictions α-synuclein-126 and -98 will show cytoplasmic diffusion in all models, and α-synuclein-112 will showcase cytoplasmic diffusion in low expressing model and aggregation in high expressing models. Compared to WT, protein expression will be higher in α-synuclein-126 and -98, while higher toxicity will be exhibited by α-synuclein-112.

higher aggregation tendencies with would be consistent with α-synuclein-112's tendencies to form aggregates (Li et al., 2005). Additionally, the deletion of Calpain cleavage site (117-122aa) has been shown to independently result in aggregation and adaptation of beta-sheet configuration of the α-synuclein protein (Dufty et al., 2007). Since this site overlaps with the deletion within the α-synuclein-112 splice variant, this further explains and supports its predisposition for aggregation. The α-synuclein-126 would not form aggregates, and instead would show cytoplasmic diffusion because the deletion of exon 3 results in lack of amino acids 41-54 (Beyer et al., 2006), which likely interrupts helices three and four that aid protein-membrane interactions (Xiong et al., 2010). This truncation also lacks two amino acids mutated in familial PD (E46K and A53T), which show characteristic plasma membrane binding (Beyer et al., 2006). Therefore, due to its hindered ability for lipid association I would hypothesize that the protein would be cytoplasmically diffused. Similarly, I hypothesize that α-synuclein-98 would lack lipid association and be unable to aggregate due to lack of exons 3 and 5 (Beyer et al. 2008). Thus, it would also showcase the phenotype of cytoplasmic diffusion.

In regard to cytotoxicity, I would expect the α-synuclein-112 and -98 to be more toxic than α-synuclein-126 because of their truncated C-terminal, which is known to serve a role in neuroprotection (Figure 20). Nevertheless, the toxicity patterns of splice variants are yet to be assesses, which is why such experiments would bring novel and insightful information. Based on results from patients' data, I would further expect the accumulation to be the highest for α-synuclein-126, followed by -98 and then -112 (Figure 20). This prediction could be supported by Beyer et al.'s finding from 2008

where the SNCA gene was upregulated for splice variants 126 and 98 in PD. Furthermore, in 2012 McLean et al. found that α-synuclein-126 and -98 seemed to be co-localized and elevated in substantia nigra and cerebellum, while α-synuclein-112 expressions was elevated only in the cerebellum.

**CONCLUSION:**

Understanding the complexities of any neurodegenerative disease is a might task for every scientist, 'big' or 'small'. Nevertheless, human curiosity and need for understanding propels scientific research on various topics with diversified study models conducted in locations all over the world. As an undergraduate student I embraced the challenge of studying a problem of protein misfolding associated with the onset of PD, and the results of my work are exemplified in this body of work.

Through the use of a simple organism such as yeast, I characterized the properties of combinatory mutants and provided greater insight into understanding the α-synuclein protein. The unexpected finding of A30P dominance gave further understanding into structural dynamics of the protein, but also generated further questions that ought to be pursued. Moreover, through the appropriate use of a simple series of PCR reactions I created two α-synuclein splice variants 126 and 112. Future independent expression of these isomers in yeast should help to understand their role in Lewy body composition and PD pathology. Hence yeast models are powerful model organisms that can provide understanding of protein's properties on the molecular level, as well as insight into human disease by uncovering the details leading to its pathology.

## References


Alberts, B., Bray, D., Hopkin, K., Johnson, A., Lewis, J., Raff, M., …Walter, P. (2010). *Essential Cell Biology*. Garland Science: New York.

Benkert, P., Tosatto, S. C. E., & Schomburg, D. (2008). QMEAN: A comprehensive scoring function for model quality assessment. *Proteins: Structure, Function, and Bioinformatics, 71*, 261-277.

Betarbet, R., Sherer, T., MacKenzie, G., Garcia-Osuna, M., Panov, A., & Greenamyr, J. (2000). Chronic systemic pesticide exposure reproduces features of Parkinson's disease. *Natural Neuroscience, 3*, 1301-1306.

Beyer, K., Domingo-Sabat, M., Humbert, J., Carrato, C., Ferrer, I., & Ariza, A. (2008). Differential expression of alpha-synuclein, parkin, and synphilin-1 isoforms in Lewy body disease. *Neurogenetics, 9*, 163-172.

Beyer, K., Lao, J. I., Carrato, C., Mate, J. L., Lopez D., Ferrer, I., & Ariza, A. (2004). Differential expression of alpha-synuclein isoforms in dementia with Lewy bodies. *Neuropathology and Applied Neurobiology, 30*, 601-607.

Beyer, K. (2006). Review: Alpha-synuclein structure, posttranslational modification and alternative splicing as aggregation enhancers. *Acta Neuropathologica, 112*, 237-251.

Beyer, K., Humbert, J., Ferrer, A., Lao, J. I., Carrato, C., López, D., Ferrer, I., & Ariza, A. (2006). Low alpha-synuclein 126 mRNA levels in dementia with Lewy bodies and Alzheimer disease. *Neuroreport, 17*, 1327-1330.

Beyer, K., Domingo-Sabat, M., Lao, J. I., Carrato, C., Ferrer, I., & Ariza, A. (2008). Identification and characterization of a new alpha-synuclein isoform and its role in Lewy body diseases. *Neurogenetics*, *9*, 15-23.

Beyer, K., & Ariza, A. (2012). Alpha-synuclein posttranslational modification and alternative splicing as a trigger for neurodegeneration. *Molecular Neurobiology*. Publlished online. DOI 10.1007/s12035-8330-5.

Bisaglia, M., Mammi, S., & Bubacco, L., (2009). Review: Structural insight physiological functions and pathological effects of alpha-synuclein. *The Federation of American Society for Experimental Biology Journal, 23*, 329-340.

Bonifati, V., Rizzu, P., van Baren, M. J., Schaap, O., Breedveld, G.J., Krieger, E., …. Heutink, P. (2003). Mutations in the DJ-1 gene associated with autosomal recessive early-onset parkinsonism. *Science, 299*, 256-259.

Bossis, G., & Melchoir, F. (2006). Regulation of SUMOylation by reversible oxidation of SUMO conjugating enzymes. *Molecular Cell, 21*, 349-357.

Brandis, K. A., Holmes, I. F., England, S. J., Sharma, N., Kukreja, L., & DebBurman, S. K. (2006). α-Synuclein fission yeast model concentration–dependent aggregation without plasma membrane localization or toxicity. *Journal of Molecular Neuroscience, 28*, 179-191.

Calne, D. B., Chu, N. S., Huang, C. C., Lu, C. S., & Olanow, W. (1994). Manganism and idiopathic parkinsonism: similarities and differences. *Neurology, 44,* 1583-1586.

Chan, S. C., Guzman, J. N., Ilijic, E., Mercer, J. N, Rick. C., Tkatch, T., … Surmeier, D.J. (2007). Rejuvenation protects neurons in mouse models of Parkinson's disease. *Nature, 447*, 1081-1086.

Choi, W., Zibaee, S., Jakes, R., Serpell, L., Davletov, B., Crowther, R.A., & Goedert, M. (2004). Mutation E64K increases phospholipid binding and assembly into filaments of human α-synuclein. *Federation of the Societies of Biochemistry and Molecular Biology Letters, 576*, 363-368

Choubey, W., Safiulina, D., Vaarmann, A., Cagalines, M., Wareski, P., Kuum, M., … Kaasik, A. (2011). Mutant A53T α-synuclein induces neuronal death by increasing mitochondrial autophagy. *Journal of Biological Chemistry, 286*, 1-18.

Clayton, D., & George, M. (1998). The synucleins: a family of proteins involved in synaptic function, plasticity, neurodegeneration and disease. *Trends in Neuroscience*, *21*, 249-254.

Conway, K. A., Harper, J. D., & Lansbury Jr., P. T. (1998). Accelerated in vitro fibril formation by a mutant α-synuclein linked to early-onset Parkinson disease. *Nature Medicine*, *4*, 1318-1320.

Conway, K. A., Lee, S. J., Rochet, J. C., Ding, T. T., Williamson R. E., & Lansbury Jr., P. T (2000). Acceleration of oligomerization, not fibrillization, is a shared property of both α-synuclein mutations linked to early-onset Parkinson's disease: Implications for pathogenesis and therapy. *Proceedings of the National Academy of Sciences, 97*, 571-576.

Dufty, B. M., Warner, L. R., Hou, S. T., Jiang, S. X., Gomez-Isla, T., Leenhouts, K. M., … Rohn, T. T. (2007). Calpain-cleavage of alpha-synuclein: connecting preteolytic processing to disease-linked aggregation. *The American Journal of Pathology, 170*, 1725-1738.

Fuller, N., Rand, R. P., George-Hyslop, S., & Fraser, P. E. (2002). Defective membrane interactions of familial Parkinson's disease mutant A30P alpha-synuclein. *Journal of Molecular Biology*, *315*, 799-807.

Emmer, K. L., Waxman, E.A., Covy, J.P., & Giasson, B.I. (2011). E46K human α-synuclein transgenic mice develop Lewy-like and Tau pathology associated with age-dependent, detrimental motor impairment. *Journal of Biological Chemistry, 286*, 1-22.

Fiske M., Valtierra, S., Solvang, K., Zorniak, M., White, M., Herrera, S., Konnikova, A., Brezinsky, R., DebBurman, S. (2011), Contribution of alanine-76 and serine phosphorylation in alpha-synuclein membrane association and aggregation in yeasts, *Parkinson's Disease,* DOI: 10.4061/2011/392180

Fredenburg, R. A., Rospigliosi, C., Meray, R. K., Kessler, J. C., Lashuel, H. A., Eliezer, D., & Lansubry Jr., P.T. (2007). The impact of the E46K mutation on the properties of α-synuclein in its monomeric and oligomeric states. *Biochemistry*, 1-14.

Fujiwara, H., Hasegawa, M., Dohmae, N., Kawashima, A., Masliah, E., Goldberg, M. … Iwatsubo, T. (2006). Alpha-synuclein is phosphorylated in synucleinopathy lesions. *Natural Cell Biology, 4,* 160-164.

Funayama, M., Hasegawa, K., Kowa, H., Saito, M., Tsuji, S., & Obata, F. (2002). A new locus for Parkinson's disease (PARK8) maps to chromosome 12p11.2-q13.1. *Annals of Neurology, 51*, 296-301.

Geiss-Friedlander, R., & Melchoir, F. (2007). Concepts in sumoylation: a decade on. *Nature Reviews Molecular Cell Biology, 8*, 947-956.

Glavin, J., Lee, V., & Trojanowski, J. (2001) Synucleiopathies: clinical and pathological implications, *Archives of Neurology, 58*, 186-190

Giasson, B. I., Duda, J. E., Quinn, S. M., Zhang, B., Trojanowski, J. Q., & Lee, V. M. Y. (2002). Neuronal α-synucleinpathy with severe movement disorder in mice expressing A53T human α-synuclein. *Neuron*, *34*, 521-533.

Giasson, B. I., Uryu, K., Trojanowski, J. Q., & Lee, V. M. Y. (1999). Mutant and wild type human α-synuclein assemble into elongated filaments with distinct morphologies in vitro. *The Journal of Biological Chemistry, 274*, 7619-7622.

Greenbaum, E. A., Graves, C. L., Mishizen-Elberz, A. J., Lupoli, M. A., Lynch, D. R., Englander, W., … Giasson, B. I. (2005). The E46K mutation in α-synuclein increases amyloid fibril formation. *The Journal of Biological Chemistry, 250*, 7800-7807.

Gromiha, M. (2003). Importance of native-state topology for determining the folding rate of two-state proteins. *Journal of Chemical Information and Computer Sciences, 43*, 1481-1485.

Herrera, S., & Shrestha, R. (2005). Newly discovered α-synuclein familial mutant E46K and key phosphorylation and nitrosylation-deficient mutants are toxic to yeast. *Eukaryon, 1*, 95-101.

Holzmann, C., Kruger, R., Saecker, A.M., Schmitt, I., Schols, L., Berger, K., & Riess, O. (2003). Polymorphisms of the α-synuclein promoter: expression analyses and association studies in Parkinson's disease. *Journal of Neural Transmission, 110*, 67-76.

Hodara, R., Norris, E., Giasson, B., Mishizen-Eberz, A., Lynch, D., Lee, M., & Ischiropoulos H. (2004). Functional consequences of alpha-synuclein tyrosine nitration: diminished binding to lipid vesicles and increased fibril formation. *The Journal of Biological Chemistry, 279*, 47746–47753.

Ikeda, M., Kawarabayashi, T., Harigaya, Y., Sasaki, A., Yama, S., Matsubara, E., … Shoji, M. (2009). *Brain Research,* 232-241.

Jenner, P., & Olanow, C. (1996). Oxidative stress and the pathogenesis of Parkinson's disease: a review. *Neurology 47,* S161-170.

Jensen, P. H., Nielsen, M. S., Jakes, R., Dotti, C. G., & Goedert, M. (1998). Binding of α-synuclein to brain vesicles is abolished by familial Parkinson's disease mutation. *The Journal of Biological Chemistry*, *273*, 26292-26294

Jo, E., Fuller, N., Rand, R., George-Hyslop, P.S., & Fraser, P.E. (2002). Defective membrane interactions of familial Parkinson's disease mutant A30P α-synuclein. *Journal of Molecular Biology*, *315*, 799-807.

Kahle, P. J., Neumann, M., Ozmen, L., Muller, V., Jacobsen, H., Schindzielorz, A., … Haass, C. (2000). Subcellular localization of wild-type and Parkinson's disease-associated mutant α-synuclein in human and transgenic mouse brain. *The Journal of Neuroscience, 20*, 6365-6373.

Kitada, T., Asakawa, S., Hattori, N., Matsumine, H., Yamamura, Y., Minoshima, S., Yokochi, M., Mizuno, Y., and Shimizu, N. (1998). Mutations in the parkin gene cause autosomal recessive juvenile parkinsonism. *Nature, 392,* 605-608.

Kim, H., Kim J., Lee, J., Park, S., & Jeon, B. (2010). Alpha-synulcein polymorphism and Parkinson's disease in a tau homogeneous population. *Neurology Asia, 15*, 61-63.

Kamiyoshihara, T., Kojima, M., Ueda, K., Tashiro, M., & Shimotakahara, S. (2007). Observation of multiple intermediates in α-synuclein fibril formation by singular value decomposition analysis. *Biochemical and Biophysical Research Communication, 355*, 398-403.

Kiely, A. P., Asi, Y. T., Kara, E., Limousin, P., Ling, H., Lewis, P., … Holton, J. L. (2013). α-Synucleinopathy associated with G51D SNCA mutation: a link between

Parkinson's disease and multiple system atrophy? *Acta Neuropathologica,* Published online DOI: 10.1007/s00401-013-1096-7.

Kitada, T., Pisani, A., Porter, D. R., Yamasuchi, H., Tscherter, A., Martella, G., … Shen, J. (2007). Impaired dopamine release and synaptic plasticity in the striatum of PINK1-deficient mice. *Proceedings of the National Academy of Sciences*, 104, 11441-11446.

Kruger, R., Kuhn, W., Muller, T., Woitalla, D., Graeber, M., Kosel, S., … Riess, O. (1998). Ala30Pro mutation in the gene encoding alpha-synuclein in parkinson's disease. *Nature Genetics, 18*, 106-108.

Langston, J. W., Ballard, P., Tetrud, J. W., & Irwin, I. (1983). Chronic Parkinsonism in humans due to a product of meperidine-analog synthesis. *Science, 219,* 979-980.

Langston, J. W., Langston, E. B., & Irwin, I. (1984). MPTP-induced parkinsonism in human and non-human primates--clinical and experimental aspects. *Acta Neurologica Scandinavica, Supplementum, 100*, 49-54.

Lelan, F., Boyer, C., Thinard, R., Remy, S., Usal, C., Tesson, L, … Lescaudron, L. (2011). Effects of human alpha-synuclein A53T-A30P mutation on SVZ and local olfactory bulb cell proliferation in a transgenic rat model of Parkinson's disease. *Parkinson's Disease,* 1-11.

Li, W., West, N., Colla, E., Pletnikova, O., Troncoso, J. C., Marsh, L., & Lee, M. K. (2005). Aggregation promoting C-terminal truncation of α-synuclein is a normal cellular process and is enhanced by the familial Parkinson's disease-linked mutations. *Proceedings of the National Academy of Sciences of the United States of America*, *102*, 2162-2167.

Liu, G., Qu, J., Suzuki, K., Nivet, E., Li, M., Montserrat, N., … Belmonte, J. C. I. (2012). Letter: Progressive degeneration of human neural stem cells caused by pathogenic LRRK2. *Nature, 491*, 603-607.

Liu, Y., Fallon, L., Lashuel, H.A., Liu, Z., & Lansbury Jr., P.T. (2002). The UCH-L1 gene encodes two opposing enzymatic activities that affect alpha-synuclein degradation and Parkinson's disease susceptibility. *Cell, 111,* 209-218.

Liu, C. W., Giasson, B. I., Lewis, K. A., Lee, V. M., Demartino, G. N., & Thomas, P. J. (2005). A precipitating role for truncated alpha-synuclein and the proteasome in alpha-synuclein aggregation: implications for pathogenesis of Parkinson disease. *The Journal of Biological Chemistry, 280*, 22670-8.

Lucking, C. B., & Brice, A. (2000). Review: Alpha-synuclein and Parkinson's disease. *Cellular and Molecular Life Sciences, 57*, 1894-1908.

Maguire-Zeiss, K. A., Short, D. W., & Federoff, H. J. (2005). Synuclein, dopamine and oxidative stress: co-conspirators in Parkinson's disease? *Molecular Brain Research, 134*, 18-23.

McLean, P. J., Kawamata, H., Ribich, S., & Hyman, B.T. (2000). Membrane association and protein conformation of α-synuclein in intact neurons. *The Journal of Biological Chemistry, 275*, 8812-8816.

McLean, J. R., Hallett, P. J., Cooper, O., Stanley, M., Isacson, O. (2012). Transcript expression levels of full-length alpha-synuclein and its three alternatively spliced variants in Parkinson's disease brain regions and in a transgenic mouse model of alpha-synuclein overexpression. *Molecular and Cellular Neuroscience, 49*, 230-239.

Myhre, R., Toft, M., Kachergus, J., Hulihan, M., Aasly, J. O., Klungland, H., & Farrer, M. J. (2008). Multiple alpha-synuclein gene polymorphisms are associated with Parkinson's disease in a Norwegian population. *Acta Neurologica Scaninavica*, *118*, 320-327.

National Institute of Neurological Disorders and Stroke (2004). Parkinson's disease: challenges, progress and promise. Retrieved from URL http://www.ninds.nih.gov/disorders/parkinsons_disease/parkinsons_research.

Neuytemans, K., Theuns, J., Cruts, M., & Van Broeckhoven, C. (2010). Genetic Etiology of Parkinson Disease Associated with Mutations in the SNCA, PARK2, PINK1, PARK7, and LRRK2 Genes: A mutation Update. *Human Mutation,* 764-780.

Olanow, C. W., & Tatton, W. G. (1999). Etiology and pathogenesis of Parkinson's disease. *Annual Review of Neuroscience, 22*, 123-144.

Outeiro, T.F., Lindquist, S. (2003). Yeast Cells Provide Insight into Alpha- Synuclein Biology and Pathobiology. *Science, 302*(5651), 1772-1775.

Paisan-Ruiz, C., Jain, S., Evans, E. W., Gilks, W. P., Simon, J., van der Brug, M., … Singleton, A. B. (2004). Cloning of the gene containing mutations that cause PARK8-linked Parkinson's disease. *Neuron, 44,* 595-600.

Paleologou, K. E., Oueslati, A., Shakked, G., Rospigliosi, C. C., Kim, H. Y., Lamberto, G. R., … Lashuel, H. A. (2010). Phosphorylation at S87 is enhanced in synucleinopathies, inhibits alpha-synuclein oligomerization, and influences synuclein-membrane interactions. *The Journal of Neuroscience, 30* (9), 3184-3198.

Pandey, N., Schimidt, R. E., & Galvin, J.E. (2005). The alpha-synuclein mutation E64K promotes aggregation in cultured cells. *Experimental Neurology*, 1-6.

Parkinson's Disease Foundation. (2012). Statistics on Parkinson's, Retrieved from URL http://www.pdf.org/en/parkinson_statistics

Parkinson, J. (1817). An essay on the shaking palsy. London: Whittingham and Rowland.

Polymeropoulos, M. H, Lavedan, C., Leroy, E., Ide, S. E., Dehejia, A., Dultra, A., … Nussbaum, R. L. (1997). Mutation in the α-synuclein gene identified in families with Parkinson's disease. *Science, 276*, 2045-2047

Prasad, K., Tarasewicz, E., Strickland, P., O'Neil, M., Mitchell, S., & Mechant, K., (2011). Biochemical and morphological consequences of human a-synuclein expression in a mouse a-synuclein null background. *European Journal of Science, 33,* 642-656.

Purves, D., Augustine, G., Fitzpatrick, D., Hall, W., Lamantia, A., McNamara, J., & White, L. (2012). *Neuroscience, Fifth Edition,* Sinauer Associates.

Raaij, M. E. V., Segers-Nolten, I. M. J., & Subramaniam, V. (2006). Quantitative morphological analysis reveals ultrastructual diversity of amyloid fibrils from α-synuclein mutants. *Biophysical Journal: Biophysical Letters,* 96-98.

Ross, C. A., & Poirier, M. A. (2004). Protein aggregation and neurodegenerative disease, *Nature Medicine, 10*, S10-7.

Schwede, T., Kopp, J., Guex, N. & Peitsch, M. C. (2003). SWISS-MODEL: an automated protein homology-modeling server. *Nucleic Acids Research*, *31,* 3381-3385.

Sian, J., Youdim, M., Riederer, P., & Gerlach, M. (1999). MPTP-Induced Parkinsonian Syndrome. *Basic Neurochemistry: Molecular, Cellular and Medical Aspects.* Philadelphia: Lippincott-Raven. Available from: http://www.ncbi.nlm.nih.gov/books/NBK27974/

Sharma, N., Brandis, K. A., Herrera, S. K., Johnson, B. E., Vaidya, T., Shrestha, R., & DebBurman, S. K. (2006). α-Synuclein budding yeast model toxicity enhanced by impaired proteasome and oxidative Stress. *Journal of Molecular Neuroscience, 28*, 161-178.

Sharon, R., Bar-Joseph, I., Frosch, M. P., Walsh, D. M, Hamilton, J. A., & Selkoe, D. J. (2003). The formation of highly soluble oligomers of α-synuclein is regulated by fatty acids and enhanced in Parkinson's disease. *Neuron, 37*, 583-595.

Sharon, R., Goldberg, M. S., Josef, I. B., Betensky, R. A., Shen, J., & Selkoe, D. J. (2001). α-synuclein occurs in lipid-rich high molecular weight complexes, binds fatty acids, and shows homology to the fatty acid- binding proteins. *Proceedings of the National Academy of Sciences, 98*, 9110-9115.

Shin, J., Dawson, V., & Dawson, T. (2009). SnapShot: pathogenesis of Parkinson's disease. *Cell, 139*, 440.

Spillantini, A. G., Crowther R. A., Jakes R., Hasegawa, M., & Goedert M. (1998). α-Synuclein in filamentous inclusions of Lewy bodies from Parkinson's disease and dementia with Lewy bodies. *Proceedings of the National Academy of Sciences, 95*, 6469-6473.

Taylor, J. P., Hardy, J., & Fischbeck, K. H. (2002). Toxic proteins in neurodegenerative disease. *Science 296*, 1991-1995.

Valente, E. M., Abou-Sleiman, P. M., Caputo, V., Muqit, M. M., Harvey, K., Gispert, S., … Wood, N. W. (2004). Hereditary early-onset Parkinson's disease caused by mutations in PINK1. *Science, 304,* 1158-1160

Vriend, G. (1990). WHAT IF: A molecular modeling and drug design program, *Journal of Molecular Graphics, 8*, 52-56.

Wersinger, C., Prou, D., Vernier, P., Niznik, H. B., & Sidhu, A. (2003). Mutations in the lipid-binding domain of α-Synuclein confer overlapping yet distinct, functional properties in the regulation of dopamine transporter activity. *Molecular and Cellular Neuroscience, 24*, 91-105.

Wilkinson, K., Knopacki, F., & Henley. J. (2012). Modification and movement: Phosphorylation and SUMOylation regulate endocytosis of GluK2-containing kainate receptors. *Communicative &Integrative Biology, 5*, 223-226

Xiong, L., Zhao, P., Guo, Z., Zhang, J., Li, D., & Mao, C. (2010). Alpha-synuclein gene structure, evolution and protein aggregation. *Neural Regeneration Research, 5*, 1423-1428.

Zarranz, J. J., Alegre, J., Gomez-Esteban, J. C., Lezcano, E., Ros, R., Ampuero, I., … de Yebenes, J. G. (2004). The new mutation, E46K, of alpha-synuclein causes Parkinson and Lewy body dementia. *Annals of Neurology, 55*, 164-173.

## APPENDIX:

### A. LOCALIZATION

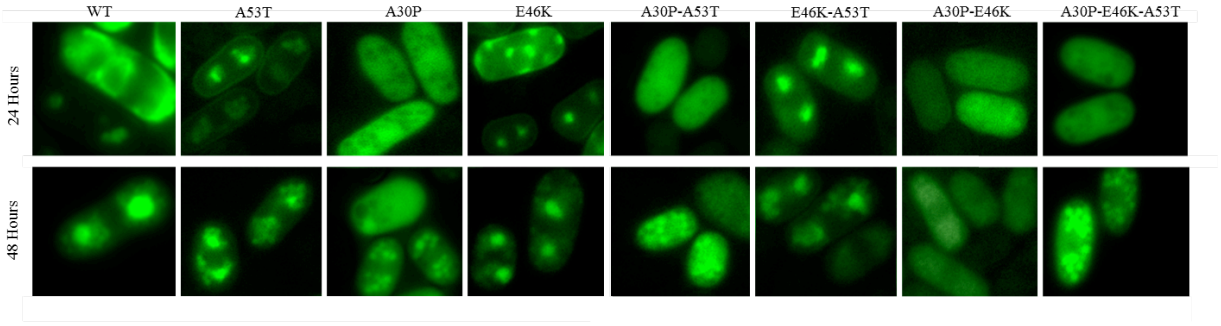


### B. QUANTIFICATION

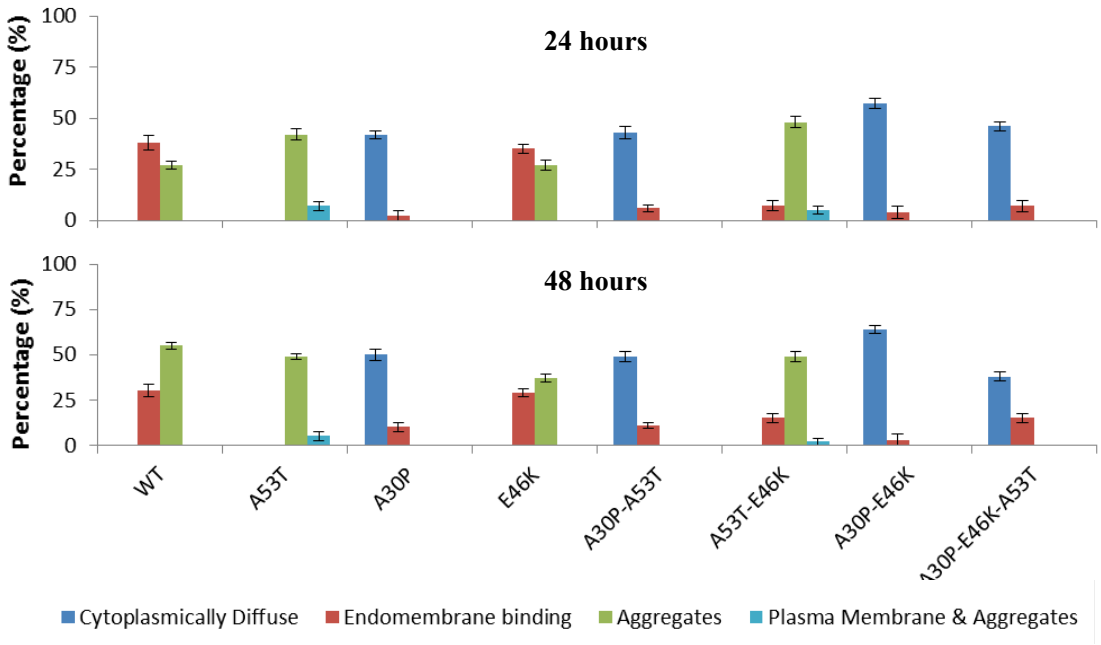


*Figure 20. Protein localization in a high expressing yeast model, (Sph+).*

A. Time course fluorescent microscopy. The following mutations of α-synuclein were evaluated in comparison to its WT localization: A53T, A30P, E46K, A30P-A53T, E46K-A53T, A30P-E46K, and A30P-E46K-A53T. The mutants were expressed in the Sph+ strain of fission yeast. Microscopy photographs were captured at 24 and 48 hours post induction with EMM-T (n=5).

B. Time course quantification. WT, A53T, A30P, E46K, A30P-A53T, E46K-A53T, A30P-E46K, and A30P-E46K-A53T were quantified for photographs captured at 24 and 48 hours post induction with EMM-T (n=5). The error bars represent standard deviation based on the averaged results.

**A. TOXICITY**

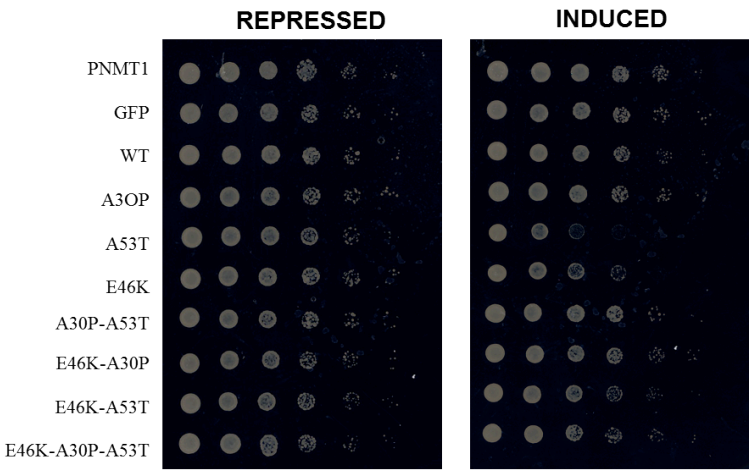


**B. EXPRESSION**

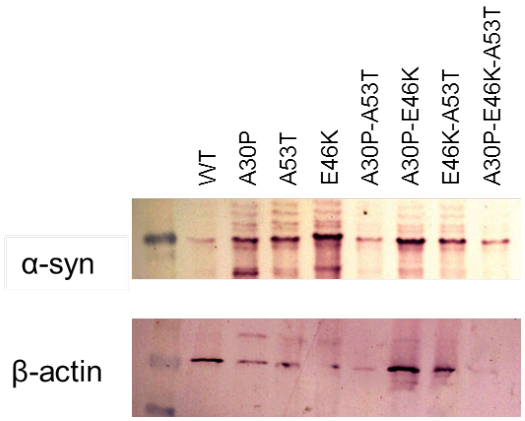


*Figure 21. Toxicity and protein accumulation in a high expressing yeast model, (Sph+).*
A. Spotting. Yeast expressing PNMT1, GFP, WT, A30P, A53T, E46K, A30P-A53T, E46K-A30P, E46K-A53T and E46K-A30P-A53T α-synuclein spotted onto a repressive media (EMM+T) and inductive media (EMM-T) after a five-fold serial dilutions (n=5).
B. Expression. Western Blot at 48 hours of WT, A30P, E46K, A53T, A30P-E46K, A30P-A53T, E46K-A53T, and E46K-A30P-A53T expression (anti-V5) with the loading control below (β-actin) (n=4).

**D. EXPERIMENTAL DESIGN**

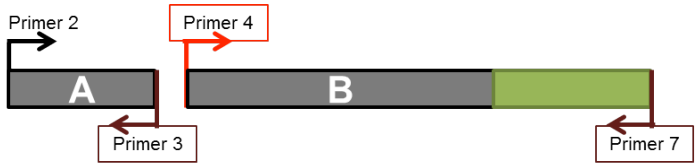


Segments for α-synuclein 126

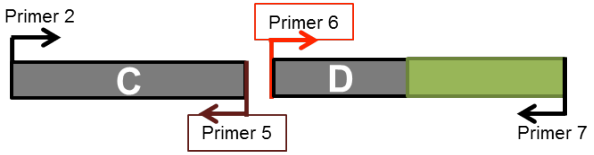


Segments for α-synuclein 112

**C. EXPERIMENTAL OUTCOME**

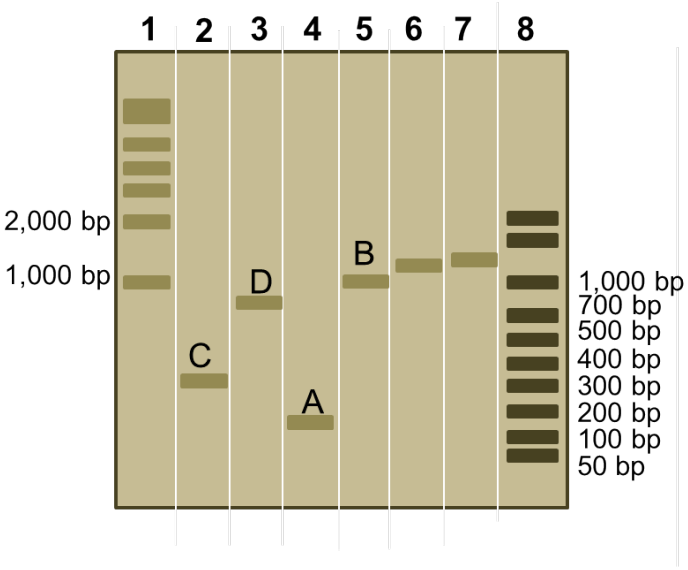


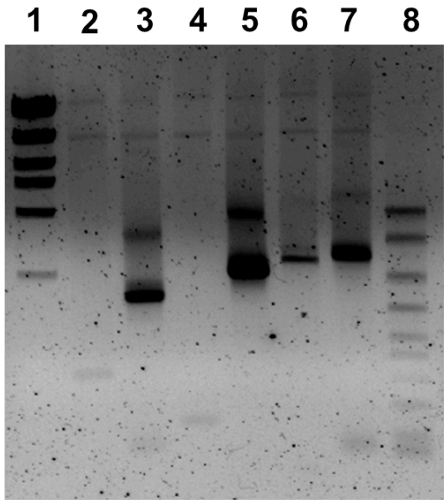


**Legend:**
1. High Mass Ladder
2. Segment C
3. Segment D
4. Segment A
5. Segment B
6. Control 1
7. Control 2
8. AmpliSize Ladder

*Figure 22. Formation of splice variants' segments (fall attempt)*

A. Experimental design. Desired segments for each splice variant created through the first round of PCR with the appropriate primers.
B. Experimental outcome. First round PCR results. Lane 1 is the high mass ladder, lane 2 is segment C, lane 3 is segment D, lane 4 is segment A and lane 5 is segments B, lane 6 is the first control and lane 7 is the second control. The two controls were utilized to ensure that the primers were functioning correctly. *Although the segments were further fused used to create α-synuclein-126 and α-synuclein-112 they were not TOPO cloned.

## A. EXPERIMENTAL DESIGN

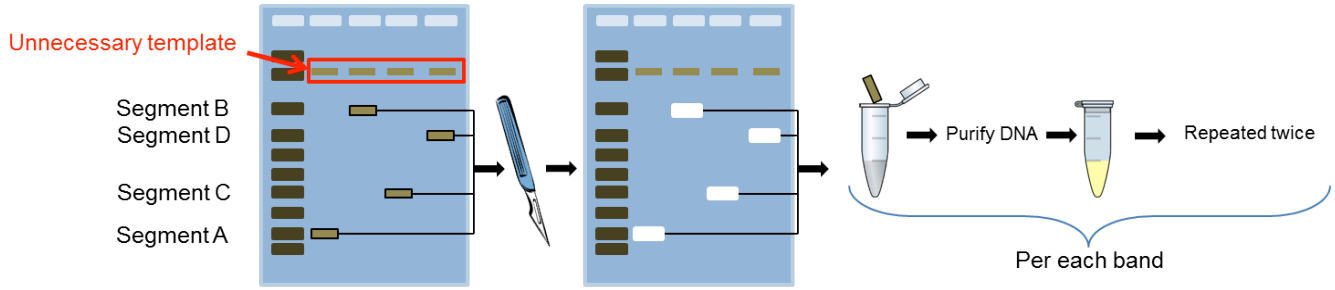


## B. EXPERIMENTAL OUTCOME

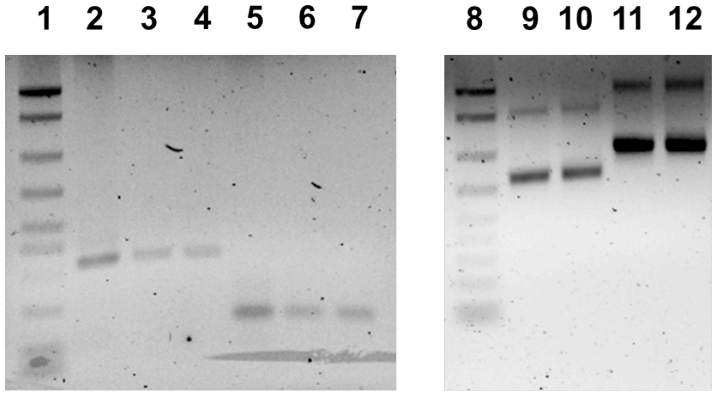


**Legend:**

1. AmpliSize Ladder
2. Segment C original PCR
3. Segment C purified PCR
4. Segment C purified PCR
5. Segment A original PCR
6. Segment A purified PCR
7. Segment A purified PCR
8. AmpliSize Ladder
9. Segment D purified PCR
10. Segment D purified PCR
11. Segment B purified PCR
12. Segment B purified PCR

*Figure 23. Purification of splice variants' segments (fall attempt).*

A. Experimental design. Exemplified is a cartoon of the purification process of the PCR product acquired for each segment. Each PCR product was run independently on the gel. The band was then cut out and purified. This process was repeated twice for each PCR product indicative of the four created segments.
B. Experimental outcome. To ensure minimal loss of product during the purification technique the original PCR product was compared to the purified product for each segment.

**A. EXPERIMENTAL DESIGN**

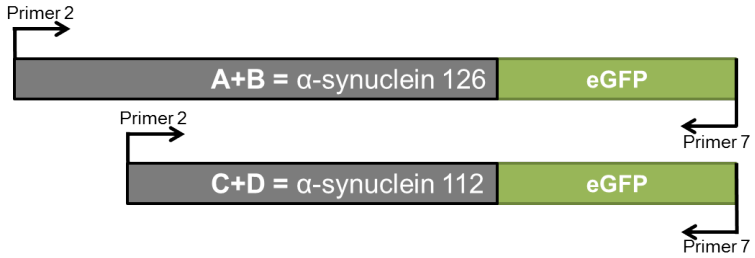


**B. EXPERIMENTAL OUTCOME**

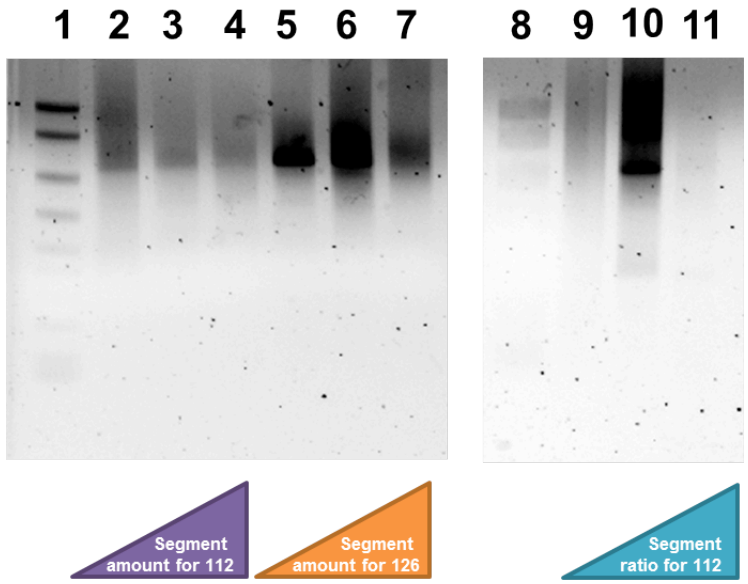


**Legend**:
1. Amp Ladder
2. 112 (low)
3. 112 (medium)
4. 112 (high)
5. 126 (low)
6. 126 (medium)
7. 126 (high)
8. Amp Ladder
9. 112 (1:1 ratio)
10. 112 (1:2 ratio)
11. 112 (1:3 ratio)

*Figure 24. Segment fusion (fall attempt).*

A. Experimental design. Desired splice variants for each α-synuclein isoform from fused segments acquired through the second round of PCR.

Experimental outcome. To acquire the best quality product two conditions were created. First: the amount of the two segments used for each splice variant was equally increased (employed for α-synuclein-112 and 126); second: the amount of the weaker product (segment C) was equal, twice or three times the amount of segment D (employed for α-synuclein-112). Lanes 1 and 8 are AmpliSize ladder. Lanes 2, 3 and 4 represent α-synuclein 112 splice variant using low, medium or high template amount respectively. Lanes 5, 6, and 7 represent α-synuclein 126 splice variant using low, medium or high template amount respectively. Lanes 9, 8 and 10 represent α-synuclein 112 splice variant using template ratios: 1:1, 1:2, 1:3.

**DISCUSSION:**

Recently, three splice variants (α-synuclein-98, -112, and -126) were identified in various synucleinopathies (Beyer et al., 2006; Beyer et al., 2008; McLean et al., 2012) and in animal PD models (McLean et al., 2012). More specifically, these splice variants of the protein were identified as components of Lewy bodies which are a hallmark characteristic of PD pathology (McLean et al., 2012). In addition to PD, other diseases such as Dementia with Lewy bodies (DLB), Lewy body variant of Alzheimer disease (LBVAD), and multiple system atrophy (MSA) can be pathologically unified by the presence of Lewy bodies with α-synuclein as their main component (Beyer et al., 2004; Beyer, 2006; Dufty et al., 2007). Whether any of the α-synuclein splice variants can directly protect or harm cells is not known, thus there is a high need for their individual expression in model organisms to assess each of their functions. Thus, my goal was to construct at least two of the α-synuclein splice variants (α-synuclein-126 and -112) to create tools for future expression in various yeast models.

**Creation of α-Synuclein Splice Variants**

As part of the second goal of my thesis, I created two splice variants, α-synuclein-126 and α-synuclein-112, but I was only successful with the process of TOPO cloning in regard to α-synuclein-126. Although the generated splice variants for α-synuclein-126 and -112 have not yet been sequenced, their base pair sizes seem appropriate for each one of the variants. The limitation of the process of splice-variant creation is that the indication of their correct splice variant acquisition is based on the

ladder utilized in gel electrophoresis. With variants that are similar in size, such as α-synuclein-126 and α-synuclein-112, the differences between exemplified segments can be miniscule. Overall, the biggest drawback in the process of forming these isoforms is that one will not know if the progression was successful until the final sequencing.

**Uncovering the Roles of Splice Variants**

Based on the available literature about the three splice variants in neurodegenerative diseases, I developed a prediction for the roles of each α-synuclein isoform. If given the opportunity to express each one of them individually in a yeast model, I would expect specific features in regard to protein localization, toxicity and expression. According to my hypothesis, in budding and fission yeasts, α-synuclein-98 and -126 would show diffusion throughout the cell, due to the impairment of regions responsible for plasma membrane binding; while α-synuclein-112 would show the formation of aggregates (Figure 20). While the formation of such aggregates would not be visible in the low expression model with the regular green fluorescent tag (GFP), we could use the higher expression budding yeast model with the enhanced green fluorescent tag (eGFP) to note possibly different results.

The reason why I believe α-synuclein-112 would form aggregates is because the deletion of amino acids 103-130 results in a characteristic shortening of the C-terminal, which makes the protein highly hydrophobic and prone for aggregation (Xiong et al., 2010). Studies have shown that C-terminally truncated α-synuclein demonstrates

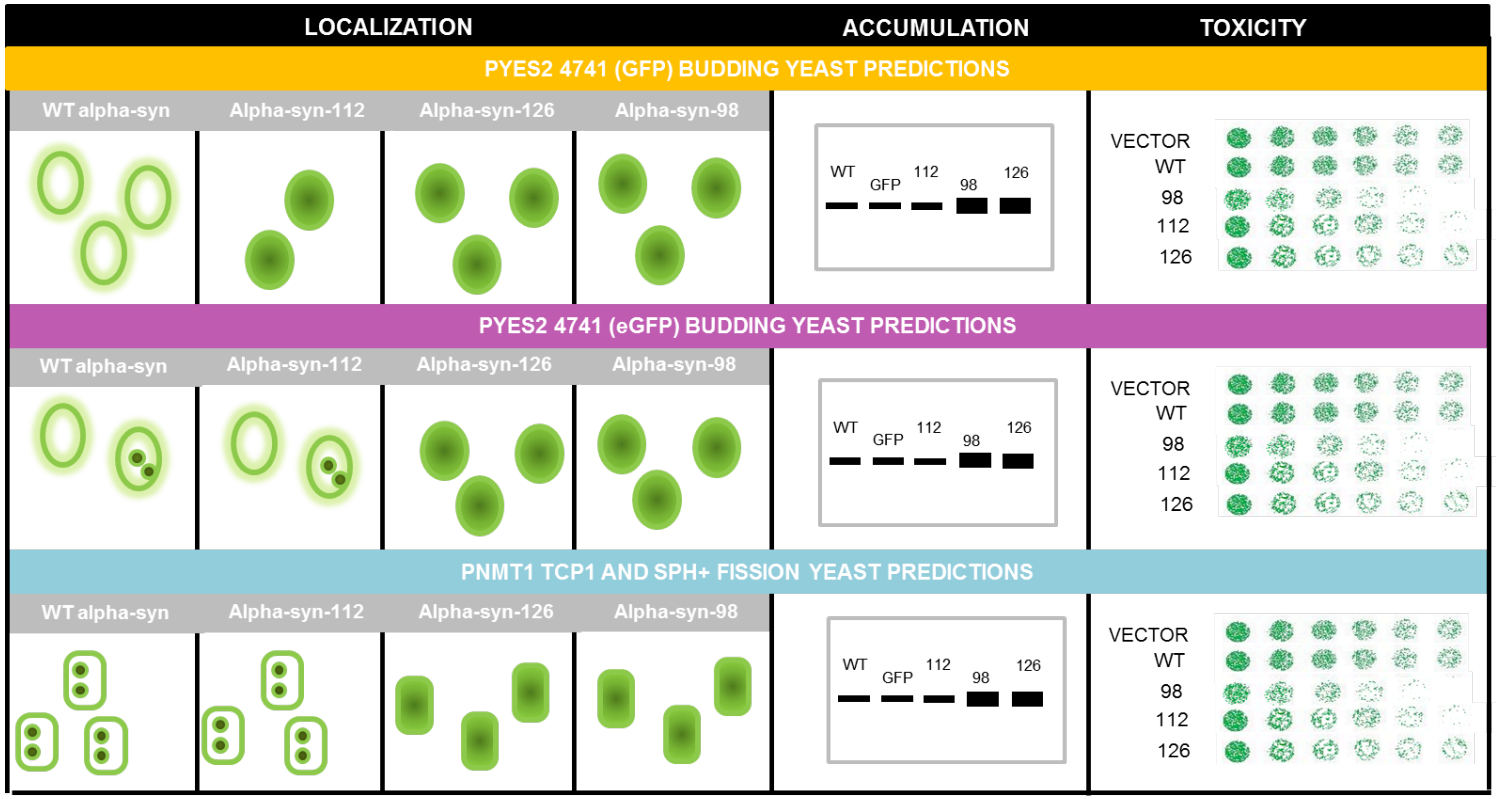


*Figure 20. Prediction for α-synuclein splice variants' properties.*

*Figure 20. Prediction for α-synuclein splice variants' properties.* This is a visual representation of the hypothesis for the behavior of splice variants in yeast models of low and high expression. The low expression model is budding yeast with GFP tag, while the high expression models are two fission yeast strains and budding yeast with eGFP tag. Localization, accumulation and toxicity were the assays of interest. According to my predictions, α-synuclein-126 and -98 will show cytoplasmic diffusion in all models, and α-synuclein-112 will showcase cytoplasmic diffusion in low expressing model and aggregation in high expressing models. Compared to WT, protein expression will be higher in α-synuclein-126 and -98, while higher toxicity will be exhibited by α-synuclein-112.

higher aggregation tendencies would be consistent with α-synuclein-112's tendencies to form aggregates (Li et al., 2005). Additionally, the deletion of the Calpain cleavage site (117-122aa) has been shown to independently result in aggregation and adaptation of beta-sheet configuration of the α-synuclein protein (Dufty et al., 2007). Since this site overlaps with the deletion within the α-synuclein-112 splice variant, this further explains and supports its predisposition for aggregation. The α-synuclein-126 would not form aggregates, and instead would show cytoplasmic diffusion because the deletion of exon 3 results in lack of amino acids 41-54 (Beyer et al., 2006), which likely interrupts helices three and four that aid protein-membrane interactions (Xiong et al., 2010). This truncation also lacks two amino acids mutated in familial PD (E46K and A53T), which show characteristic plasma membrane binding (Beyer et al., 2006). Therefore, due to its hindered ability for lipid association, I would hypothesize that the protein would be cytoplasmically diffused. Similarly, I hypothesize that α-synuclein-98 would lack lipid association and be unable to aggregate due to lack of exons 3 and 5 (Beyer et al. 2008). Thus, it would also showcase the phenotype of cytoplasmic diffusion.

In regard to cytotoxicity, I would expect the α-synuclein-112 and -98 to be more toxic than α-synuclein-126 because of its truncated C-terminal, which is known to serve a role in neuroprotection (Figure 20). Nevertheless, the toxicity patterns of splice variants are yet to be assessed, which is why such experiments would bring novel and insightful information. Based on results from patients' data, I would further expect the accumulation to be the highest for α-synuclein-126, followed by -98 and then -112 (Figure 20). This prediction could be supported by Beyer et al.'s finding from 2008,

where the SNCA gene was upregulated for splice variants 126 and 98 in PD. Furthermore, in 2012 McLean et al. found that α-synuclein-126 and -98 seemed to be co-localized and elevated in substantia nigra and cerebellum, while α-synuclein-112 expressions was elevated only in the cerebellum.

**CONCLUSION:**

Understanding the complexities of any neurodegenerative disease is a mighty task for every scientist, whether “big” or “small”. Nevertheless, human curiosity and need for understanding propels scientific research on various topics with diversified study models conducted all over the world. As an undergraduate student I embraced the challenge of studying a problem of protein misfolding associated with the onset of PD, and the results of my work are exemplified in this body of work.

Through the use of a simple organism such as yeast, I characterized the properties of combinatory mutants and provided greater insight into understanding the α-synuclein protein. The unexpected finding of A30P dominance gave further understanding into structural dynamics of the protein, but also generated further questions that ought to be pursued. Moreover, through the appropriate use of a simple series of PCR reactions, I created two α-synuclein splice variants 126 and 112. Future independent expression of these isomers in yeast should help to understand their role in Lewy body composition and PD pathology. Hence yeast models are powerful model organisms that can provide understanding of protein’s properties on the molecular level, as well as insight into human disease by uncovering the details leading to its pathology.

## References


Alberts, B., Bray, D., Hopkin, K., Johnson, A., Lewis, J., Raff, M., …&Walter, P. (2010). *Essential Cell Biology*. Garland Science: New York.

Benkert, P., Tosatto, S. C. E., & Schomburg, D. (2008). QMEAN: A comprehensive scoring function for model quality assessment. *Proteins: Structure, Function, and Bioinformatics, 71*, 261-277.

Betarbet, R., Sherer, T., MacKenzie, G., Garcia-Osuna, M., Panov, A., & Greenamyr, J. (2000). Chronic systemic pesticide exposure reproduces features of Parkinson's disease. *Natural Neuroscience, 3*, 1301-1306.

Beyer, K., Domingo-Sabat, M., Humbert, J., Carrato, C., Ferrer, I., & Ariza, A. (2008). Differential expression of alpha-synuclein, parkin, and synphilin-1 isoforms in Lewy body disease. *Neurogenetics, 9*, 163-172.

Beyer, K., Lao, J. I., Carrato, C., Mate, J. L., Lopez D., Ferrer, I., & Ariza, A. (2004). Differential expression of alpha-synuclein isoforms in dementia with Lewy bodies. *Neuropathology and Applied Neurobiology, 30*, 601-607.

Beyer, K. (2006). Review: Alpha-synuclein structure, posttranslational modification and alternative splicing as aggregation enhancers. *Acta Neuropathologica, 112*, 237-251.

Beyer, K., Humbert, J., Ferrer, A., Lao, J. I., Carrato, C., López, D., Ferrer, I., & Ariza, A. (2006). Low alpha-synuclein 126 mRNA levels in dementia with Lewy bodies and Alzheimer disease. *Neuroreport, 17*, 1327-1330.

Beyer, K., Domingo-Sabat, M., Lao, J. I., Carrato, C., Ferrer, I., & Ariza, A. (2008). Identification and characterization of a new alpha-synuclein isoform and its role in Lewy body diseases. *Neurogenetics*, *9*, 15-23.

Beyer, K., & Ariza, A. (2012). Alpha-synuclein posttranslational modification and alternative splicing as a trigger for neurodegeneration. *Molecular Neurobiology*. Published online. DOI 10.1007/s12035-8330-5.

Bisaglia, M., Mammi, S., & Bubacco, L., (2009). Review: Structural insight, physiological functions, and pathological effects of alpha-synuclein. *The Federation of American Society for Experimental Biology Journal, 23*, 329-340.

Bonifati, V., Rizzu, P., van Baren, M. J., Schaap, O., Breedveld, G.J., Krieger, E., …. Heutink, P. (2003). Mutations in the DJ-1 gene associated with autosomal recessive early-onset parkinsonism. *Science, 299*, 256-259.

Bossis, G., & Melchoir, F. (2006). Regulation of SUMOylation by reversible oxidation of SUMO conjugating enzymes. *Molecular Cell, 21*, 349-357.

Brandis, K. A., Holmes, I. F., England, S. J., Sharma, N., Kukreja, L., & DebBurman, S. K. (2006). α-Synuclein fission yeast model concentration–dependent aggregation without plasma membrane localization or toxicity. *Journal of Molecular Neuroscience, 28*, 179-191.

Calne, D. B., Chu, N. S., Huang, C. C., Lu, C. S., & Olanow, W. (1994). Manganism and idiopathic parkinsonism: similarities and differences. *Neurology, 44,* 1583-1586.

Chan, S. C., Guzman, J. N., Ilijic, E., Mercer, J. N, Rick. C., Tkatch, T., … & Surmeier, D.J. (2007). Rejuvenation protects neurons in mouse models of Parkinson's disease. *Nature, 447*, 1081-1086.

Choi, W., Zibaee, S., Jakes, R., Serpell, L., Davletov, B., Crowther, R.A., & Goedert, M. (2004). Mutation E64K increases phospholipid binding and assembly into filaments of human α-synuclein. *Federation of the Societies of Biochemistry and Molecular Biology Letters, 576*, 363-368

Choubey, W., Safiulina, D., Vaarmann, A., Cagalines, M., Wareski, P., Kuum, M., … Kaasik, A. (2011). Mutant A53T α-synuclein induces neuronal death by increasing mitochondrial autophagy. *Journal of Biological Chemistry, 286*, 1-18.

Clayton, D., & George, M. (1998). The synucleins: a family of proteins involved in synaptic function, plasticity, neurodegeneration, and disease. *Trends in Neuroscience*, *21*, 249-254.

Conway, K. A., Harper, J. D., & Lansbury Jr., P. T. (1998). Accelerated in vitro fibril formation by a mutant α-synuclein linked to early-onset Parkinson disease. *Nature Medicine*, *4*, 1318-1320.

Conway, K. A., Lee, S. J., Rochet, J. C., Ding, T. T., Williamson R. E., & Lansbury Jr., P. T (2000). Acceleration of oligomerization, not fibrillization, is a shared property of both α-synuclein mutations linked to early-onset Parkinson's disease: Implications for pathogenesis and therapy. *Proceedings of the National Academy of Sciences, 97*, 571-576.

Dufty, B. M., Warner, L. R., Hou, S. T., Jiang, S. X., Gomez-Isla, T., Leenhouts, K. M., … & Rohn, T. T. (2007). Calpain-cleavage of alpha-synuclein: connecting preteolytic processing to disease-linked aggregation. *The American Journal of Pathology, 170*, 1725-1738.

Fuller, N., Rand, R. P., George-Hyslop, S., & Fraser, P. E. (2002). Defective membrane interactions of familial Parkinson's disease mutant A30P alpha-synuclein. *Journal of Molecular Biology*, *315*, 799-807.

Emmer, K. L., Waxman, E.A., Covy, J.P., & Giasson, B.I. (2011). E46K human α-synuclein transgenic mice develop Lewy-like and Tau pathology associated with age-dependent, detrimental motor impairment. *Journal of Biological Chemistry, 286*, 1-22.

Fiske M., Valtierra, S., Solvang, K., Zorniak, M., White, M., Herrera, S., Konnikova, A., Brezinsky, R., DebBurman, S. (2011), Contribution of alanine-76 and serine phosphorylation in alpha-synuclein membrane association and aggregation in yeasts, *Parkinson's Disease,* DOI: 10.4061/2011/392180

Fredenburg, R. A., Rospigliosi, C., Meray, R. K., Kessler, J. C., Lashuel, H. A., Eliezer, D., & Lansubry Jr., P.T. (2007). The impact of the E46K mutation on the properties of α-synuclein in its monomeric and oligomeric states. *Biochemistry*, 1-14.

Fujiwara, H., Hasegawa, M., Dohmae, N., Kawashima, A., Masliah, E., Goldberg, M. … Iwatsubo, T. (2006). Alpha-synuclein is phosphorylated in synucleinopathy lesions. *Natural Cell Biology, 4,* 160-164.

Funayama, M., Hasegawa, K., Kowa, H., Saito, M., Tsuji, S., & Obata, F. (2002). A new locus for Parkinson's disease (PARK8) maps to chromosome 12p11.2-q13.1. *Annals of Neurology, 51*, 296-301.

Geiss-Friedlander, R., & Melchoir, F. (2007). Concepts in sumoylation: a decade on. *Nature Reviews Molecular Cell Biology, 8*, 947-956.

Glavin, J., Lee, V., & Trojanowski, J. (2001) Synucleiopathies: clinical and pathological implications, *Archives of Neurology, 58*, 186-190

Giasson, B. I., Duda, J. E., Quinn, S. M., Zhang, B., Trojanowski, J. Q., & Lee, V. M. Y. (2002). Neuronal α-synucleinpathy with severe movement disorder in mice expressing A53T human α-synuclein. *Neuron*, *34*, 521-533.

Giasson, B. I., Uryu, K., Trojanowski, J. Q., & Lee, V. M. Y. (1999). Mutant and wild type human α-synuclein assemble into elongated filaments with distinct morphologies in vitro. *The Journal of Biological Chemistry, 274*, 7619-7622.

Greenbaum, E. A., Graves, C. L., Mishizen-Elberz, A. J., Lupoli, M. A., Lynch, D. R., Englander, W., … & Giasson, B. I. (2005). The E46K mutation in α-synuclein increases amyloid fibril formation. *The Journal of Biological Chemistry, 250*, 7800-7807.

Gromiha, M. (2003). Importance of native-state topology for determining the folding rate of two-state proteins. *Journal of Chemical Information and Computer Sciences, 43*, 1481-1485.

Herrera, S., & Shrestha, R. (2005). Newly discovered α-synuclein familial mutant E46K and key phosphorylation and nitrosylation-deficient mutants are toxic to yeast. *Eukaryon, 1*, 95-101.

Holzmann, C., Kruger, R., Saecker, A.M., Schmitt, I., Schols, L., Berger, K., & Riess, O. (2003). Polymorphisms of the α-synuclein promoter: expression analyses and association studies in Parkinson's disease. *Journal of Neural Transmission, 110*, 67-76.

Hodara, R., Norris, E., Giasson, B., Mishizen-Eberz, A., Lynch, D., Lee, M., & Ischiropoulos H. (2004). Functional consequences of alpha-synuclein tyrosine nitration: diminished binding to lipid vesicles and increased fibril formation. *The Journal of Biological Chemistry, 279*, 47746–47753.

Ikeda, M., Kawarabayashi, T., Harigaya, Y., Sasaki, A., Yama, S., Matsubara, E., … Shoji, M. (2009). *Brain Research,* 232-241.

Jenner, P., & Olanow, C. (1996). Oxidative stress and the pathogenesis of Parkinson's disease: a review. *Neurology, 47,* S161-170.

Jensen, P. H., Nielsen, M. S., Jakes, R., Dotti, C. G., & Goedert, M. (1998). Binding of α-synuclein to brain vesicles is abolished by familial Parkinson's disease mutation. *The Journal of Biological Chemistry*, *273*, 26292-26294

Jo, E., Fuller, N., Rand, R., George-Hyslop, P.S., & Fraser, P.E. (2002). Defective membrane interactions of familial Parkinson's disease mutant A30P α-synuclein. *Journal of Molecular Biology*, *315*, 799-807.

Kahle, P. J., Neumann, M., Ozmen, L., Muller, V., Jacobsen, H., Schindzielorz, A., … Haass, C. (2000). Subcellular localization of wild-type and Parkinson's disease-associated mutant α-synuclein in human and transgenic mouse brain. *The Journal of Neuroscience, 20*, 6365-6373.

Kitada, T., Asakawa, S., Hattori, N., Matsumine, H., Yamamura, Y., Minoshima, S., Yokochi, M., Mizuno, Y., and Shimizu, N. (1998). Mutations in the parkin gene cause autosomal recessive juvenile parkinsonism. *Nature, 392,* 605-608.

Kim, H., Kim J., Lee, J., Park, S., & Jeon, B. (2010). Alpha-synulcein polymorphism and Parkinson's disease in a tau homogeneous population. *Neurology Asia, 15*, 61-63.

Kamiyoshihara, T., Kojima, M., Ueda, K., Tashiro, M., & Shimotakahara, S. (2007). Observation of multiple intermediates in α-synuclein fibril formation by singular value decomposition analysis. *Biochemical and Biophysical Research Communication, 355*, 398-403.

Kiely, A. P., Asi, Y. T., Kara, E., Limousin, P., Ling, H., Lewis, P., … & Holton, J. L. (2013). α-Synucleinopathy associated with G51D SNCA mutation: a link between

Parkinson's disease and multiple system atrophy? *Acta Neuropathologica,* Published online DOI: 10.1007/s00401-013-1096-7.

Kitada, T., Pisani, A., Porter, D. R., Yamasuchi, H., Tscherter, A., Martella, G., …& Shen, J. (2007). Impaired dopamine release and synaptic plasticity in the striatum of PINK1-deficient mice. *Proceedings of the National Academy of Sciences*, 104, 11441-11446.

Kruger, R., Kuhn, W., Muller, T., Woitalla, D., Graeber, M., Kosel, S., …& Riess, O. (1998). Ala30Pro mutation in the gene encoding alpha-synuclein in parkinson's disease. *Nature Genetics, 18*, 106-108.

Langston, J. W., Ballard, P., Tetrud, J. W., & Irwin, I. (1983). Chronic Parkinsonism in humans due to a product of meperidine-analog synthesis. *Science, 219,* 979-980.

Langston, J. W., Langston, E. B., & Irwin, I. (1984). MPTP-induced parkinsonism in human and non-human primates--clinical and experimental aspects. *Acta Neurologica Scandinavica, Supplementum, 100*, 49-54.

Lelan, F., Boyer, C., Thinard, R., Remy, S., Usal, C., Tesson, L, … & Lescaudron, L. (2011). Effects of human alpha-synuclein A53T-A30P mutation on SVZ and local olfactory bulb cell proliferation in a transgenic rat model of Parkinson's disease. *Parkinson's Disease,* 1-11.

Li, W., West, N., Colla, E., Pletnikova, O., Troncoso, J. C., Marsh, L., & Lee, M. K. (2005). Aggregation promoting C-terminal truncation of α-synuclein is a normal cellular process and is enhanced by the familial Parkinson's disease-linked mutations. *Proceedings of the National Academy of Sciences of the United States of America*, *102*, 2162-2167.

Liu, G., Qu, J., Suzuki, K., Nivet, E., Li, M., Montserrat, N., … & Belmonte, J. C. I. (2012). Letter: Progressive degeneration of human neural stem cells caused by pathogenic LRRK2. *Nature, 491*, 603-607.

Liu, Y., Fallon, L., Lashuel, H.A., Liu, Z., & Lansbury Jr., P.T. (2002). The UCH-L1 gene encodes two opposing enzymatic activities that affect alpha-synuclein degradation and Parkinson's disease susceptibility. *Cell, 111,* 209-218.

Liu, C. W., Giasson, B. I., Lewis, K. A., Lee, V. M., Demartino, G. N., & Thomas, P. J. (2005). A precipitating role for truncated alpha-synuclein and the proteasome in alpha-synuclein aggregation: implications for pathogenesis of Parkinson disease. *The Journal of Biological Chemistry, 280*, 22670-8.

Lucking, C. B., & Brice, A. (2000). Review: Alpha-synuclein and Parkinson's disease. *Cellular and Molecular Life Sciences, 57*, 1894-1908.

Maguire-Zeiss, K. A., Short, D. W., & Federoff, H. J. (2005). Synuclein, dopamine, and oxidative stress: co-conspirators in Parkinson's disease? *Molecular Brain Research, 134*, 18-23.

McLean, P. J., Kawamata, H., Ribich, S., & Hyman, B.T. (2000). Membrane association and protein conformation of α-synuclein in intact neurons. *The Journal of Biological Chemistry, 275*, 8812-8816.

McLean, J. R., Hallett, P. J., Cooper, O., Stanley, M., & Isacson, O. (2012). Transcript expression levels of full-length alpha-synuclein and its three alternatively spliced variants in Parkinson's disease brain regions and in a transgenic mouse model of alpha-synuclein overexpression. *Molecular and Cellular Neuroscience, 49*, 230-239.

Myhre, R., Toft, M., Kachergus, J., Hulihan, M., Aasly, J. O., Klungland, H., & Farrer, M. J. (2008). Multiple alpha-synuclein gene polymorphisms are associated with Parkinson's disease in a Norwegian population. *Acta Neurologica Scaninavica*, *118*, 320-327.

National Institute of Neurological Disorders and Stroke (2004). Parkinson's disease: challenges, progress and promise. Retrieved from URL http://www.ninds.nih.gov/disorders/parkinsons_disease/parkinsons_research.

Neuytemans, K., Theuns, J., Cruts, M., & Van Broeckhoven, C. (2010). Genetic Etiology of Parkinson Disease Associated with Mutations in the SNCA, PARK2, PINK1, PARK7, and LRRK2 Genes: A Mutation Update. *Human Mutation,* 764-780.

Olanow, C. W., & Tatton, W. G. (1999). Etiology and pathogenesis of Parkinson's disease. *Annual Review of Neuroscience, 22*, 123-144.

Outeiro, T.F., Lindquist, S. (2003). Yeast Cells Provide Insight into Alpha- Synuclein Biology and Pathobiology. *Science, 302*(5651), 1772-1775.

Paisan-Ruiz, C., Jain, S., Evans, E. W., Gilks, W. P., Simon, J., van der Brug, M., …& Singleton, A. B. (2004). Cloning of the gene containing mutations that cause PARK8-linked Parkinson's disease. *Neuron, 44,* 595-600.

Paleologou, K. E., Oueslati, A., Shakked, G., Rospigliosi, C. C., Kim, H. Y., Lamberto, G. R., …& Lashuel, H. A. (2010). Phosphorylation at S87 is enhanced in synucleinopathies, inhibits alpha-synuclein oligomerization, and influences synuclein-membrane interactions. *The Journal of Neuroscience, 30* (9), 3184-3198.

Pandey, N., Schimidt, R. E., & Galvin, J.E. (2005). The alpha-synuclein mutation E64K promotes aggregation in cultured cells. *Experimental Neurology*, 1-6.

Parkinson's Disease Foundation. (2012). Statistics on Parkinson's, Retrieved from URL http://www.pdf.org/en/parkinson_statistics

Parkinson, J. (1817). An essay on the shaking palsy. London: Whittingham and Rowland.

Polymeropoulos, M. H, Lavedan, C., Leroy, E., Ide, S. E., Dehejia, A., Dultra, A., …& Nussbaum, R. L. (1997). Mutation in the α-synuclein gene identified in families with Parkinson's disease. *Science, 276*, 2045-2047

Prasad, K., Tarasewicz, E., Strickland, P., O'Neil, M., Mitchell, S., & Mechant, K., (2011). Biochemical and morphological consequences of human a-synuclein expression in a mouse a-synuclein null background. *European Journal of Science, 33,* 642-656.

Purves, D., Augustine, G., Fitzpatrick, D., Hall, W., Lamantia, A., McNamara, J., & White, L. (2012). *Neuroscience, Fifth Edition,* Sinauer Associates.

Raaij, M. E. V., Segers-Nolten, I. M. J., & Subramaniam, V. (2006). Quantitative morphological analysis reveals ultrastructual diversity of amyloid fibrils from α-synuclein mutants. *Biophysical Journal: Biophysical Letters,* 96-98.

Ross, C. A., & Poirier, M. A. (2004). Protein aggregation and neurodegenerative disease, *Nature Medicine, 10*, S10-7.

Schwede, T., Kopp, J., Guex, N. & Peitsch, M. C. (2003). SWISS-MODEL: an automated protein homology-modeling server. *Nucleic Acids Research*, *31,* 3381-3385.

Sian, J., Youdim, M., Riederer, P., & Gerlach, M. (1999). MPTP-Induced Parkinsonian Syndrome. *Basic Neurochemistry: Molecular, Cellular and Medical Aspects.* Philadelphia: Lippincott-Raven. Available from: http://www.ncbi.nlm.nih.gov/books/NBK27974/

Sharma, N., Brandis, K. A., Herrera, S. K., Johnson, B. E., Vaidya, T., Shrestha, R., & DebBurman, S. K. (2006). α-Synuclein budding yeast model toxicity enhanced by impaired proteasome and oxidative stress. *Journal of Molecular Neuroscience, 28*, 161-178.

Sharon, R., Bar-Joseph, I., Frosch, M. P., Walsh, D. M, Hamilton, J. A., & Selkoe, D. J. (2003). The formation of highly soluble oligomers of α-synuclein is regulated by fatty acids and enhanced in Parkinson's disease. *Neuron, 37*, 583-595.

Sharon, R., Goldberg, M. S., Josef, I. B., Betensky, R. A., Shen, J., & Selkoe, D. J. (2001). α-synuclein occurs in lipid-rich high molecular weight complexes, binds fatty acids, and shows homology to the fatty acid-binding proteins. *Proceedings of the National Academy of Sciences, 98*, 9110-9115.

Shin, J., Dawson, V., & Dawson, T. (2009). SnapShot: pathogenesis of Parkinson's disease. *Cell, 139*, 440.

Spillantini, A. G., Crowther R. A., Jakes R., Hasegawa, M., & Goedert M. (1998). α-Synuclein in filamentous inclusions of Lewy bodies from Parkinson's disease and dementia with Lewy bodies. *Proceedings of the National Academy of Sciences, 95*, 6469-6473.

Taylor, J. P., Hardy, J., & Fischbeck, K. H. (2002). Toxic proteins in neurodegenerative disease. *Science 296*, 1991-1995.

Valente, E. M., Abou-Sleiman, P. M., Caputo, V., Muqit, M. M., Harvey, K., Gispert, S., … & Wood, N. W. (2004). Hereditary early-onset Parkinson's disease caused by mutations in PINK1. *Science, 304,* 1158-1160

Vriend, G. (1990). WHAT IF: A molecular modeling and drug design program, *Journal of Molecular Graphics, 8*, 52-56.

Wersinger, C., Prou, D., Vernier, P., Niznik, H. B., & Sidhu, A. (2003). Mutations in the lipid-binding domain of α-Synuclein confer overlapping yet distinct, functional properties in the regulation of dopamine transporter activity. *Molecular and Cellular Neuroscience, 24*, 91-105.

Wilkinson, K., Knopacki, F., & Henley. J. (2012). Modification and movement: Phosphorylation and SUMOylation regulate endocytosis of GluK2-containing kainate receptors. *Communicative &Integrative Biology, 5*, 223-226

Xiong, L., Zhao, P., Guo, Z., Zhang, J., Li, D., & Mao, C. (2010). Alpha-synuclein gene structure, evolution, and protein aggregation. *Neural Regeneration Research, 5*, 1423-1428.

Zarranz, J. J., Alegre, J., Gomez-Esteban, J. C., Lezcano, E., Ros, R., Ampuero, I., … & De Yebenes, J. G. (2004). The new mutation, E46K, of alpha-synuclein causes Parkinson and Lewy body dementia. *Annals of Neurology, 55*, 164-173.

## APPENDIX:

### A. LOCALIZATION

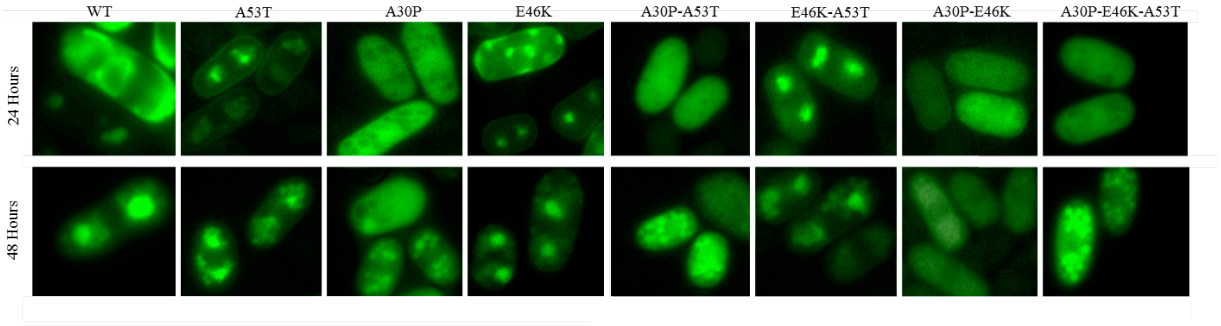


### B. QUANTIFICATION

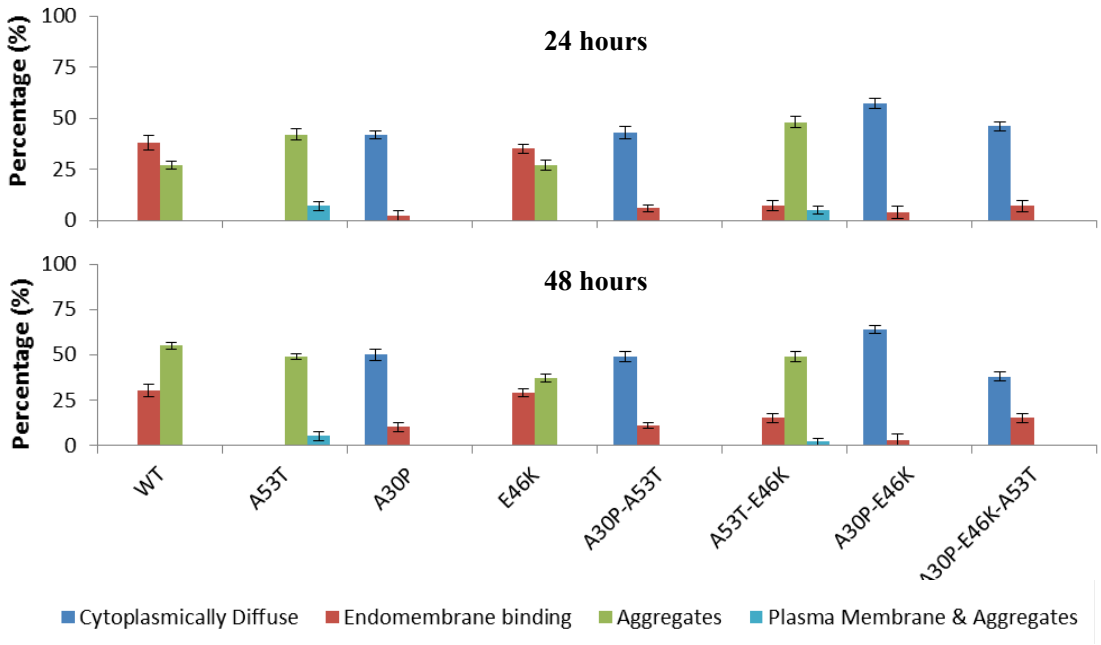


*Figure 20. Protein localization in a high expressing yeast model, (Sph+).*

C. Time course fluorescent microscopy. The following mutations of α-synuclein were evaluated in comparison to its WT localization: A53T, A30P, E46K, A30P-A53T, E46K-A53T, A30P-E46K, and A30P-E46K-A53T. The mutants were expressed in the Sph+ strain of fission yeast. Microscopy photographs were captured at 24 and 48 hours post induction with EMM-T (n=5).

D. Time course quantification. WT, A53T, A30P, E46K, A30P-A53T, E46K-A53T, A30P-E46K, and A30P-E46K-A53T were quantified for photographs captured at 24 and 48 hours post induction with EMM-T (n=5). The error bars represent standard deviation based on the averaged results.

**A. TOXICITY**

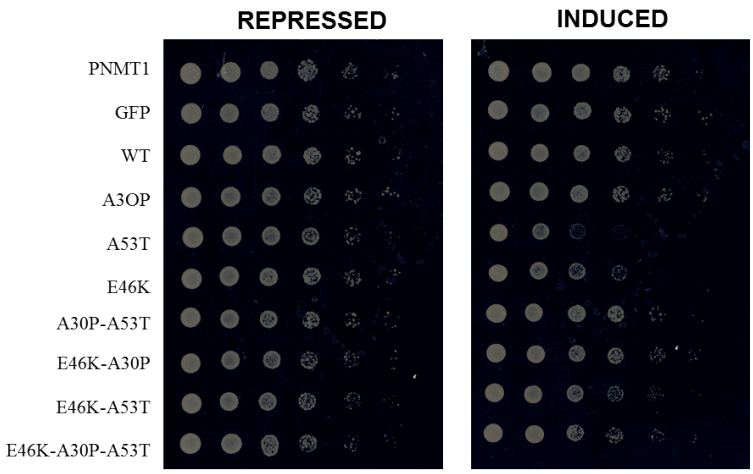


**B. EXPRESSION**

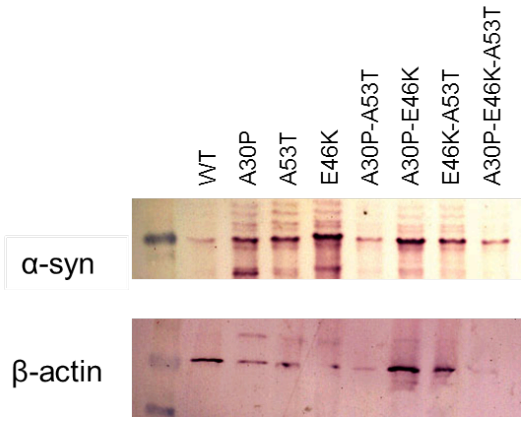


*Figure 21. Toxicity and protein accumulation in a high expressing yeast model, (Sph+).*
A. Spotting. Yeast expressing PNMT1, GFP, WT, A30P, A53T, E46K, A30P-A53T, E46K-A30P, E46K-A53T and E46K-A30P-A53T α-synuclein spotted onto a repressive media (EMM+T) and inductive media (EMM-T) after a five-fold serial dilutions (n=5).
B. Expression. Western Blot at 48 hours of WT, A30P, E46K, A53T, A30P-E46K, A30P-A53T, E46K-A53T, and E46K-A30P-A53T expression (anti-V5) with the loading control below (β-actin) (n=4).

## F. EXPERIMENTAL DESIGN

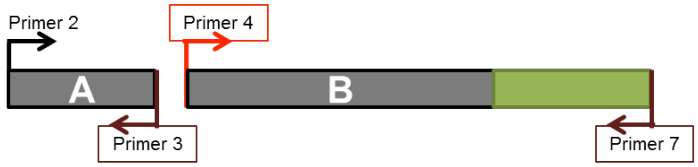


Segments for α-synuclein 126

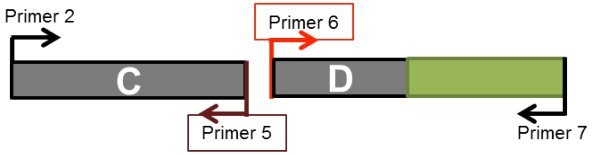


Segments for α-synuclein 112

## E. EXPERIMENTAL OUTCOME

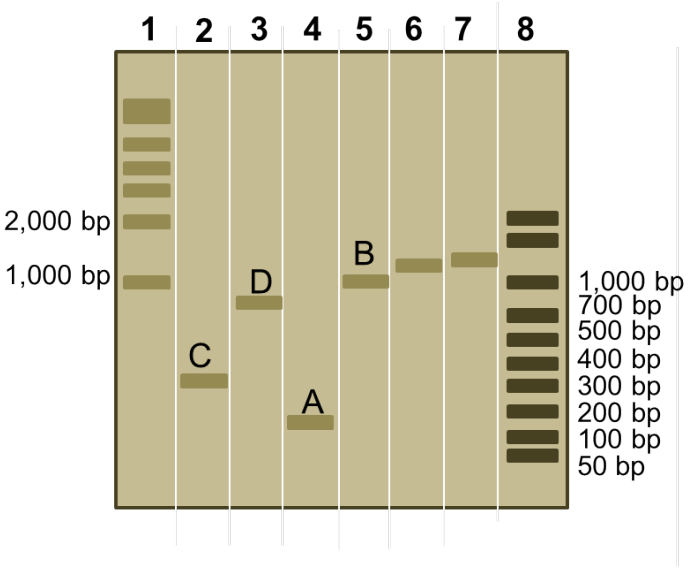


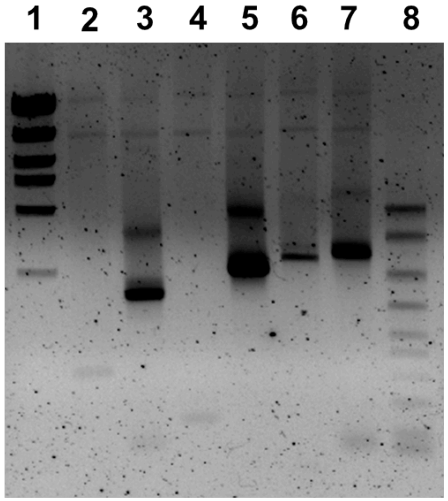


**Legend:**
1. High Mass Ladder
2. Segment C
3. Segment D
4. Segment A
5. Segment B
6. Control 1
7. Control 2
8. AmpliSize Ladder

*Figure 22. Formation of splice variants' segments (fall attempt)*

C. Experimental design. Desired segments for each splice variant created through the first round of PCR with the appropriate primers.

D. Experimental outcome. First round PCR results. Lane 1 is the high mass ladder, lane 2 is segment C, lane 3 is segment D, lane 4 is segment A and lane 5 is segments B, lane 6 is the first control, and lane 7 is the second control. The two controls were utilized to ensure that the primers were functioning correctly. *Although the segments were further fused used to create α-synuclein-126 and α-synuclein-112, they were not TOPO cloned.

## B. EXPERIMENTAL DESIGN

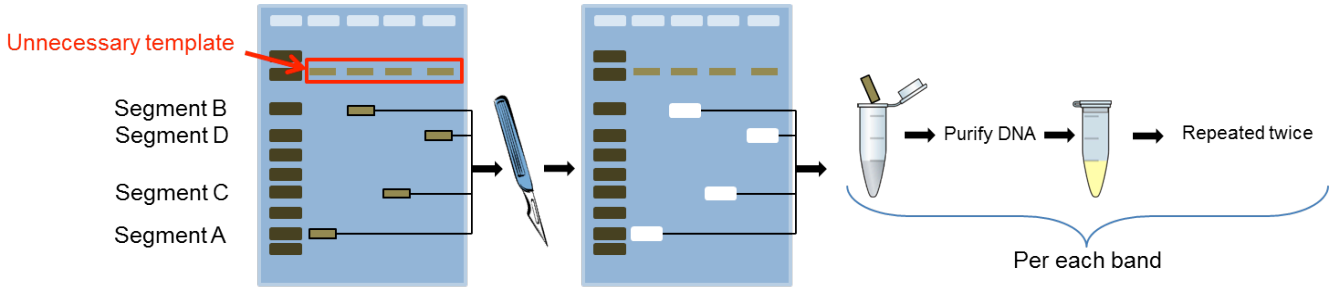


## C. EXPERIMENTAL OUTCOME

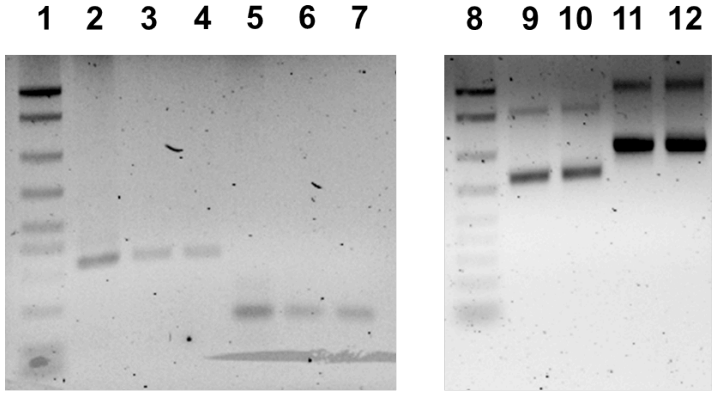


**Legend:**

1. AmpliSize Ladder
2. Segment C original PCR
3. Segment C purified PCR
4. Segment C purified PCR
5. Segment A original PCR
6. Segment A purified PCR
7. Segment A purified PCR
8. AmpliSize Ladder
9. Segment D purified PCR
10. Segment D purified PCR
11. Segment B purified PCR
12. Segment B purified PCR

*Figure 23. Purification of splice variants' segments (fall attempt).*

C. Experimental design. Exemplified is a cartoon of the purification process of the PCR product acquired for each segment. Each PCR product was run independently on the gel. The band was then cut out and purified. This process was repeated twice for each PCR product indicative of the four created segments.

D. Experimental outcome. To ensure minimal loss of product during the purification technique, the original PCR product was compared to the purified product for each segment.

**B. EXPERIMENTAL DESIGN**

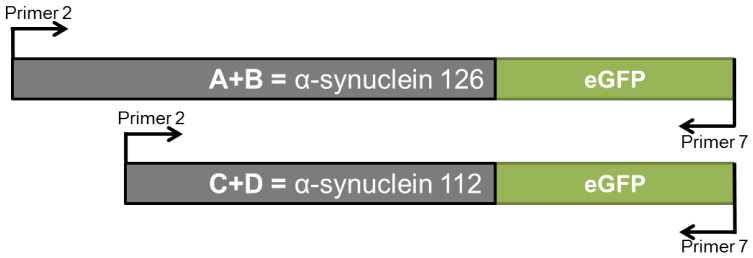


**C. EXPERIMENTAL OUTCOME**

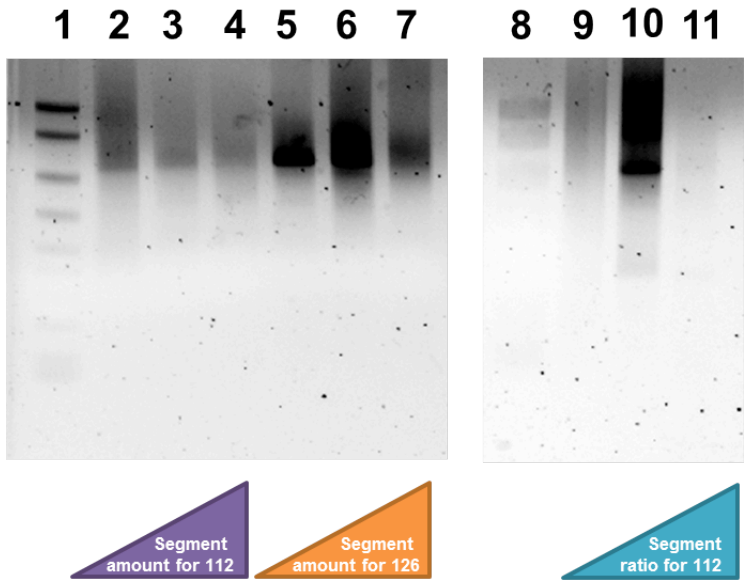


**Legend**:
1. Amp Ladder
2. 112 (low)
3. 112 (medium)
4. 112 (high)
5. 126 (low)
6. 126 (medium)
7. 126 (high)
8. Amp Ladder
9. 112 (1:1 ratio)
10. 112 (1:2 ratio)
11. 112 (1:3 ratio)

*Figure 24. Segment fusion (fall attempt).*

B. Experimental design. Desired splice variants for each α-synuclein isoform from fused segments acquired through the second round of PCR.

C. Experimental outcome. To acquire the best quality product, two conditions were created. First: the amount of the two segments used for each splice variant was equally increased (employed for α-synuclein-112 and 126); secondly, the amount of the weaker product (segment C) was equal, twice, or three times the amount of segment D (employed for α-synuclein-112). Lanes 1 and 8 are AmpliSize ladder. Lanes 2, 3 and 4 represent α-synuclein 112 splice variant using low, medium, or high template amount respectively. Lanes 5, 6, and 7 represent α-synuclein 126 splice variant using low, medium, or high template amount respectively. Lanes 9, 8 and 10 represent α-synuclein 112 splice variant using template ratios: 1:1, 1:2, 1:3.